Collider Particle Physics
- Chapter 11 -

LHC Physics

Claudio Luci

SAPIENZA
UNIVERSITÀ DI ROMA

last update : 070117

Chapter Summary

- ☐ Cross-Section Measurements
- ☐ W mass measurement
- ☐ $\mathrm{Sin}^2\theta_W$
- ☐ Gauge Boson Couplings
- ☐ Higgs Discovery in Run1
- ☐ Higgs Physics Dedicated Lecture
- ☐ Top quark
- ☐ Example of Dark Matter Search at LHC
- ☐ Example of SuSy particles search at LHC

A few Cross-Sections Measurements

Reminder: proton-proton collisions

Parton-parton collision

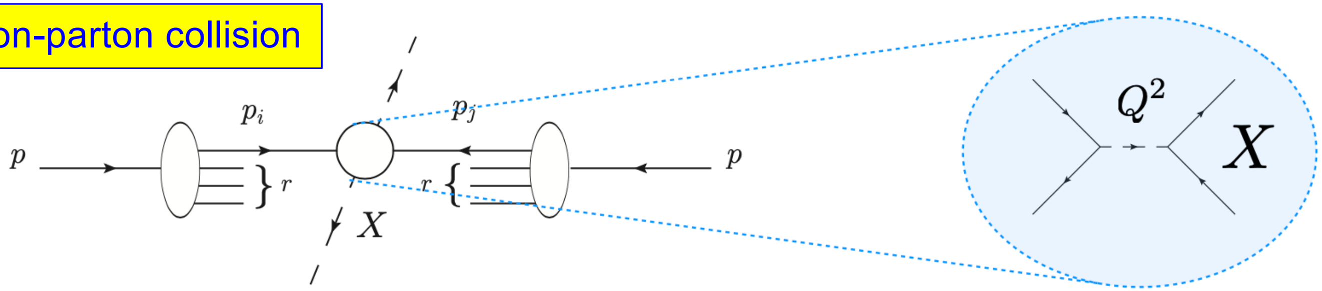

Having no knowledge a priori of the type and momentum fraction of the initial partons, the predictions need to be integrated w.r.t. to all parton types and momenta.

$$\sigma(pp \to X) = \sum_{i,j} \int_0^1 dx_i dx_j f_i(x_i, Q^2) f_j(x_j, Q^2) d\hat{\sigma}(q_i q_j \to X, \hat{s}, Q^2)$$

Q^2 *'Resolution scale'*

In the case depicted above M_X^2

- q_1 and q_2 are the initial partons
- x_1 and x_2 are the momentum fraction of each parton.

Important messages

(1) The centre-of-mass energy of the interaction is not known a priori (and essentially impossible to reconstruct due to limited resolution and part of the event being undetected)

(2) At LHC making predictions that are:
- Exact is not possible.
- Accurate and precise is however possible… but difficult.

(3) Predictions rely on the knowledge of the number and types of partons and the distributions of their momenta in the protons.

Reminder: PDFs

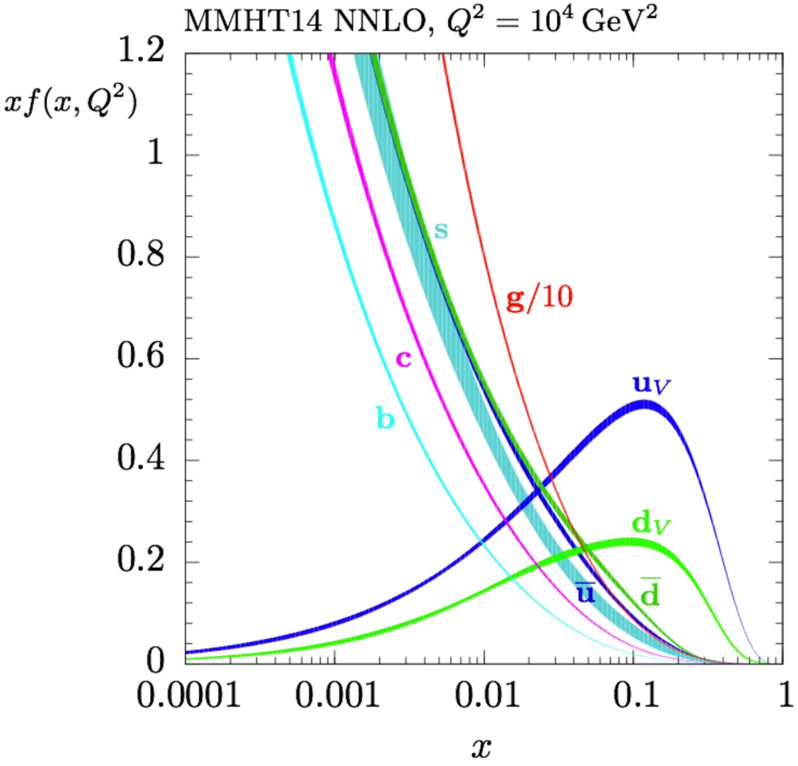

PDFs Sum rules

Momentum sum rule

$$\sum_i \int_0^1 dx\, x f_i(x,Q^2) = 1$$

Flavour conservation sum rules

$$\int_0^1 (f_u(x,Q^2) - f_{\overline{u}}(x,Q^2))dx = 2$$

$$\int_0^1 (f_d(x,Q^2) - f_{\overline{d}}(x,Q^2))dx = 1$$

$$\int_0^1 (f_s(x,Q^2) - f_{\overline{s}}(x,Q^2))dx = 0$$

- PDFs are the probability to find a parton with a momentum fraction of x.
- PDFs are not calculable, but measured in DIS experiments (with electron and neutrino scattering on nucleons).
- PDFs evolution in Q^2 are calculable (with Altarelli-Parisi equations).

Measurement of the Total pp Cross Section

From the initial O(80) mb naive estimate of the total cross section of pp collisions.

The total cross section is dominated (60 mb) by inelastic interactions.

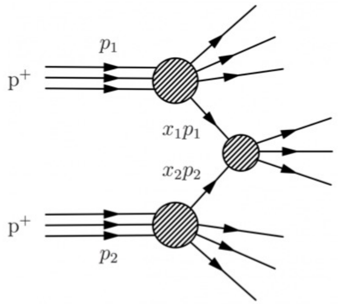

The main subject of these lectures.

Includes elastic interactions from exchange of photons or pomerons (20 mb).

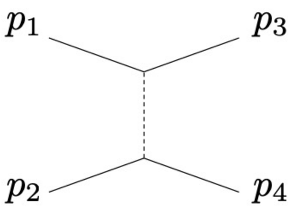

$$t = (p_1 - p_3)^2$$

(very naive view of the pomeron is a colorless pair of gluons)

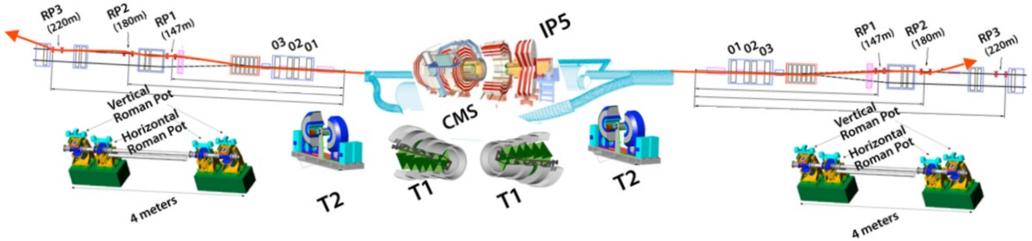

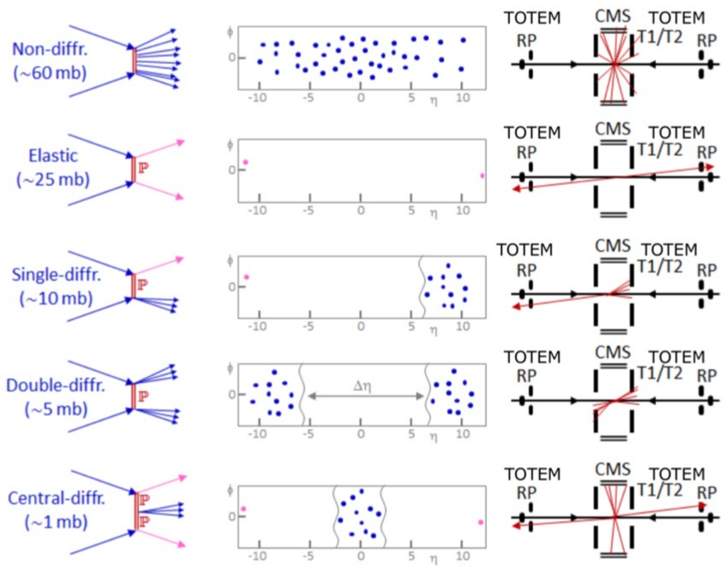

QCD bckg

QCD bckg

QCD bckg

QCD bckg

The measurement of the total cross section requires the measurement of the elastic cross section at (very) low momentum transfer.

The simplest measurement of the cross section counting events:

$$\sigma_{tot} = \frac{N_{el} + N_{inel}}{\mathcal{L}}$$

QCD background

- ☐ High-p_T events are dominated by QCD jet production

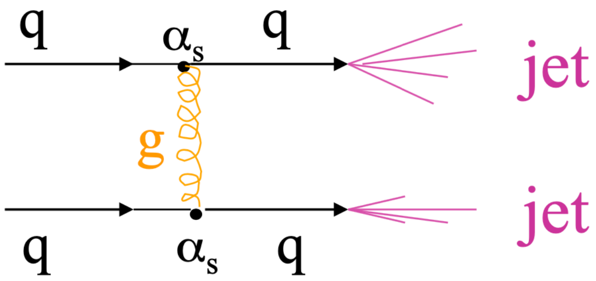

- ☐ Strong interaction → large cross-section
- ☐ Many diagrams contribute: qq → qq ; qg → qg ; gg → gg; etc …
- ☐ They are called "QCD background "

- ☐ Most interesting processes are rare processes:
  - involve heavy particles
  - have weak cross-sections (e.g. W cross-sections)
  - to extract signal over QCD jet background must look at decays to photons and leptons → pay a prize in branching ratio

Example of Total Cross Sections for LHC main processes

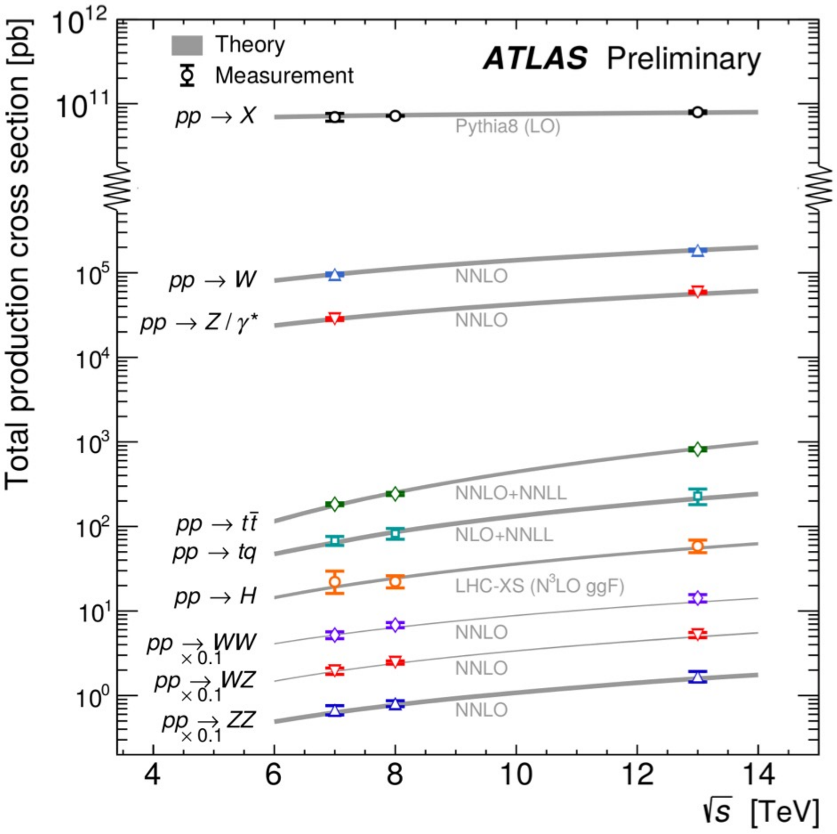

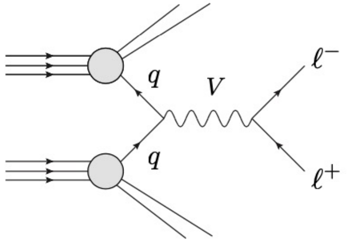

Vector boson production (often referred to as Drell Yan).

LEP ~4 M Z per experiment
LHC ~100 M (leptonic) / exp.
(for 100 fb^{-1})

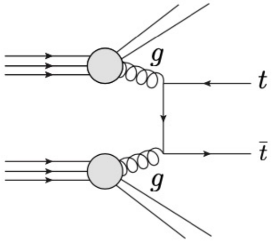

Top pair production

$$t\bar{t} \sim 1\,\mathrm{nb}$$

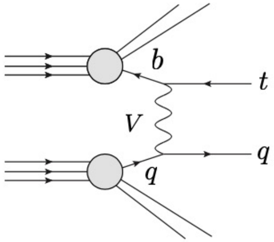

Single top production

$$tq \sim 200\,\mathrm{pb}$$

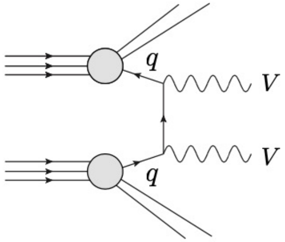

Diboson production

$$WW \sim 100\,\mathrm{pb}$$

$$ZZ \sim 20\,\mathrm{pb}$$

Drell-Yan Processes Cross Sections

Flavour content of the $pp \to \mathrm{Z}, \mathrm{W}^{\pm}$ process

In pp collisions a sizeable charge asymmetry due to the valence quarks (2u vs 1d) in the proton (difference reduces with the COM energy as W production occurs at lower x).

For 13 TeV collisions predictions are:

$$\sigma_{W^-} = 8.54\,^{+0.21}_{-0.24}\,(\mathrm{PDF}) \pm 0.16\,(\mathrm{TH})\ \mathrm{nb}$$

$$\sigma_{W^+} = 11.54\,^{+0.32}_{-0.31}\,(\mathrm{PDF}) \pm 0.22\,(\mathrm{TH})\ \mathrm{nb}$$

$$\sigma_{Z} = 1.89 \pm 0.05\,(\mathrm{PDF}) \pm 0.04\,(\mathrm{TH})\ \mathrm{nb}$$

Note: PDF uncertainties are dominant.

Overall this process is O(3M) times smaller than the total inelastic cross section.

Still O(2) Billion W boson events produced !!

flavour decomposition of W cross sections

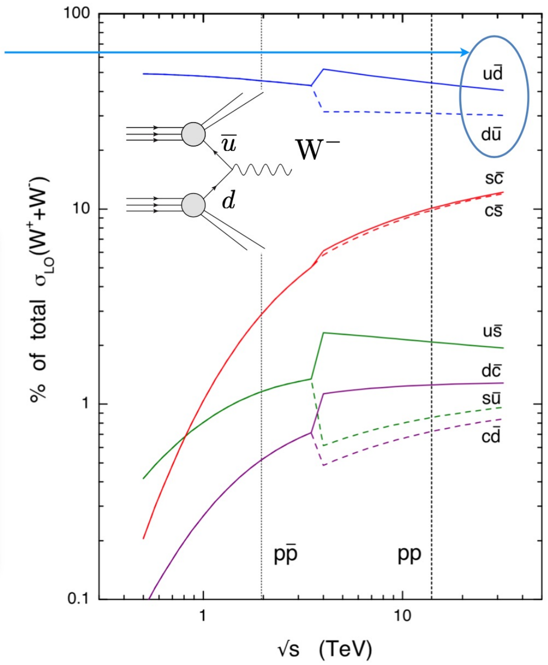

Typically in pp in leptonic modes $\ell = e, \mu, \tau$

$$\mathrm{Br}(\mathrm{W} \to \mathrm{q}\overline{\mathrm{q}'}) \sim 70\%$$

$$\mathrm{Br}(\mathrm{W} \to \ell^{\pm}\nu) \sim 10\%$$

flavour decomposition of Z⁰ cross sections

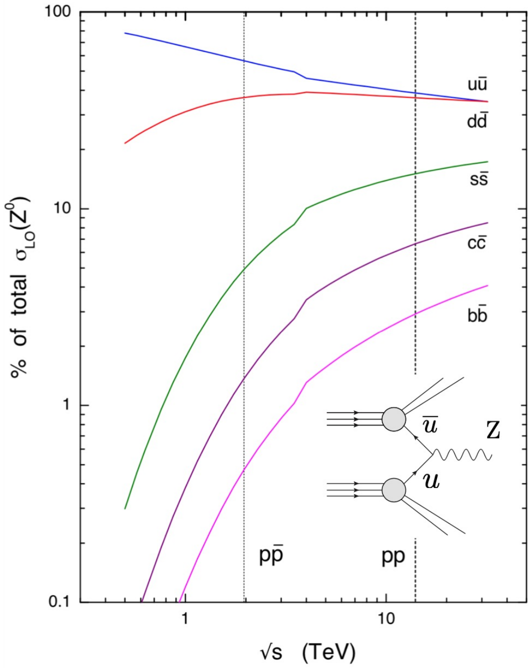

$$\mathrm{Br}(\mathrm{Z} \to \nu\overline{\nu}) \sim 20\%$$

$$\mathrm{Br}(\mathrm{Z} \to \mathrm{q}\overline{\mathrm{q}}) \sim 70\%$$

$$\mathrm{Br}(\mathrm{Z} \to \ell^{+}\ell^{-}) \sim 3\%$$

The di-lepton mass spectrum at LHC

Inclusive mass distributions

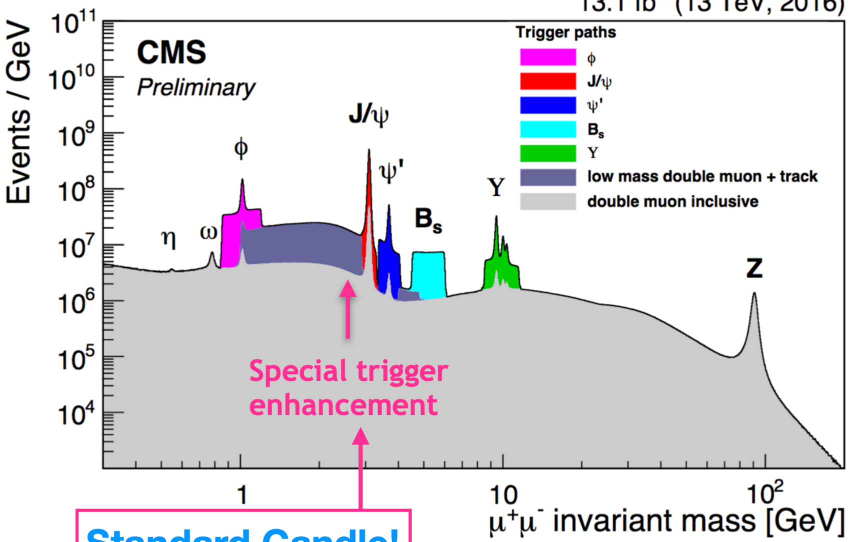

Special trigger enhancement

Standard Candle!

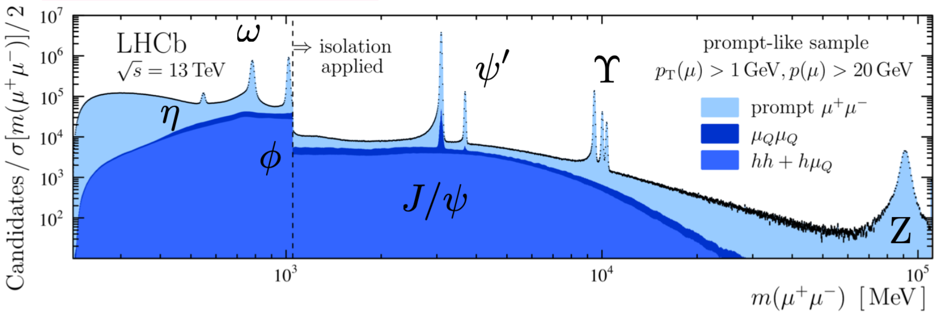

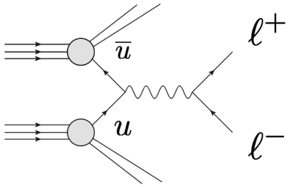

Z, J/Psi and Upsilon in electrons and muons are extremely important standard candles for calibration.

Standard Candle!

LEP

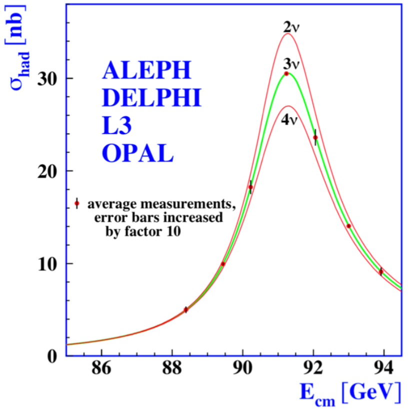

$$m_Z = 91.1875 \pm 0.0021 \text{ GeV}$$

$$\Gamma_Z = 2.4952 \pm 0.0023 \text{ GeV}$$

$$\rho = 1.0050 \pm 0.0010$$

An exclusive analysis scrutinising the Bs mass region

$$\text{Br}(B_s^0 \rightarrow \mu^+\mu^-) =$$
$$(3.65 \pm 0.23) \times 10^{-9}$$

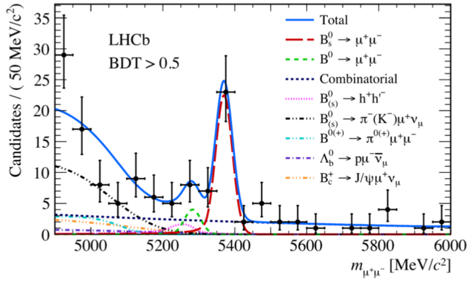

SM Cross Section Measurements

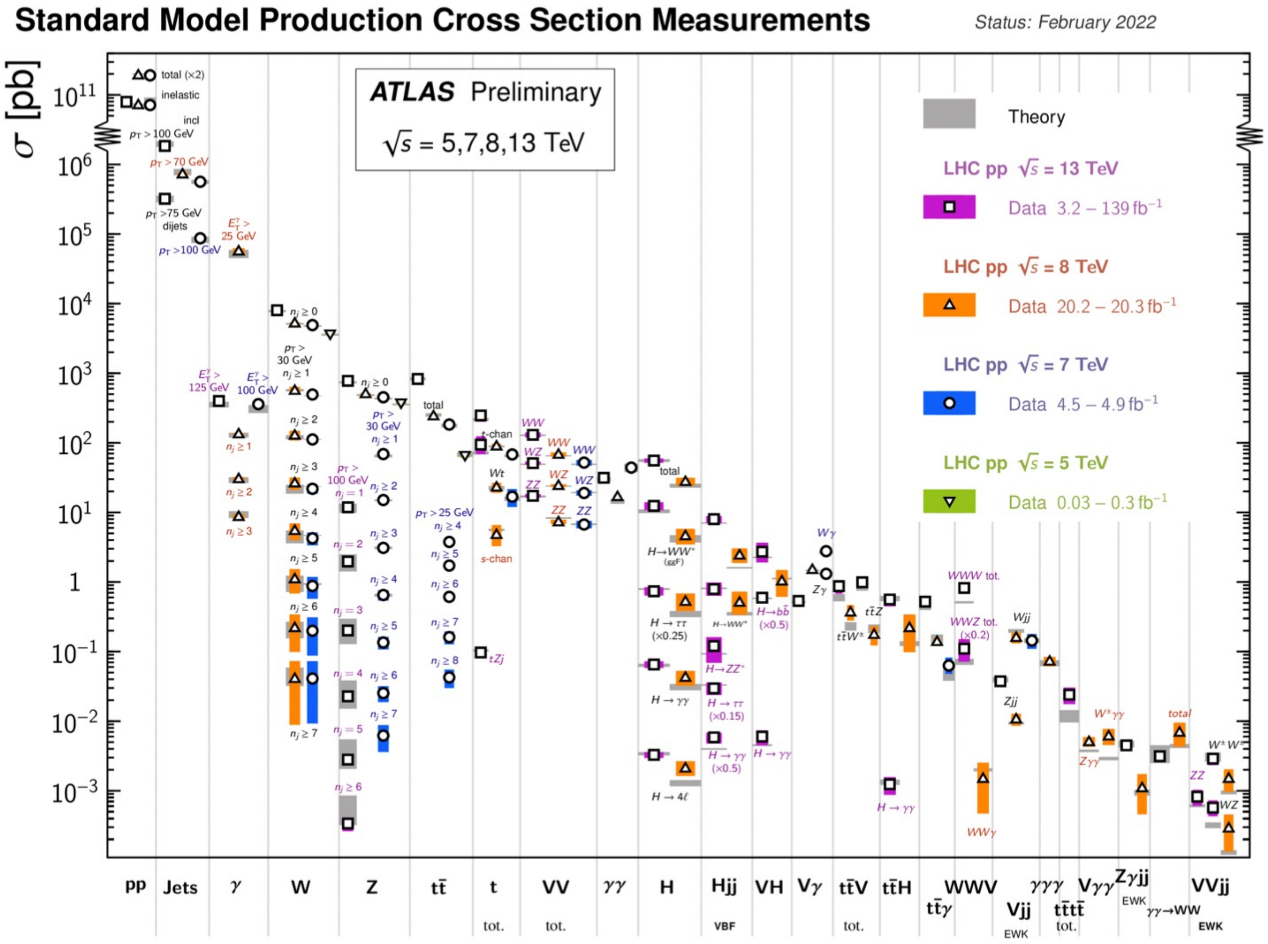
Standard Model Production Cross Section Measurements

Status: February 2022

Very large number of fiducial cross section measurement made at the LHC

Down to processes as rare as three boson production

Now measured VBS diboson production (VVjj)

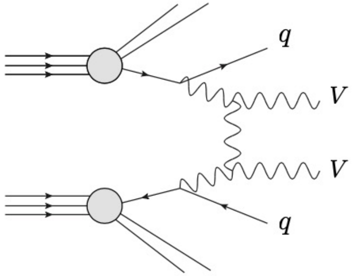

See later

Jet Cross Section and Measurement of α_s

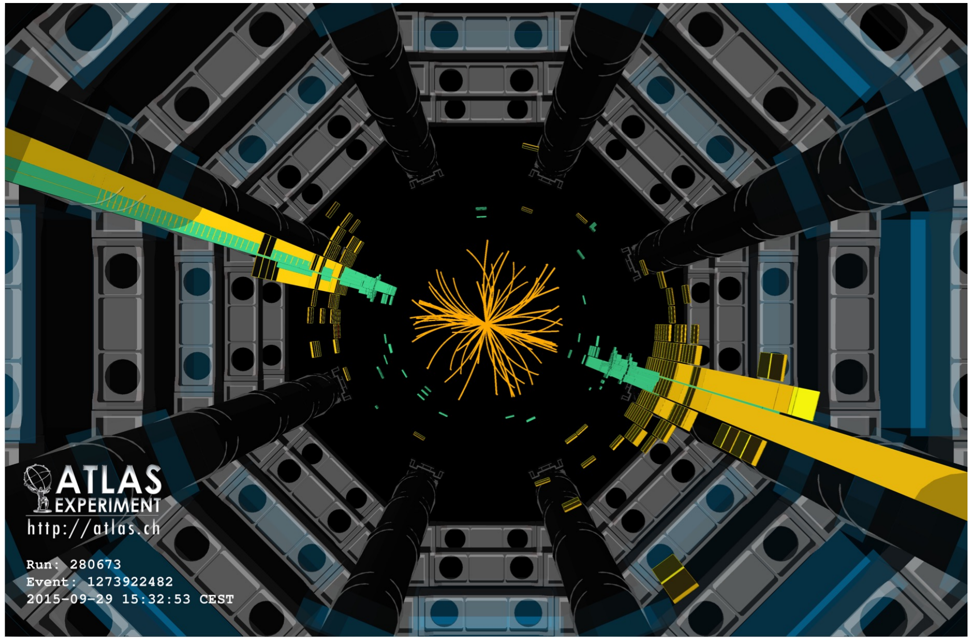

$$\frac{d^2\sigma}{dp_T dy} = \frac{1}{\varepsilon \mathcal{L}} \frac{N_j}{\Delta p_T \Delta y}$$

Double differential cross section

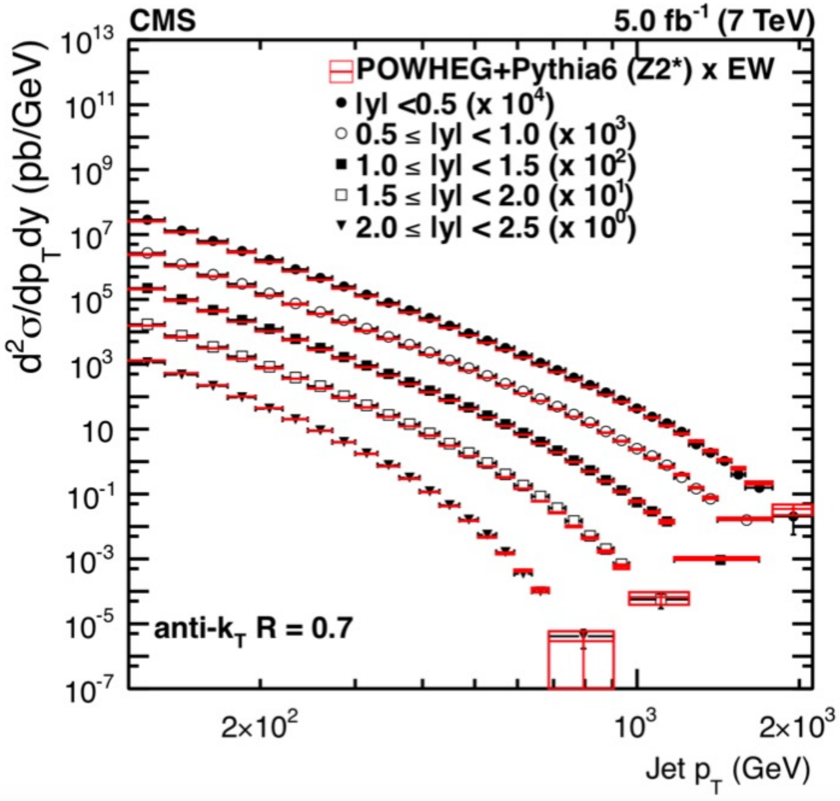

anti-k_T is a clusterisation algorithm

α_S Measurement at LHC

Ratio of Differential Jet Production Cross Sections

$$R_{3/2} = \frac{\sigma_{3-jets}}{\sigma_{2-jets}} =$$

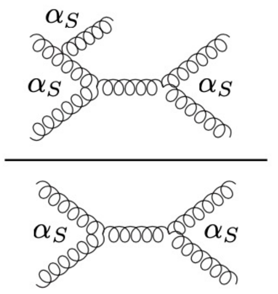

$$\propto \alpha_S$$

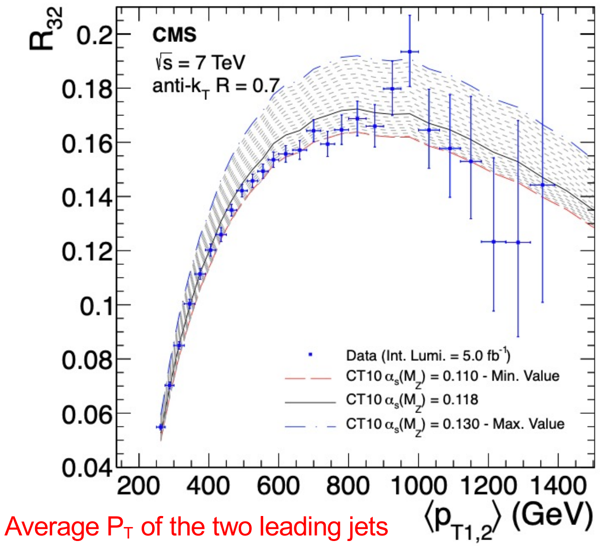

Average P_T of the two leading jets

From the measurements of jet cross sections and their ratios, the strong coupling constant can be measured at the highest energy scales!

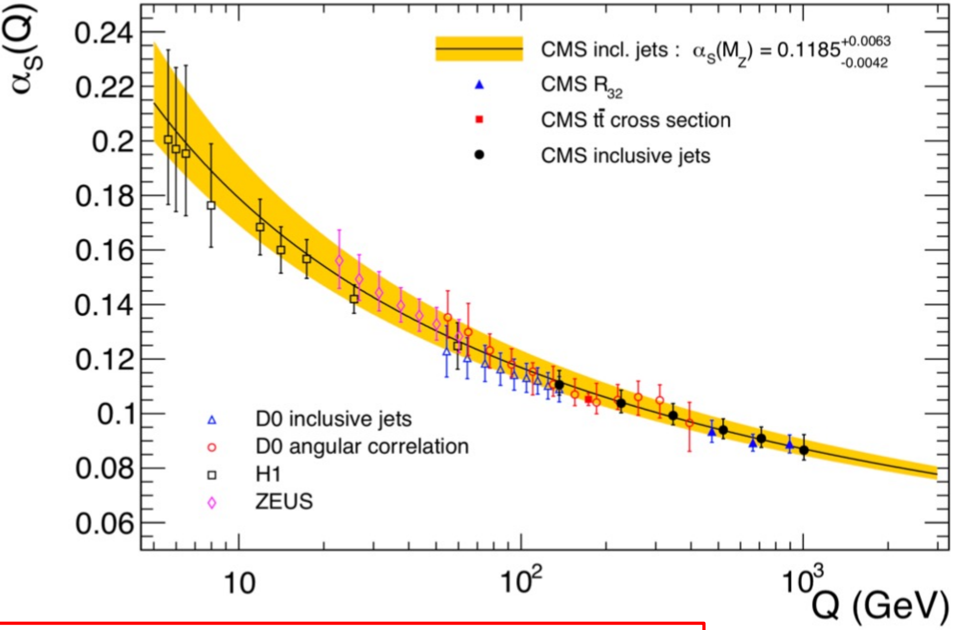

$$\alpha_S^{-1}(Q^2) = \alpha_S^{-1}(Q_0^2)\left[1+\frac{33-2n_f}{12\pi}\alpha_S(Q_0^2)\ln\left(\frac{Q^2}{Q_0^2}\right)\right]$$

M_W at Atlas

One W event in the muon-neutrino channel

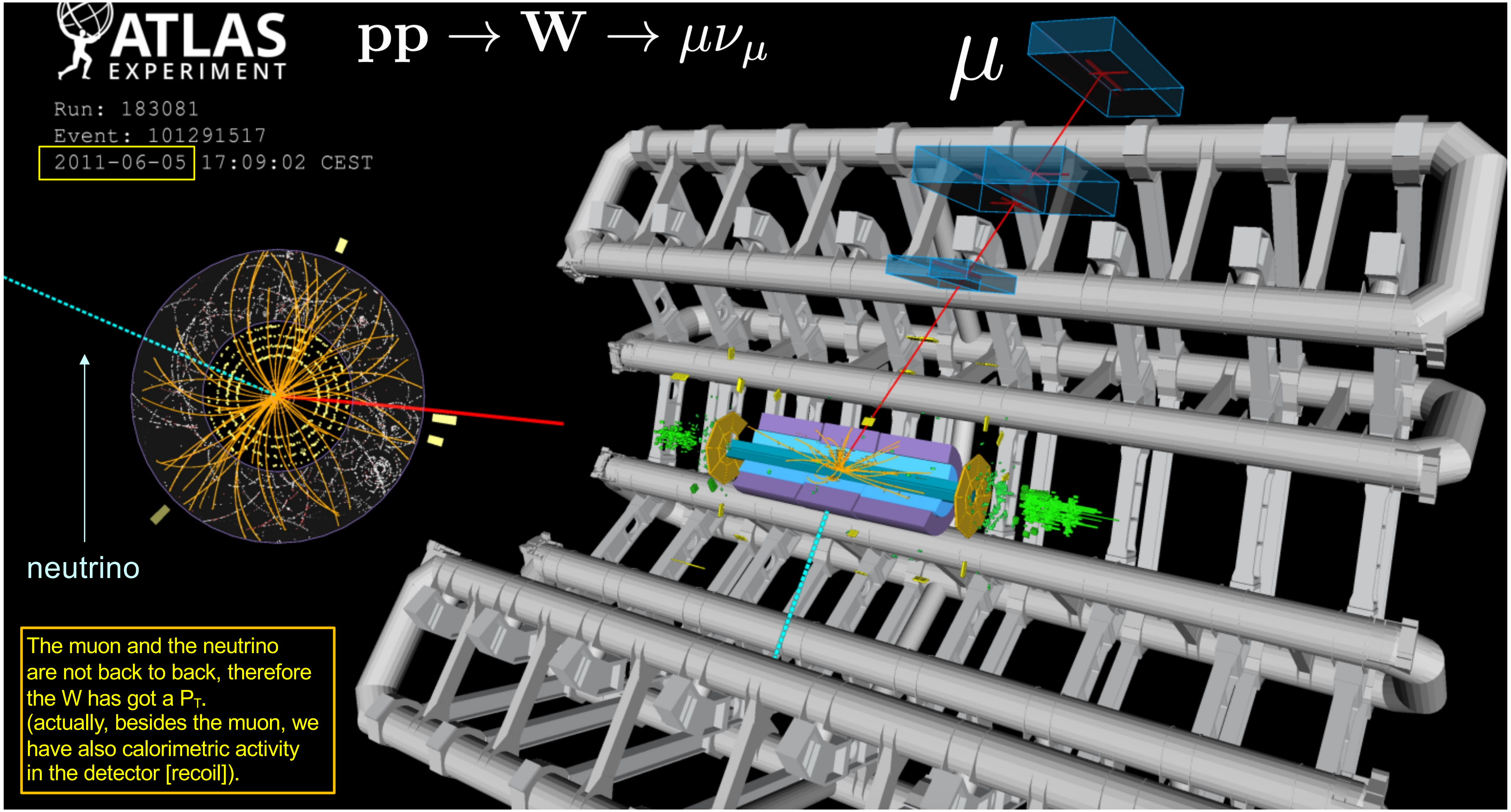

The muon and the neutrino are not back to back, therefore the W has got a P_T.
(actually, besides the muon, we have also calorimetric activity in the detector [recoil]).

One W event in the electron-neutrino channel

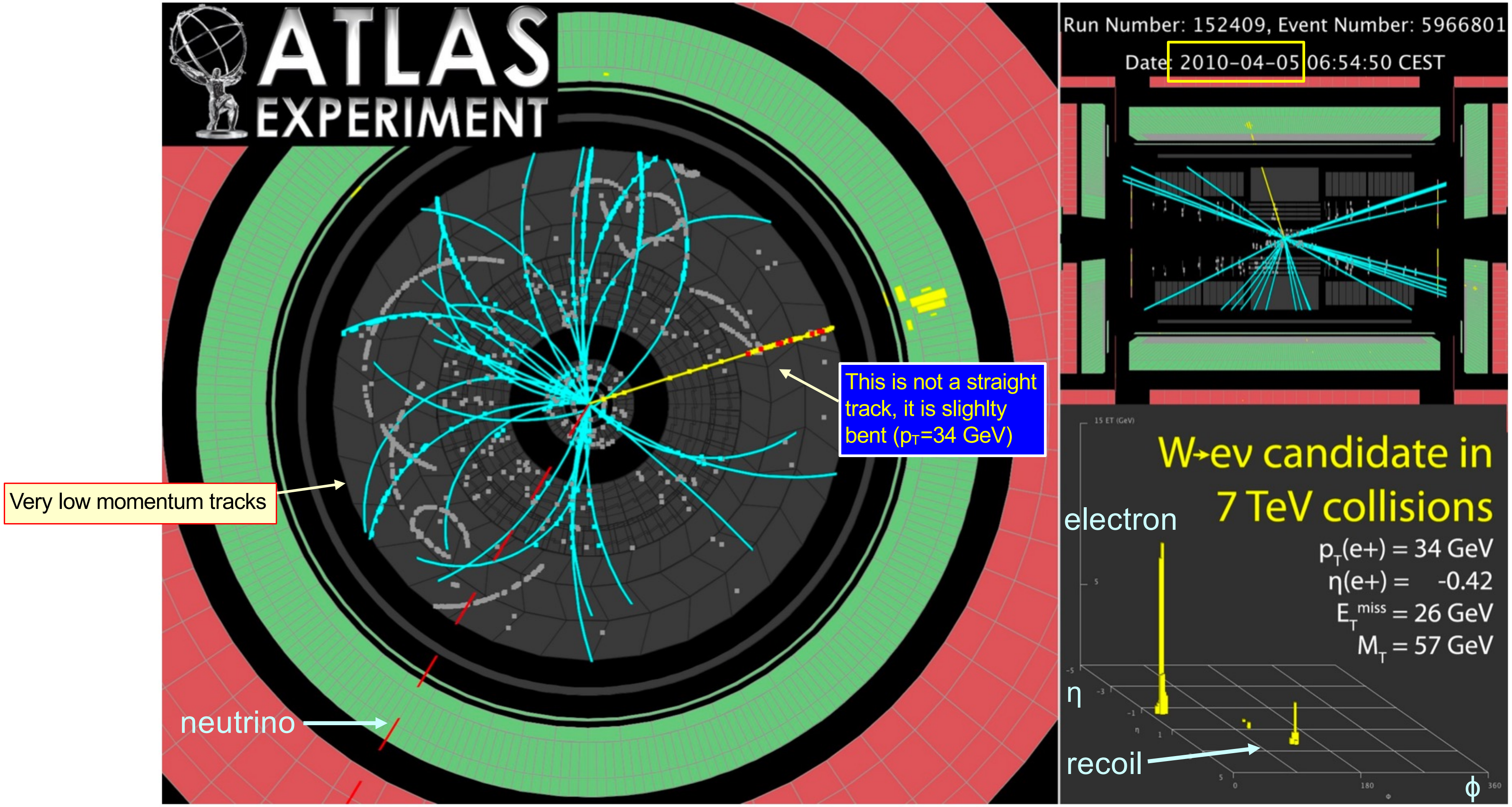

This is not a straight track, it is slighlty bent (p_T=34 GeV)

Very low momentum tracks

W→eν candidate in 7 TeV collisions

$p_T(e+) = 34$ GeV
$\eta(e+) = -0.42$
$E_T^{miss} = 26$ GeV
$M_T = 57$ GeV

ATLAS W mass: measurement strategy

2011 data set: E_{CM}=7 TeV; $\mathcal{L}$=4.6 fb^{-1}

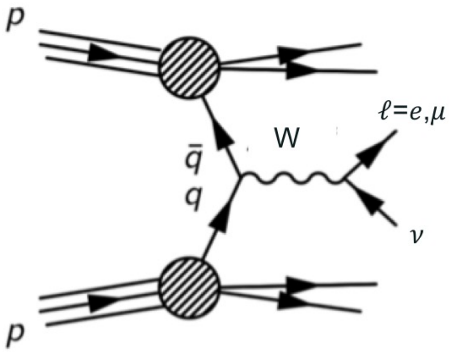

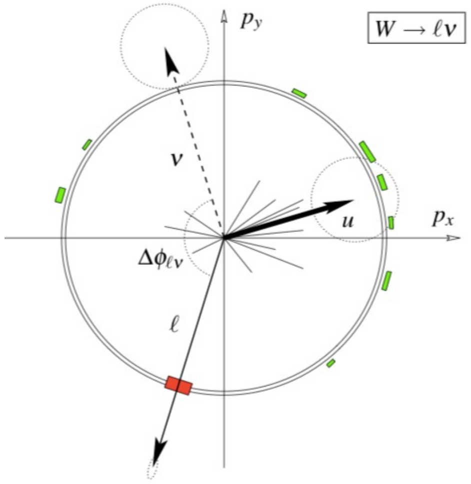

The W has a transverse momentum

Due to the neutrino the W invariant mass can not be reconstructed and we are forced to consider other variables sensitive to the W mass, like:

- The lepton transverse momentum: $\vec{p}_T^{\,\ell}$
- The W transverse mass: $m_T^W \equiv \sqrt{2\vec{p}_T^{\,\ell}\vec{p}_T^{\,miss}\left(1-\cos\Delta\phi\right)}$

where $\vec{p}_T^{\,miss} = -\left(\vec{p}_T^{\,\ell} + \vec{u}_T\right)$ is the neutrino missing p_T

and u_T is the **recoil**: $\vec{u}_T = \sum_i \vec{E}_{T,i}$ (calorimeter cells)

Event selection

- Muons: |η|<2.4
- Electrons : |η|<1.2 OR 1.8<|η|<2.4
- Lepton isolation
- $p_T^{\,l}$>30 GeV
- p_T^{miss}>30 GeV
- u_T<30 GeV
- m_T>60 GeV

Event sample

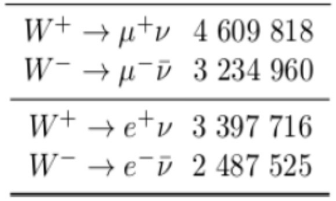

$W^+ \to \mu^+\nu$	4 609 818
$W^- \to \mu^-\bar{\nu}$	3 234 960
$W^+ \to e^+\nu$	3 397 716
$W^- \to e^-\bar{\nu}$	2 487 525

Sample of 13.7 M events: 5 times larger than combined (D0 + CDF) Tevatron sample

Statistics is not an issue; the challenge is the control of systematics (theoretical and experimental) to aim at 10 MeV error

How the W get a transverse momentum

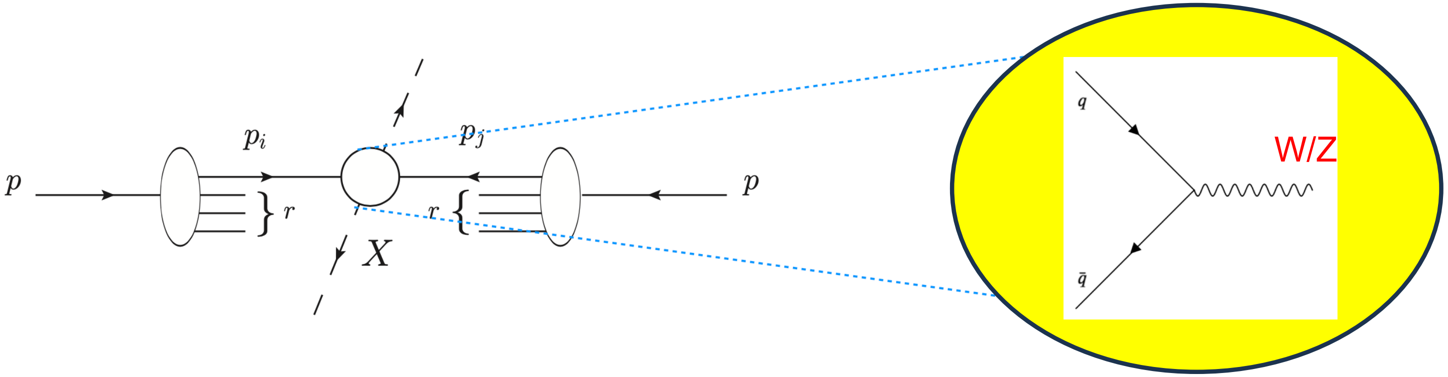

Feynman Assumption: infinite momentum frame.

Partons have only longitudinal momentum, therefore the W/Z does not have a transverse momentum

BUT … we have to take into account the QCD higher order corrections, namely the emission of gluons from the initial state.

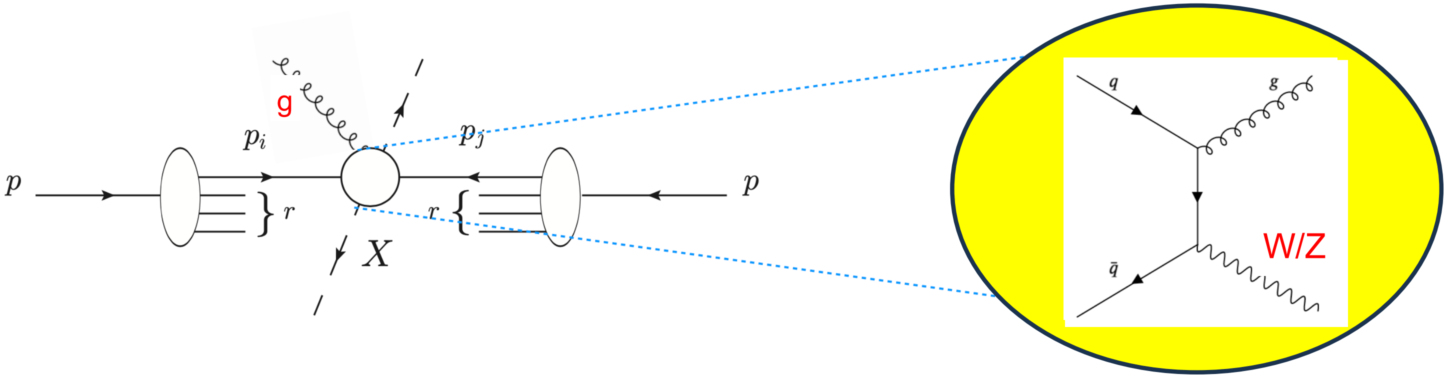

Now the W/Z has got a transverse momentum

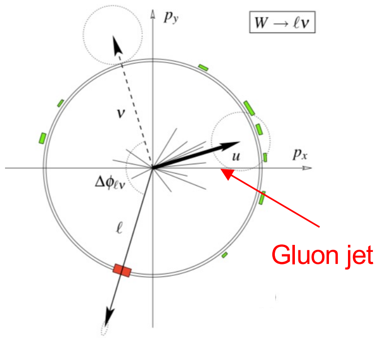

W mass: effects of p_T^W, PDF and pile up

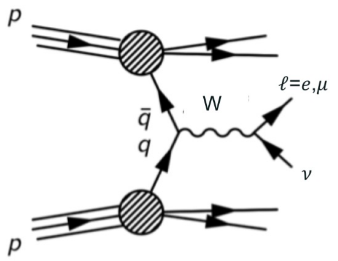

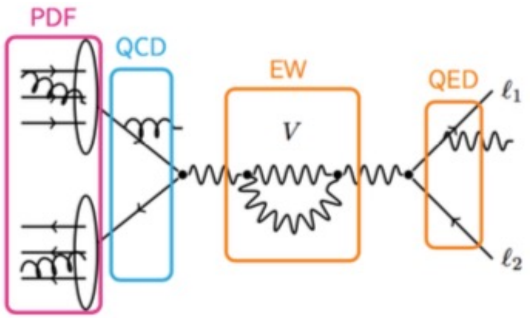

- At Leading Order the W is emitted along the beam pipe:

$$\vec{p}_T^{\,W} = 0$$

- High Order corrections modify the spectrum:

$$\vec{p}_T^{\,W} \neq 0$$

Example taken from an ATLAS note (2008) arxiv:0901.0512

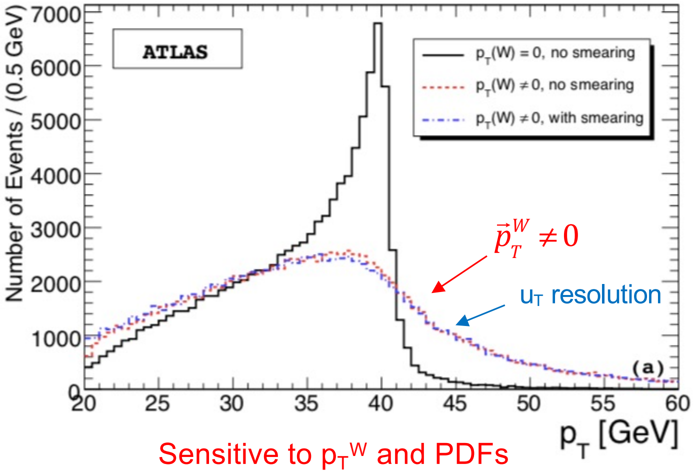

$\vec{p}_T^{\,W} \neq 0$

u_T resolution

Sensitive to p_T^W and PDFs

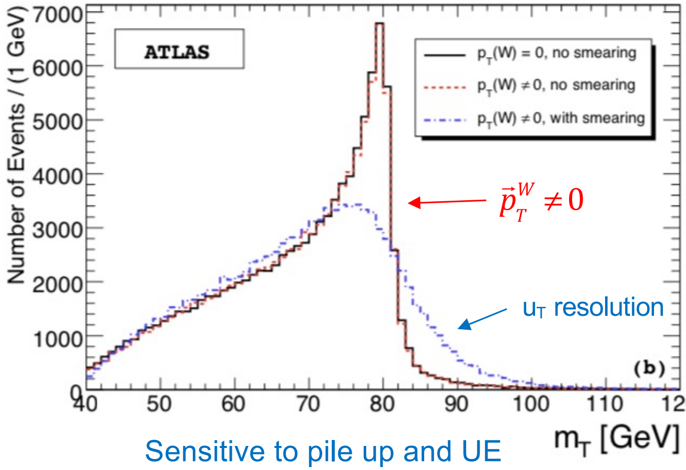

$\vec{p}_T^{\,W} \neq 0$

u_T resolution

Sensitive to pile up and UE

UE: underlying events

A closer look at the two distributions

- ☐ **W width and W transverse momentum effects.**

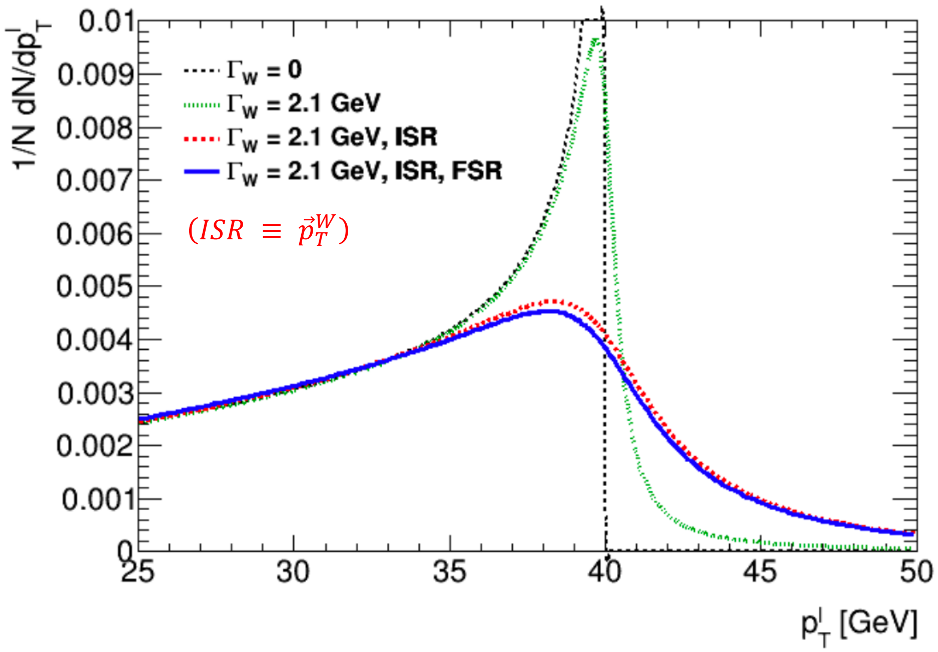

W width and W transverse momentum smear the jacobian peak of the lepton transverse momentum. The FSR has no significant impact.

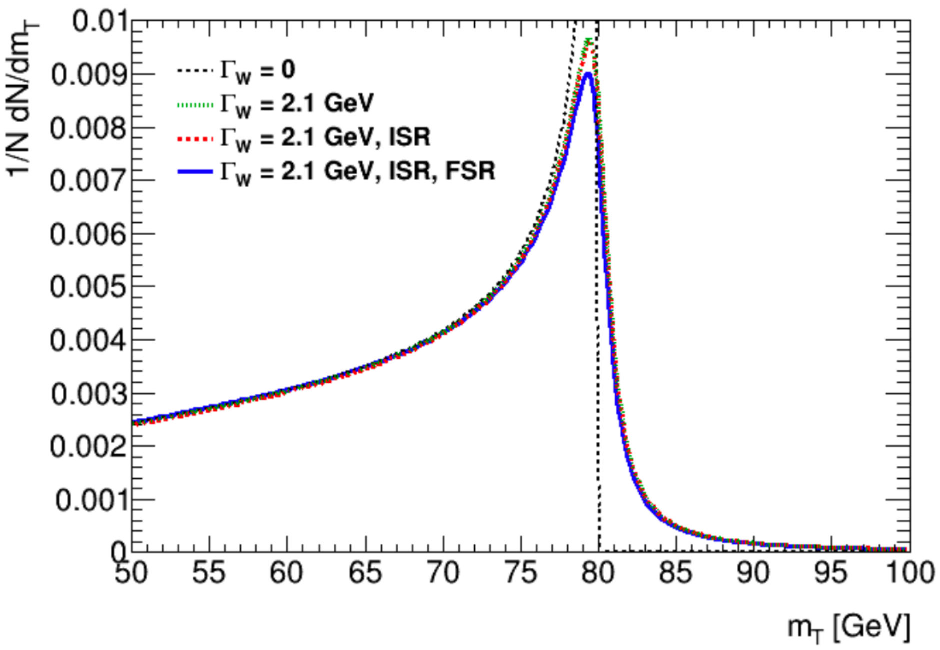

The W transverse mass is only slightly affected by W width and ISR has no significant effect, so it seems to be a more robust estimator of the W mass, but… wait for the detector effect.

A closer look at the two distributions

- ❑ **W width and W transverse momentum effects.**
- ❑ **Detector effects:**
  - ➢ **lepton calibration (~10^{-4}); recoil resolution (~5-15 GeV); acceptance (~ 15%)**

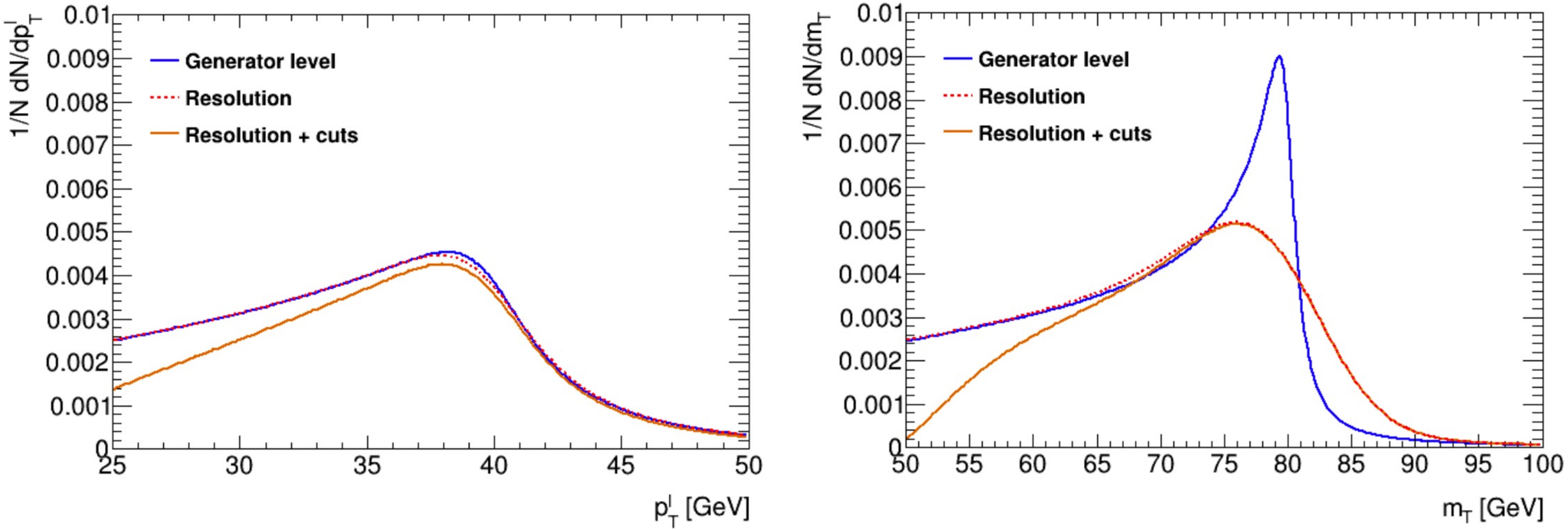

Lepton transverse momentum is slightly affected by detector effect since the lepton momentum is well measured and the recoil does not enter in this measurement.

On the contrary, W transverse mass depends heavily on the recoil resolution. So, the two measurements are really complementary.

Lepton energy/momentum scale calibration

❑Lepton momentum scales are measured using Z->ll and events and corrected in MC

❑ Scale known better than ~2 x 10-4 (except for muons at highest rapidity)

❑ Translates into an uncertainty on m_W of approx. 8-9 MeV

❑ Reconstruction, identification and trigger efficiency studied from Z sample, small effects for muon, of similar size as the energy scale for electrons.

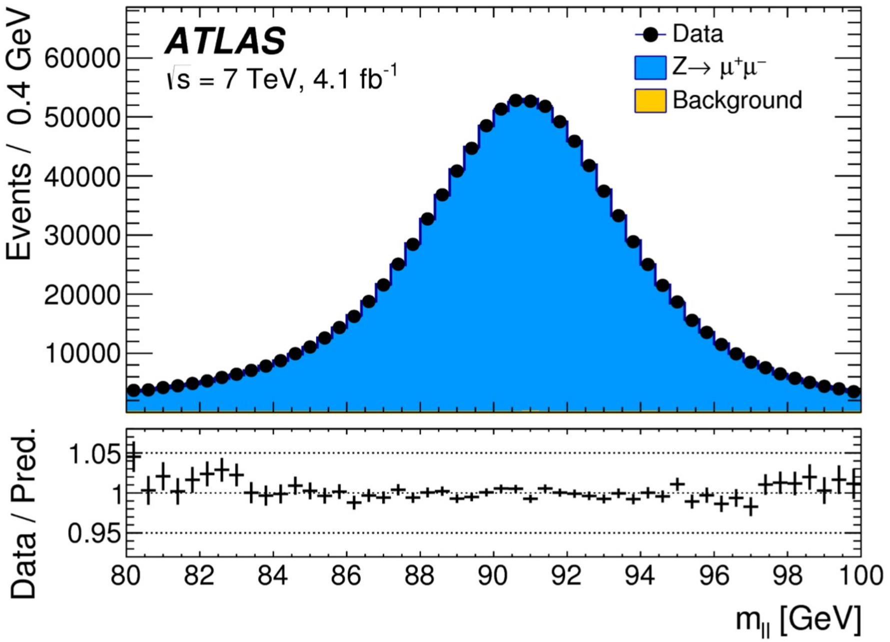

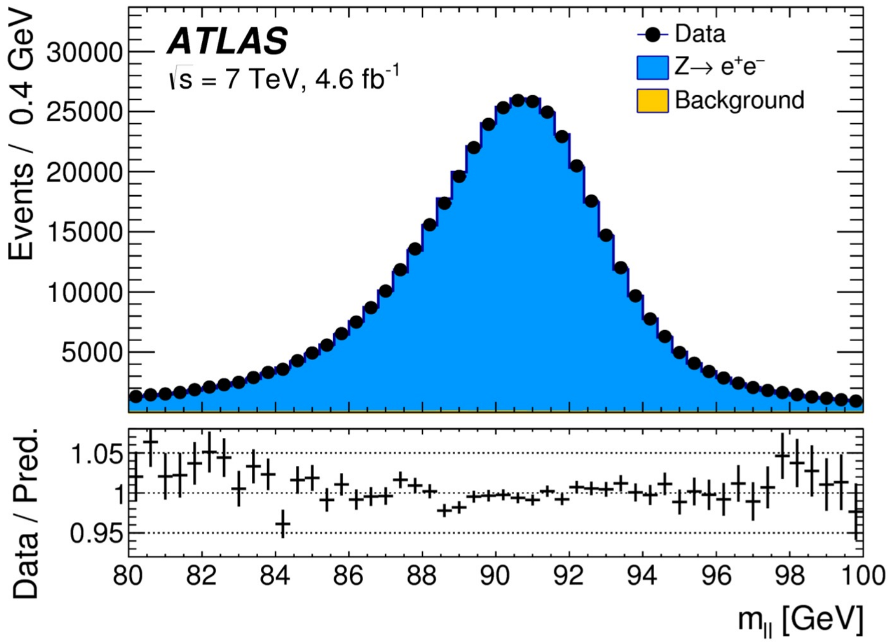

Recoil reconstruction

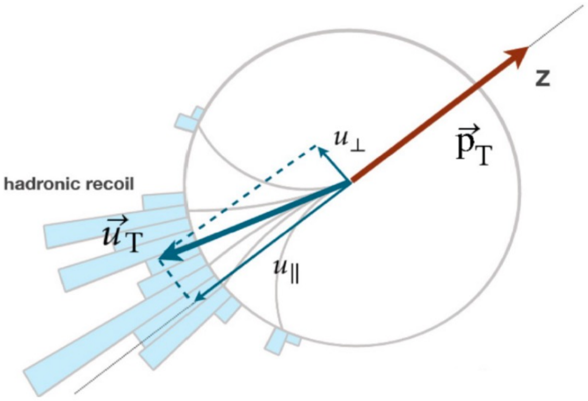

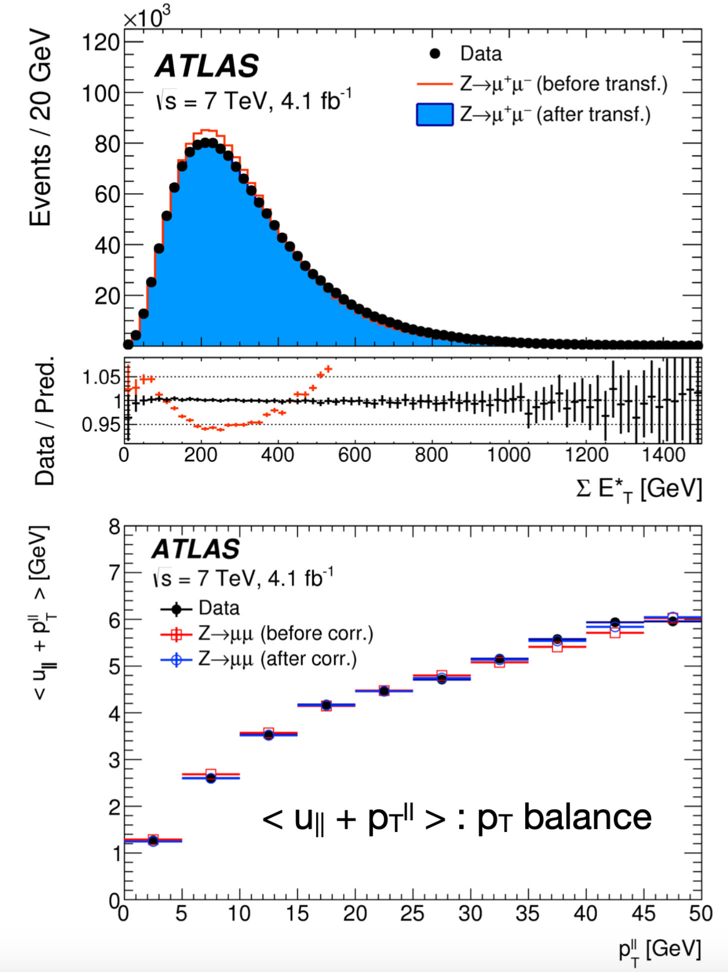

$< u_{||} + p_T^{ll} >$: p_T balance

❑ The reconstruction of the hadronic recoil depends strongly on the total E_T in the event, three corrections are needed:

1. Pileup distribution: data/MC equalisation.
2. Correction of residual differences in the total E_T distribution (activity mis-modeling)
3. Calibration obtained by the p_T balance in Z event

❑ Uncertainty on m_W ~ 11 MeV for m_T fits (smaller for p_T^l), dominated by the total E_T correction.

Z cross-checks

- ☐ Good data/MC agreement in Z→ ll
- ☐ Test: m_Z from fits to m_T and p_T^l
- ☐ Result consistent with m_Z within experimental uncertainties.

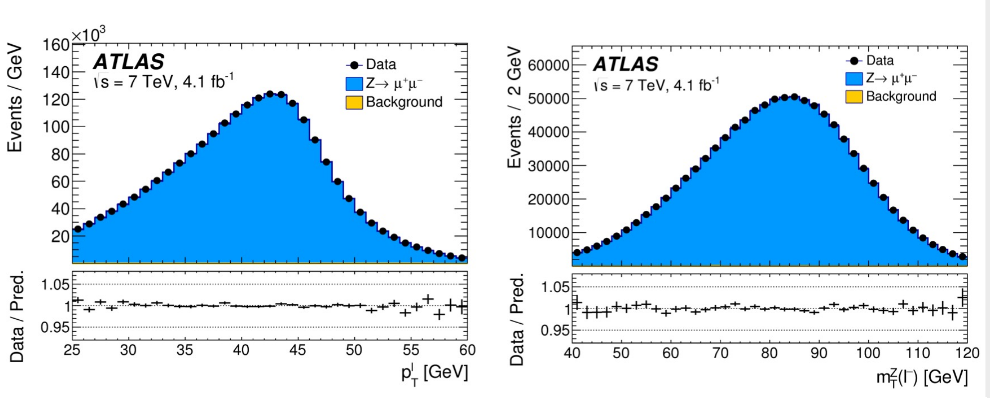

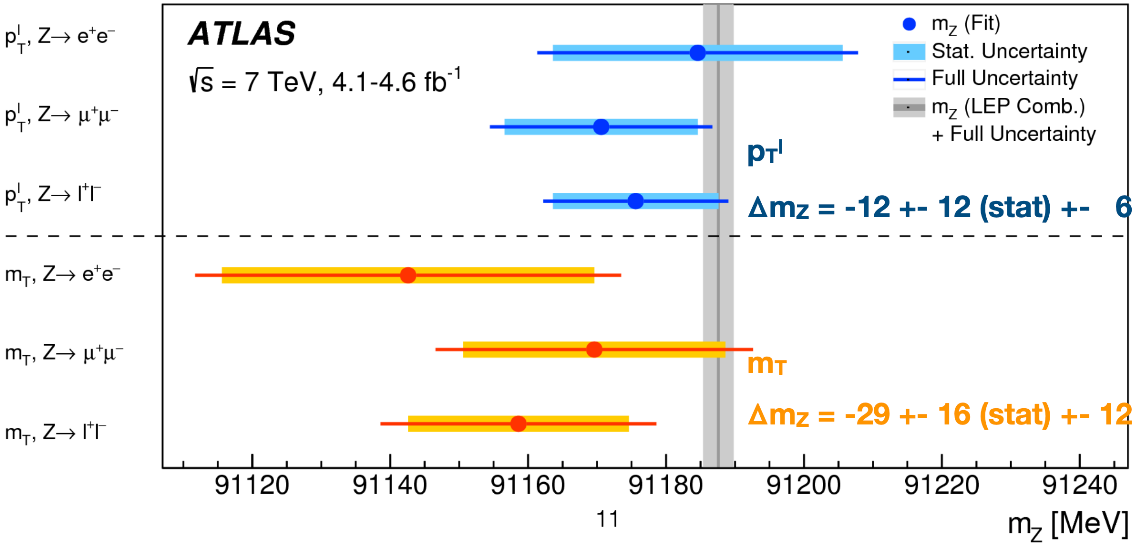

p_T^l

Δm_Z = -12 +- 12 (stat) +- 6 (syst) MeV

m_T

Δm_Z = -29 +- 16 (stat) +- 12 (syst) MeV

W Mass Fits

- Fit from MC templates with different mass generated in steps of 1 - 10 MeV
- 28 χ^2 fits, separeted for lepton type (μ,e), W charge (+/-), rapidity interval (4 for μ, 3 for e) and fit variable (m_T, p_T^l).
- Many other fits were performed as consistency checks by varying fit range, etc …

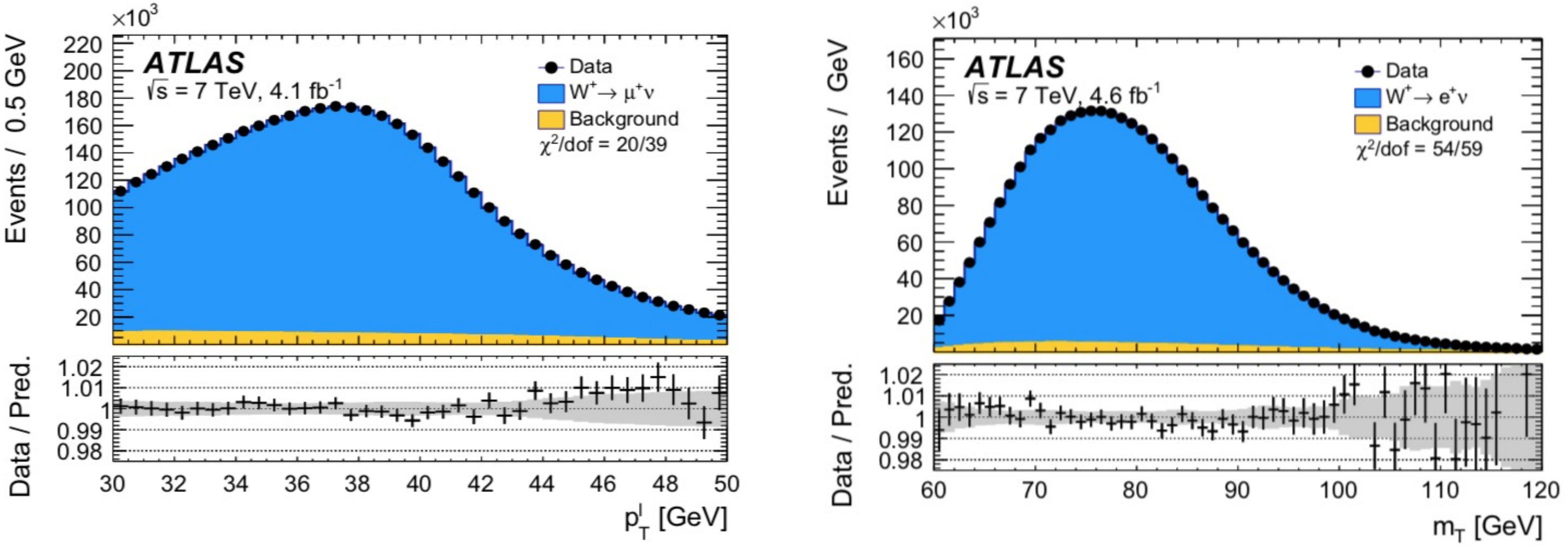

Combined result

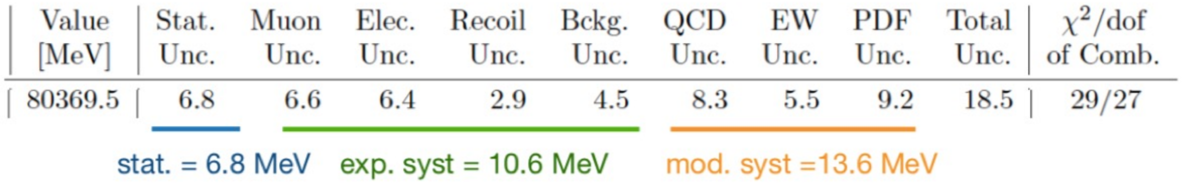

Value [MeV]	Stat. Unc.	Muon Unc.	Elec. Unc.	Recoil Unc.	Bckg. Unc.	QCD Unc.	EW Unc.	PDF Unc.	Total Unc.	χ^2/dof of Comb.
80369.5	6.8	6.6	6.4	2.9	4.5	8.3	5.5	9.2	18.5	29/27

stat. = 6.8 MeV exp. syst = 10.6 MeV mod. syst =13.6 MeV

M_W = 80370 ± 19 MeV

m_W = 80370 ± 7 (stat.) ± 18 (sys.) MeV

Comparison with previous results and SM

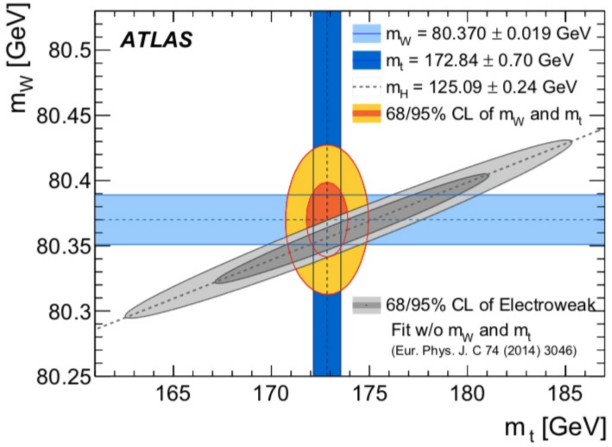

Good agreement with SM EWK fits (Gfitter)

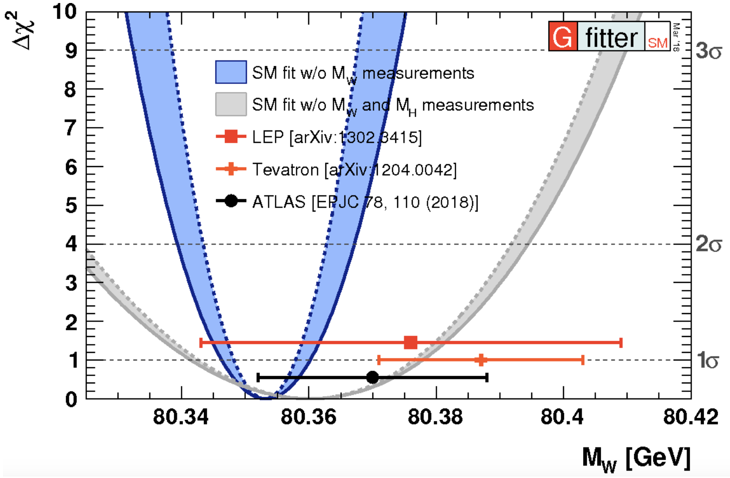

The ATLAS measurement has the same precision of the previous most precise single measurement (CDF) and is consistent with previous results.

From PDG 2019

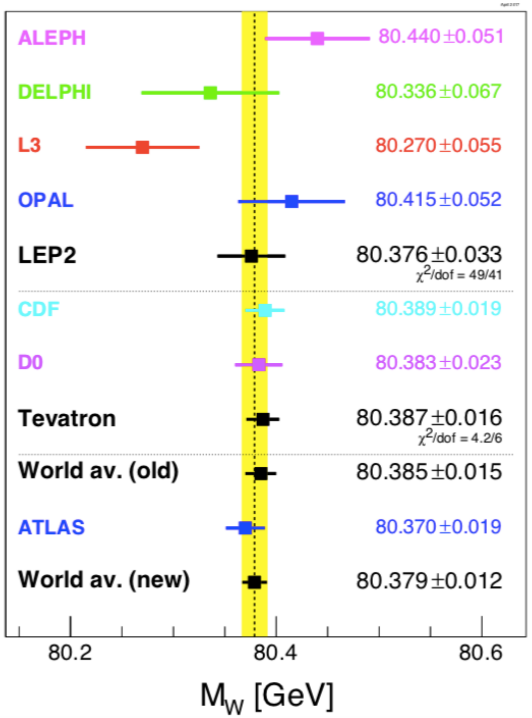

Prospects for M_W measurements

Major source of uncertainties are p_T^W (from QCD and PDF) and recoil (from pile-up)

exploit dedicated low pile up runs ($<\mu>\simeq 2$) to get p_T^W from data

ATLAS: ATL-PHYS-PUB-2017-021

Low-mu datasets: ATLAS/CMS 380/200 pb^{-1} at 13 TeV; 260/300 pb^{-1} 5 TeV

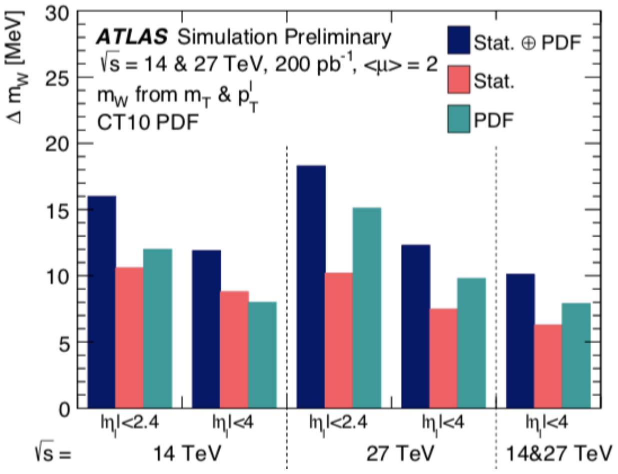

ATLAS-CMS High_Lumi perspective arxiv:1902.10229

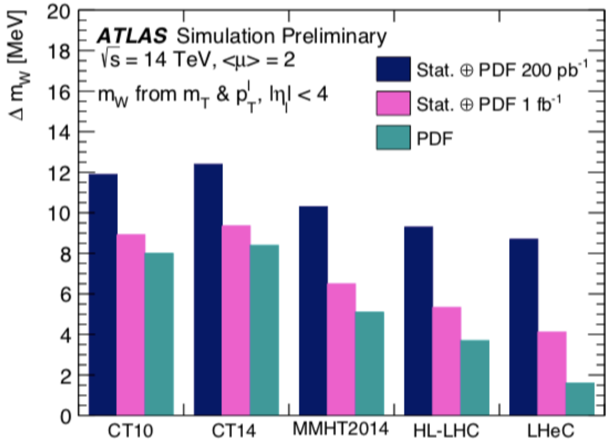

Different set of PDF functions

- ❑ **Total uncertainty of ~11 MeV with 200 pb-1 of data at each energy (~one week of data taking)**
- ❑ **With HL-LHC PDF and 1 fb^{-1} we could reach of precision of 6 MeV**
- ❑ **With Future LHeC PDF set from DIS data we could aim at a precision of 4 MeV**

CAVEAT: experimental systematics are not included, but they are of statistical nature and could be reduced

M_W at CDF

Let’s open a parenthesis

FERMILAB and the Tevatron

Fermilab and the accelerator complex

Fermilab and accelerators

Fermilab

- **National Accelerator Laboratory** founded 1967
  - Named after **Enrico Fermi** and dedicated (“Fermilab”) in 1974
- Central facility: proton synchrotron “Main Ring”
  - 2π km circumference and initial energy of 200 GeV (1972)
  - Used for fixed target experiments
- Higher energy with **superconducting magnets**
  - **First** superconducting synchrotron
  - Initial name “Energy Doubler” or “Energy Saver”. **512 GeV** (1983) ; then **800 GeV** (1984) and **900 GeV** (1986)
- **Antiproton source** added in 1985
  - Stochastic cooling **built on success of SppS at CERN**
  - First **collisions** at 1.6 TeV in 1985, 1.8 TeV in 1986: **TeVatron**
- **Run II (2001 – 2011)**
  - beam energy: **980 GeV**
  - main ring in another tunnerl

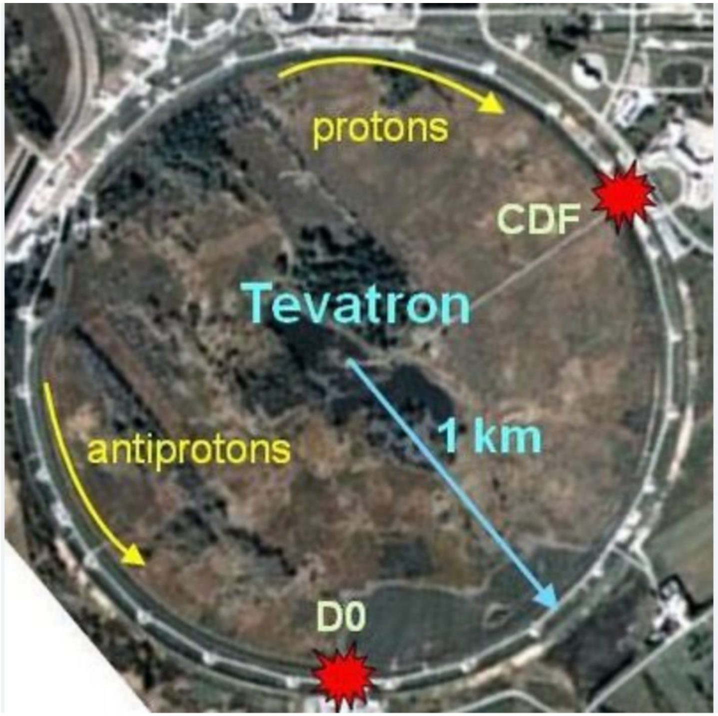

Timeline

1983
W and Z bosons
discovered at
UA1 and UA2

1985
First collisions
at Tevatron

1988-1989
Tevatron Run 0

1989
LEP first
collisions

1992
Tevatron Run I
begins

1992
HERA
collisions
begin

1995
Top discovery

1996
Tevatron Run I
ends

2000
LEP collisions
end

2001
Tevatron Run II
begins

2007
HERA
collisions end

2008
LHC first
collisions

2011
Tevatron Run II
ends

2012
Higgs boson
discovered at
ATLAS and CMS

Tevatron

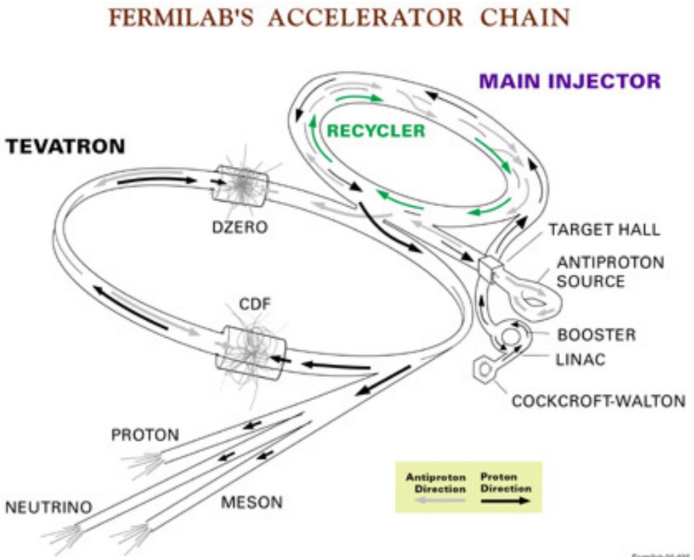

Fermilab is placed in natural areas, which are designated as a National Environmental Research Park. It is a federal area.

Some of Fermilab inhabitants

Fermilab's first director brought bison to the lab in 1969 as a symbol of the history of the Midwestern prairie and the laboratory's research at the frontiers of particle physics.

First baby bison of 2021

How to get to Fermilab !

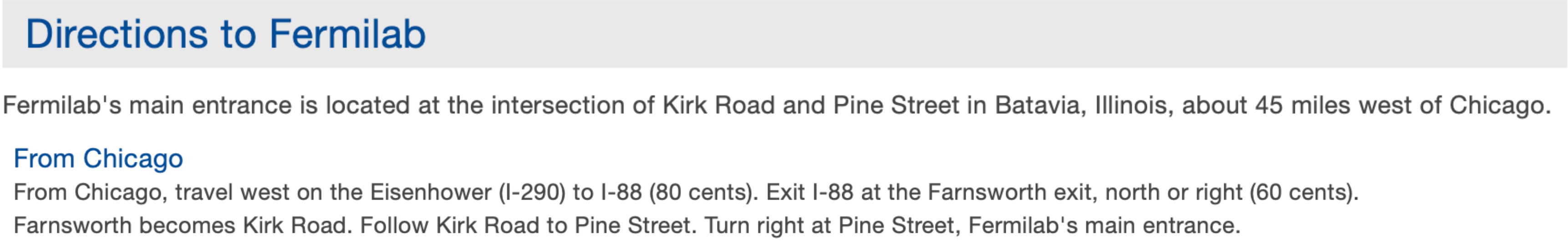

Directions to Fermilab

Fermilab's main entrance is located at the intersection of Kirk Road and Pine Street in Batavia, Illinois, about 45 miles west of Chicago.

From Chicago

From Chicago, travel west on the Eisenhower (I-290) to I-88 (80 cents). Exit I-88 at the Farnsworth exit, north or right (60 cents). Farnsworth becomes Kirk Road. Follow Kirk Road to Pine Street. Turn right at Pine Street, Fermilab's main entrance.

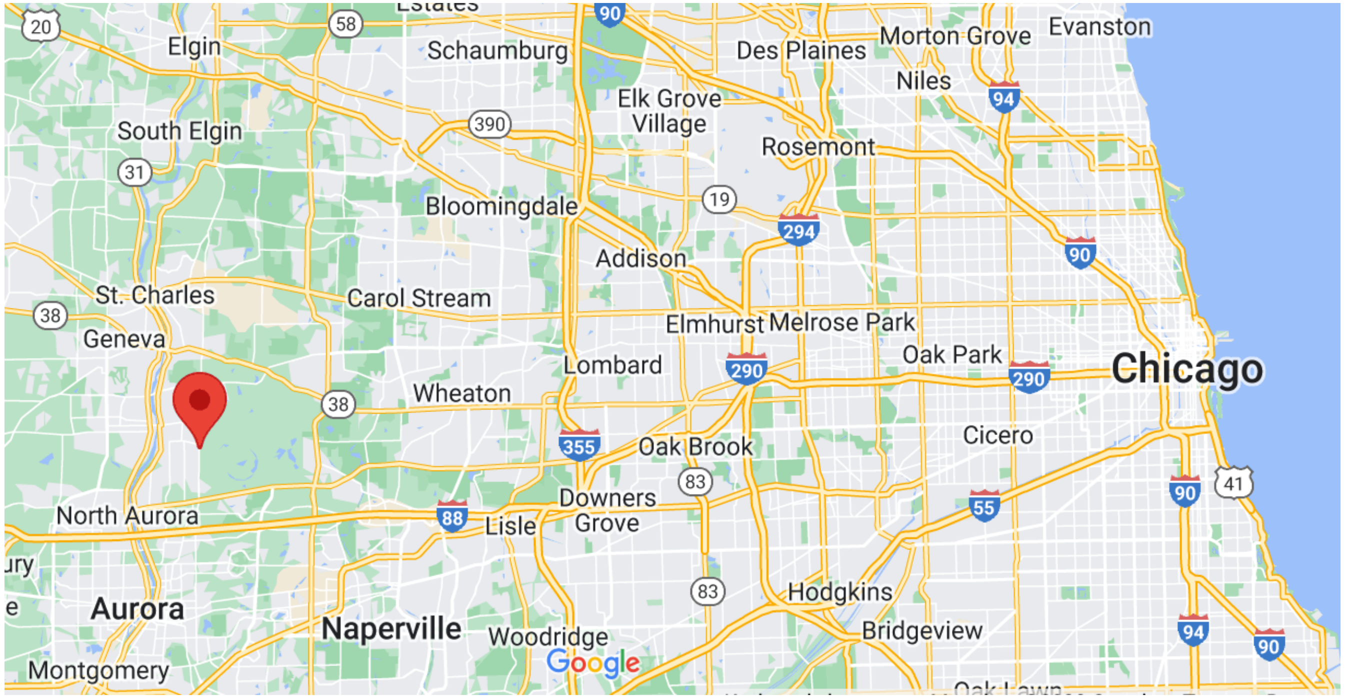

Tevatron experiments: CDF and D0

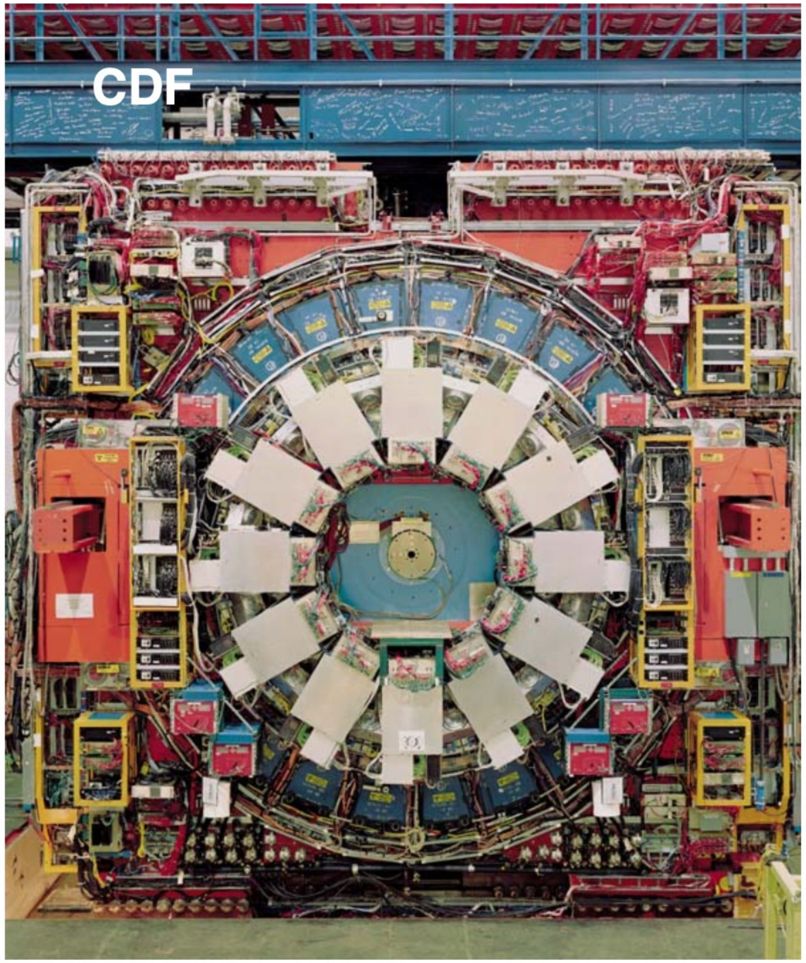

Early Tevatron results

- Tevatron first run 1988-1989
  - Retroactively named “Run 0”
  - 4 pb^{-1} lumi delivered to CDF
    - DØ still under construction at this time

- Ability to measure W and Z bosons?
  - Precision measurements *seemed* well out of reach
    - Limiting factor: calorimeter energy resolution
    - Breakthrough: **calibrating with E/p** (including tracker)

- SLC starting up around the same time
  - Who would be first to see Z bosons in the Western Hemisphere?

New York Times 19-Jul-1988

Search Quickens for Ultimate Particles

Two new American colliders start up, with a European one soon to follow.

By MALCOLM W. BROWNE

FOR the first time in five years, high-energy physicists in the United States are poised to seize a commanding lead from colleagues in Europe as they bring powerful new particle accelerators to bear on mysteries shrouding the ultimate basis of matter.

Full-scale experiments have begun at America's two largest accelerator laboratories, in California and Illinois, both of which recently completed machines even more powerful than European counterparts.

The Stanford Linear Collider (S.L.C.) in California, the Stanford Linear Accelerator Center's new entry in the high-energy physics race, began its ambitious experimental program last month. The machine hurls clusters of negatively charged electrons into oncoming clusters of their antimatter counterparts, positrons. Scientists at Stanford hope these collisions will soon produce large numbers of Z^0, or Z-zero, particles — ephemeral particles whose properties illuminate some of the enigmas that underlie material existence.

At America's other leading high-energy accelerator, the Fermi National Accelerator Laboratory (Fermilab) in Batavia, Ill., scientists are also expecting important results soon. "We have just started our first real series of experiments using the new Tevatron collider," said Dr. Leon M. Lederman, its director.

One object of their work is to make progress toward testing the theory that everything in nature is made up of some combination of 16 ingredients: four classes of vector particles, six massless leptons and six heavier quarks, one of which, called the top quark, has not yet been detected.

"We think we will soon have the top quark in the bag; that's the missing quark physicists have been looking for," he said. "But in this business you learn to keep your fingers crossed."

But the technological supremacy the S.L.C. and Tevatron offer may be short-lived. A Western European scientific consortium is nearing completion of an underground accelerator 17 miles in circumference, by far the largest such machine in the world. Last Wednesday scientists successfully tested the first two-mile segment of the European Large Electron-Positron collider, prompting acclaim from scientists at competing institutions in the United States. The LEP will not be ready for experiments until 1990, however, and until then physicists in the United States are pressing their temporary advantage.

Much farther down the road, American physicists hope to build an accelerator about 52 miles in circumference, the Superconducting Supercollider, which would dwarf even the European LEP ring. The cost of the S.S.C. is so daunting, however, that even some of its proponents have begun to express doubts that it will ever be paid for. Meanwhile, the leaders of American laboratories are focusing on current developments.

"This will be a very interesting summer but a very tense one," Dr. Burton Richter, director of the Stanford Linear Accelerator Center and winner of a Nobel prize in physics, said in an interview. "In the next few weeks we hope to start producing Z^3 particles, one of the types of particle the S.L.C. was designed to make, but you never can be certain of a result until you achieve it."

"While we wait," he added with a laugh, "I've asked my department directors to go to a synagogue or a church to pray for divine help."

Dr. Richter's uneasiness stems from the fact that his S.L.C. represents an accelerator design that has never been tried. A conventional particle collider spins counter-rotating clusters of particles around a ring. In the machine Dr. Richter conceived and built, however, the opposing particle beams, each one much thinner than a human hair, are initially accelerated together down a straight, two-mile-long linear accelerator. At the end of the line, the two beams diverge and are ducted around two semi-circular arms resembling crab claws. The tips of the claws point toward each other, aiming the two beams directly at each other.

The Z^0 particle that scientists hope the S.L.C. will soon produce in large numbers is a very heavy, short-lived particle that conveys the weak nuclear force from one subnuclear particle to another. (The weak force is responsible for one form of radioactive nuclear decay.)

Five years ago, physicists in Europe created and observed Z^0 particles and two other carriers of the weak force, the W+ (W-plus) and W-

Continued on Page C13

Fermi National Accelerator Laboratory

Aerial view of Fermi National Accelerator Laboratory in Batavia, Illinois, showing circular main accelerator.

The Design of the Future?

Stanford's new linear collider uses an unusual design, avoiding some of the energy losses of the more common circular design. Electrons are fired into the system, and some are diverted to bombard a tungsten target, creating positrons, their antimatter equivalents. The beams, which are shaped in damping rings, end their two-mile journey when magnets bend them around opposing arms. The beams collide in a detector that records resulting particles.

Steve Hart/The New York Times

Tevatron Run I (1992-1996): “top” result

- 140 pb^{-1} of 1.8 TeV collisions delivered to both experiments
  - DØ fully online in 1992
- The top quark
  - Evidence in 1994
  - **Discovery** by both experiments in 1995

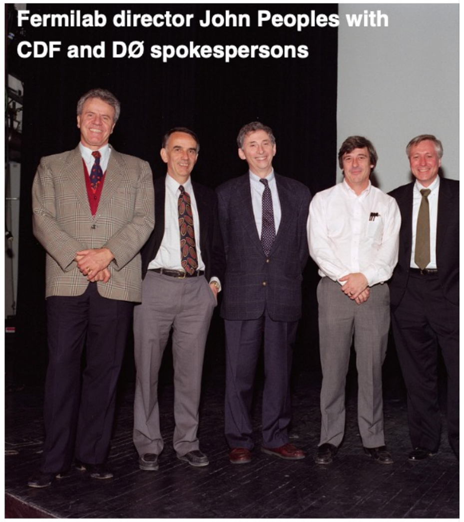
Fermilab director John Peoples with CDF and DØ spokespersons

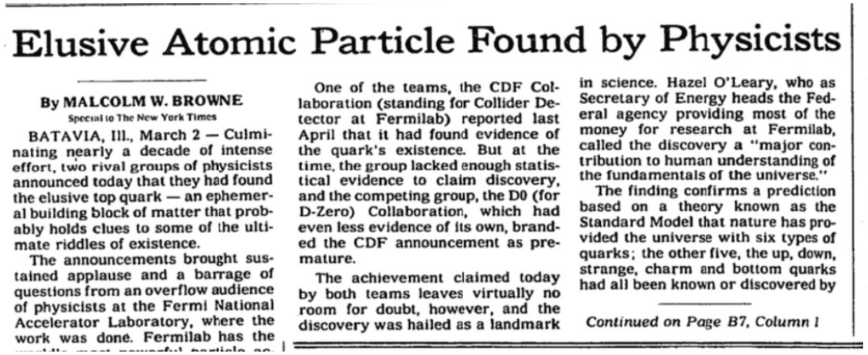

Elusive Atomic Particle Found by Physicists

By MALCOLM W. BROWNE

Special to The New York Times

BATAVIA, Ill., March 2 — Culminating nearly a decade of intense effort, two rival groups of physicists announced today that they had found the elusive top quark — an ephemeral building block of matter that probably holds clues to some of the ultimate riddles of existence.

The announcements brought sustained applause and a barrage of questions from an overflow audience of physicists at the Fermi National Accelerator Laboratory, where the work was done. Fermilab has the

One of the teams, the CDF Collaboration (standing for Collider Detector at Fermilab) reported last April that it had found evidence of the quark's existence. But at the time, the group lacked enough statistical evidence to claim discovery, and the competing group, the D0 (for D-Zero) Collaboration, which had even less evidence of its own, branded the CDF announcement as premature.

The achievement claimed today by both teams leaves virtually no room for doubt, however, and the discovery was hailed as a landmark in science. Hazel O'Leary, who as Secretary of Energy heads the Federal agency providing most of the money for research at Fermilab, called the discovery a "major contribution to human understanding of the fundamentals of the universe."

The finding confirms a prediction based on a theory known as the Standard Model that nature has provided the universe with six types of quarks; the other five, the up, down, strange, charm and bottom quarks had all been known or discovered by

Continued on Page B7, Column 1

Tevatron Run II

- Major upgrade after Run I ended (1996)
  - Increase in peak luminosity from 10^{30} cm^{-2} s^{-1} to over **$4\mathrm{x}10^{32}$ cm^{-2} s^{-1}**
  - Increase of beam energy from 900 GeV to **980 GeV**
- Construction of **Main Injector**
  - New 150 GeV accelerator stage
  - Essential in increase in luminosity
  - Still used at Fermilab for neutrino experiments
- Significant upgrades to both CDF and DØ
  - e.g. upgraded trackers and triggers
  - Solenoid magnet in DØ
- Run II delivered data from **2001-2011**
  - **12 fb^{-1}** to each experiment

Main Injector

Main Injector tunnel

CDF Central Outer Tracker installation

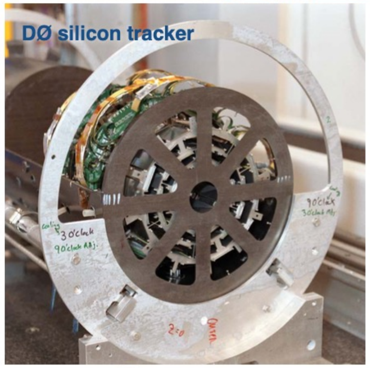

DØ silicon tracker

W boson mass: toward unprecedented precision

- LEP set the standard by 2004
  - Uncertainty: 33 MeV combined (51 MeV single best)
- CDF/DØ goals
  - Exceed single best LEP measurement
    - ~0.2 fb^{-1} CDF, ~1 fb^{-1} DØ
  - Exceed world average with single measurement
    - ~2 fb^{-1} CDF, ~5 fb^{-1} DØ

Unblinding first Run II W mass measurement at CDF
16 Dec 2006

First Run II measurements

80413 ± 48 MeV (CDF, 2006)

80401 ± 43 MeV (DØ, 2009)

PRL **103** 141801 (2009)

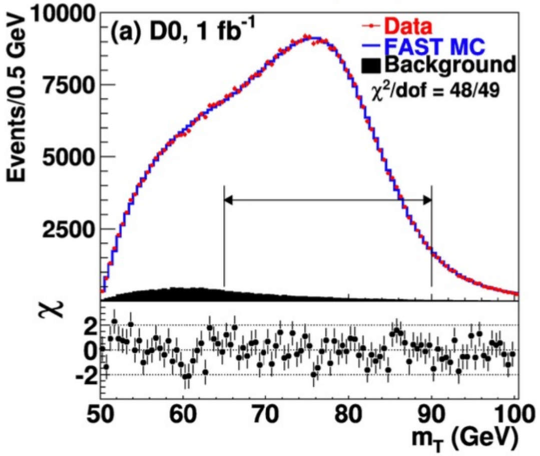

PRL **99** 151801 (2007)

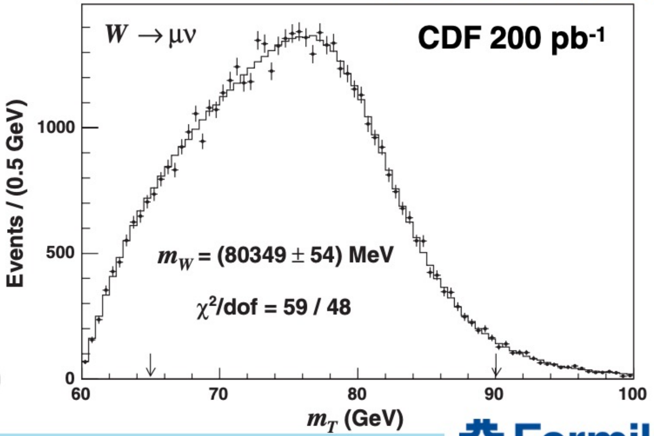

nb. CDF e+μ, DØ e only

W boson mass: achieving unprecedented precision

Calibrating with well-known resonances:
J/ψ,Υ, Z at CDF; Z at DØ

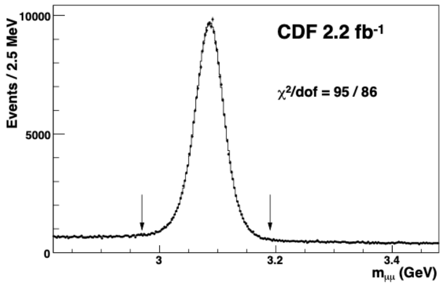

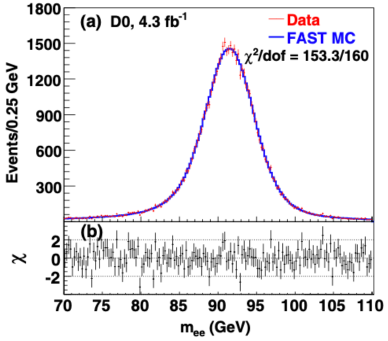

Calibrating hadronic recoil with Z, validate with W

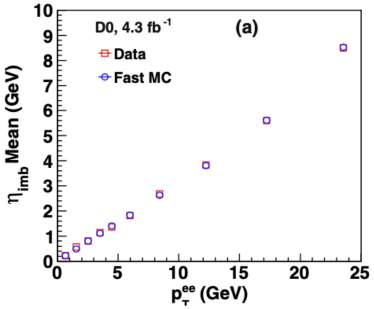

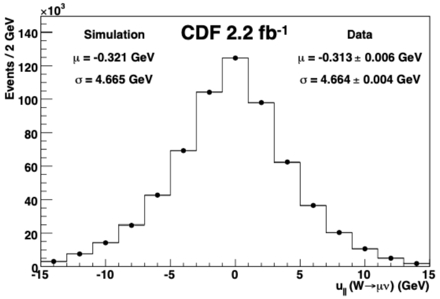

Fits to m_T, lepton p_T, missing p_T,
Combined for final result

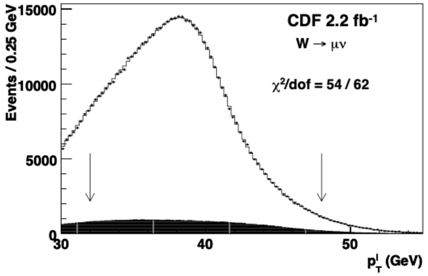

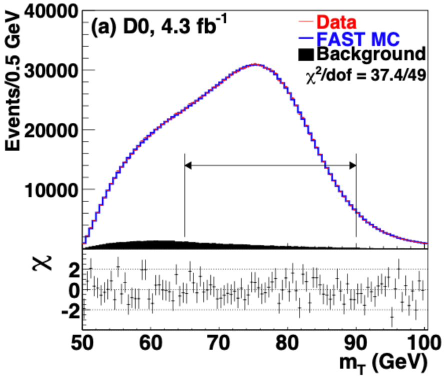

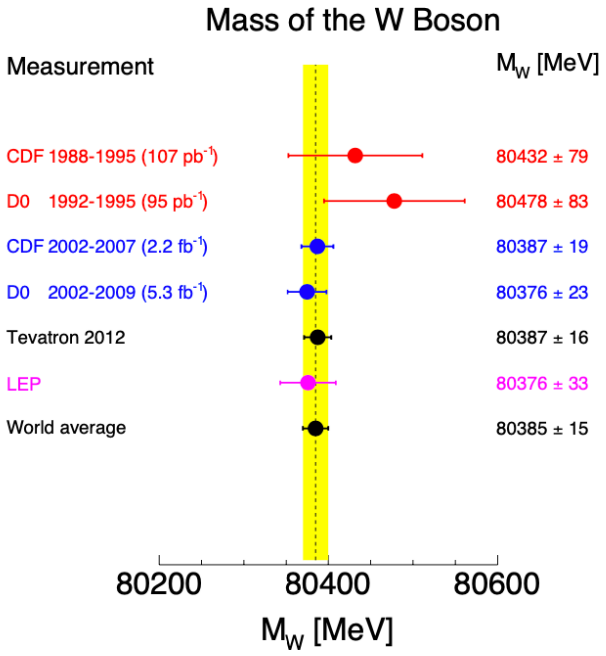

CDF: PRD **89**, 072003 (2014)
DØ: PRD **89**, 012005 (2014)
CDF+DØ: PRD **88**, 052018 (2013)

W boson mass: one final surprise?

- CDF goal with the **full** Tevatron dataset
  - Once again exceed world average precision
  - < 10 MeV total uncertainty
    - Nearly every systematic uncertainty constrained by data

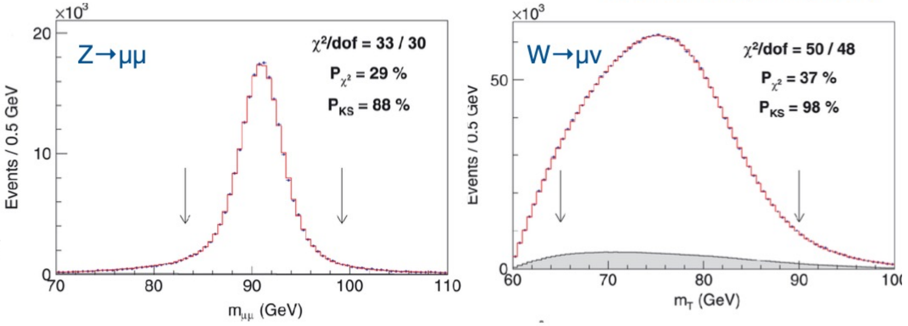

Science **376**, 170 (2022)

- Powerful validation: independent Z mass
  - M_Z = 91192.0±7.5 MeV (muons)
    - Single most precise hadron collider measurement!

- **M_W =** Wait a few slides

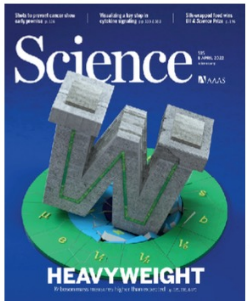

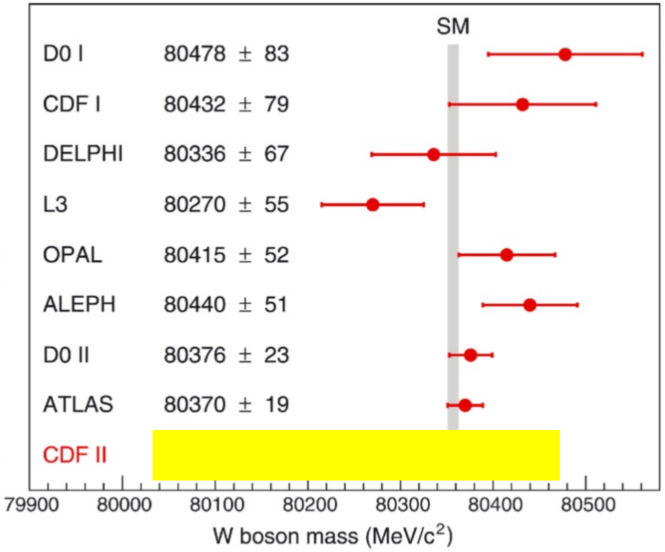

Let’s close the parenthesis }

…. but ….

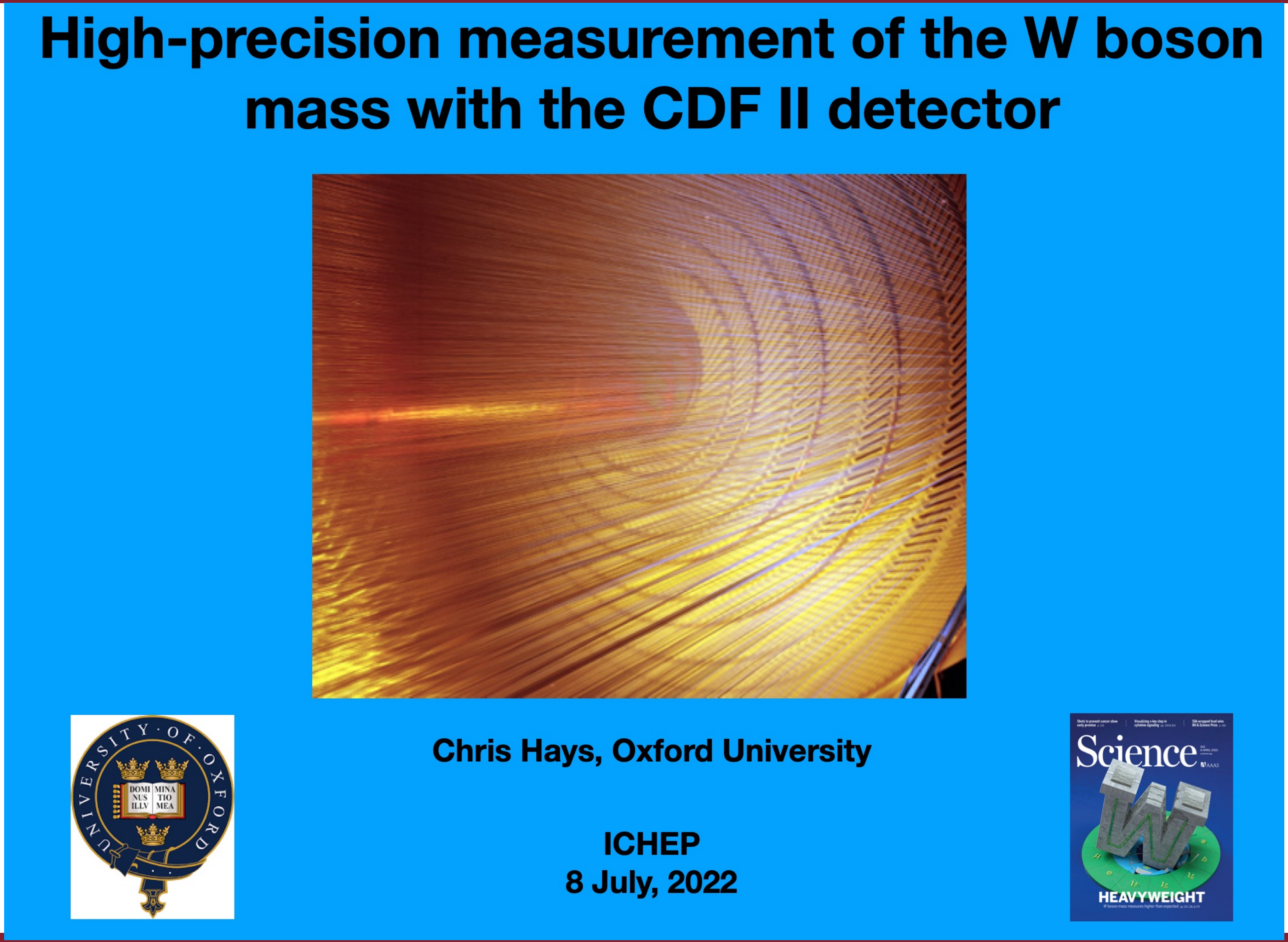

High-precision measurement of the W boson mass with the CDF II detector

Chris Hays, Oxford University

ICHEP
8 July, 2022

CDF II measurement of the W boson mass

$\sqrt{s} = 1.96$ TeV proton-antiproton collisions from the Fermilab Tevatron

Measurement uses complete Tevatron Run II data set

8.8 fb^{-1} of integrated luminosity

4.2 M selected W boson candidates

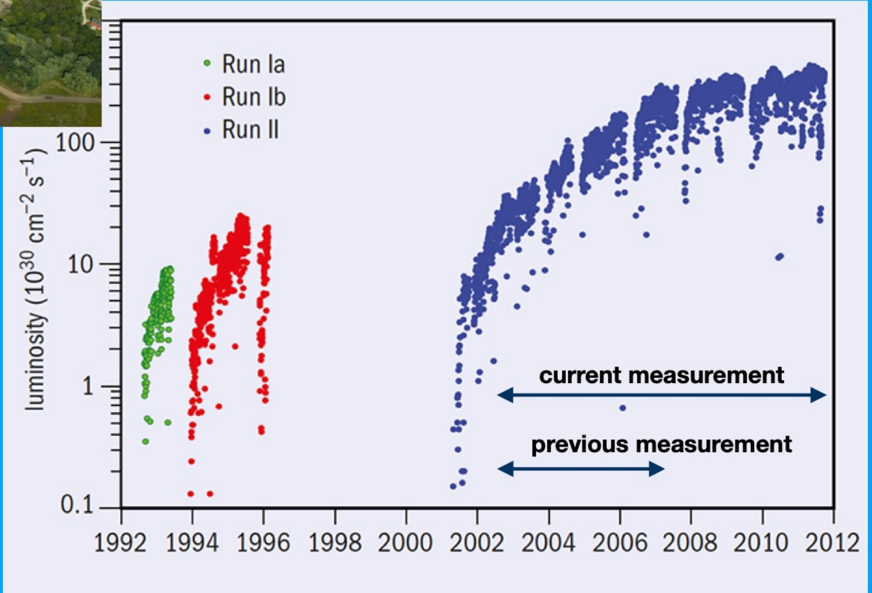

CDF II measurement of the W boson mass

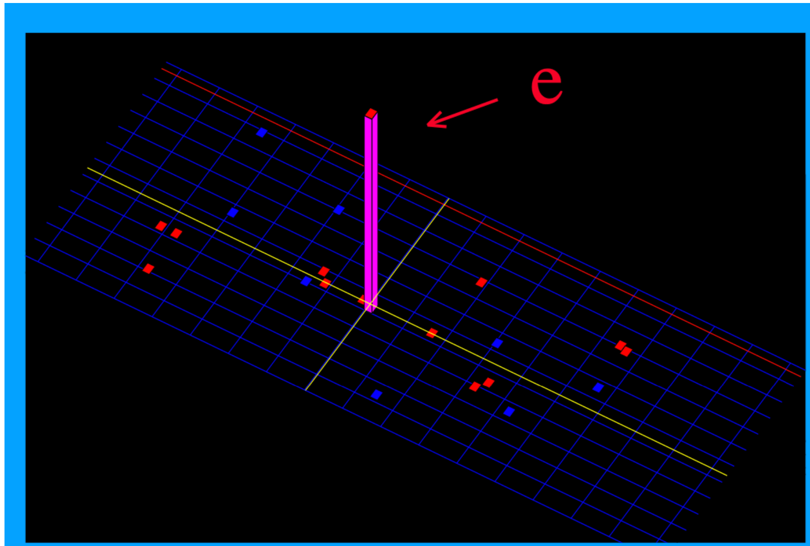

W bosons identified in their decays to $e\nu$ and $\mu\nu$

Mass measured by fitting template distributions of transverse momentum and mass

$$m_T = \sqrt{2 p_T^l \not{p}_T \left(1 - \cos\Delta\phi\right)}$$

$$\vec{\not{p}}_T = -(\vec{p}_T^{\,l} + \vec{u}_T)$$

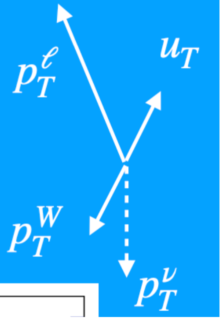

Muon momentum calibration

Final step is to measure the Z boson mass

$$M_Z = 91\ 192.0 \pm 6.4_{stat} \pm 4.0_{sys}\ \text{MeV}$$

Result blinded with [-50,50] MeV offset until previous steps were complete
Combine all measurements into a final charged-track momentum scale

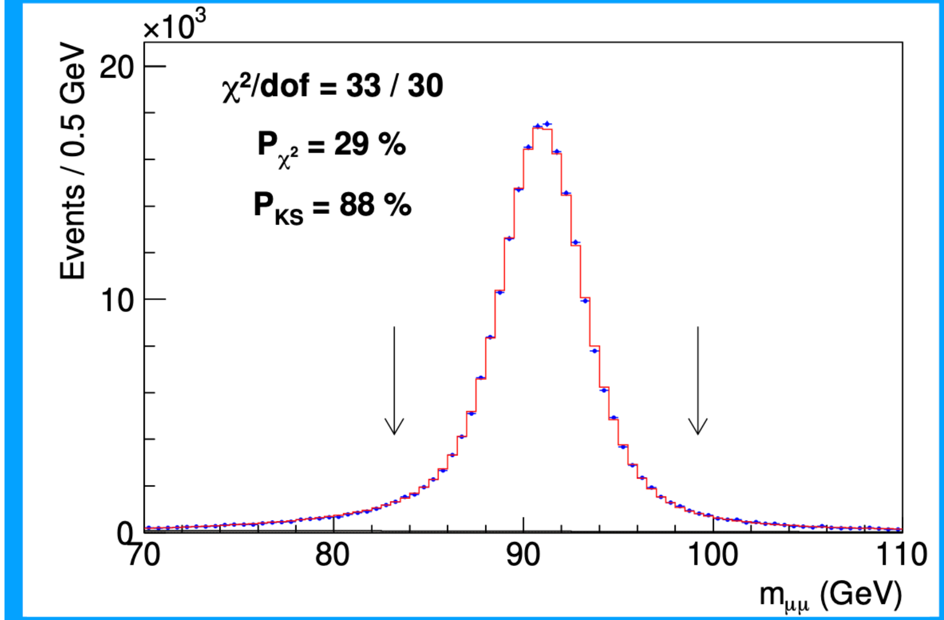

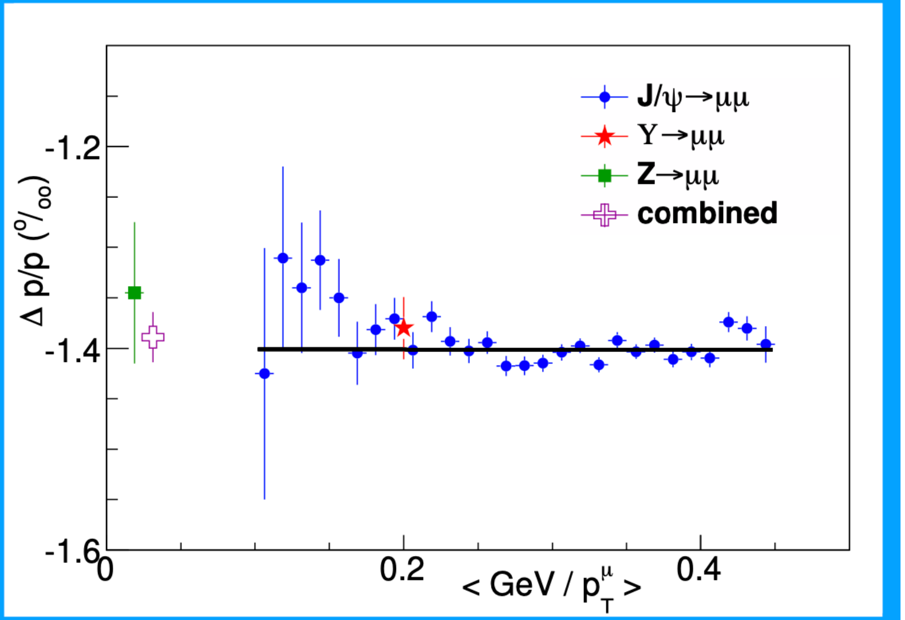

Electron momentum calibration

Second step is the measurement of the Z boson mass

$$M_Z = 91\ 194.3 \pm 13.8_{stat} \pm 7.6_{sys}\ \mathrm{MeV}$$

Same blinding as for muon channel

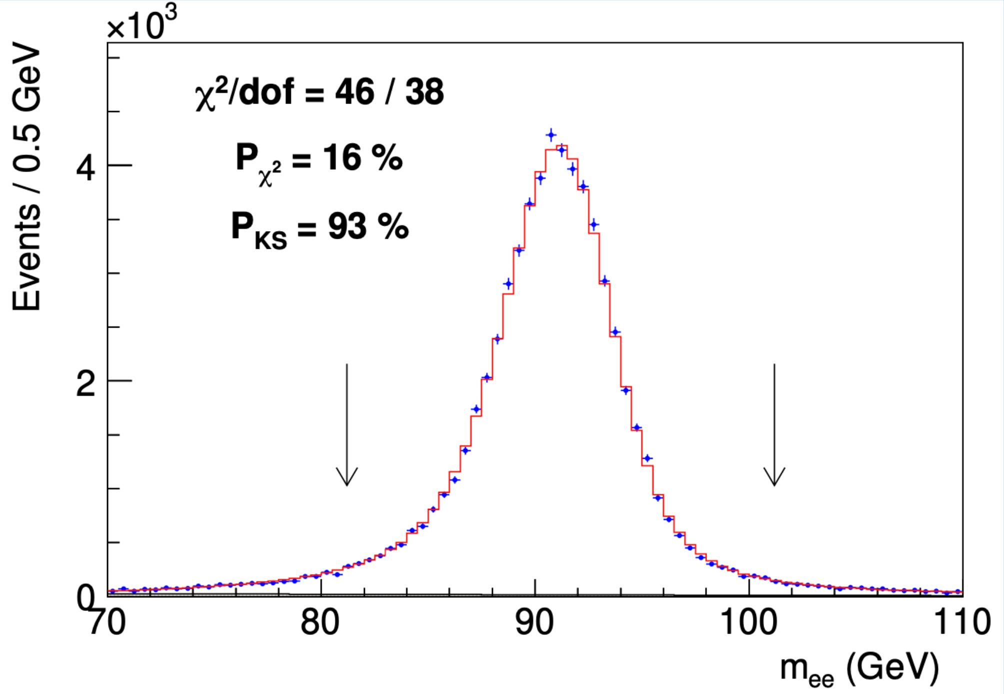

Recoil momentum calibration

First step is the alignment of the calorimeters

Misalignments relative to the beam axis cause a modulation in the recoil direction

Alignment performed separately for each run period using minimum-bias data

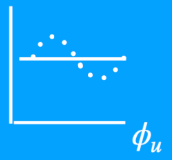

Second step is the reconstruction of the recoil

Remove towers traversed by identified leptons

Remove corresponding recoil energy in simulation using towers rotated by 90°

validate using towers rotated by 180°

Third step is the calibration of the recoil response

Check calibration using ratio of recoil magnitude to p_T^Z along direction of p_T^Z (R_{rec})

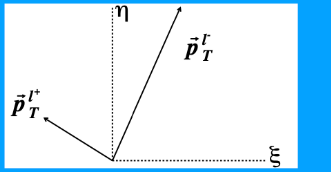

Fourth step is the calibration of the recoil resolution

Includes jet-like energy and angular resolution, additional dijet fraction term, and pileup

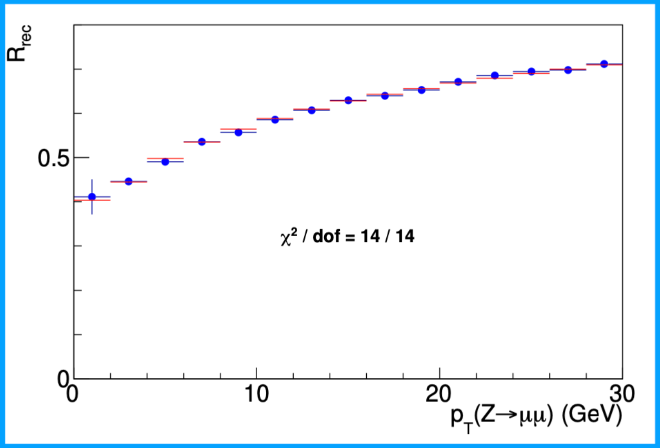

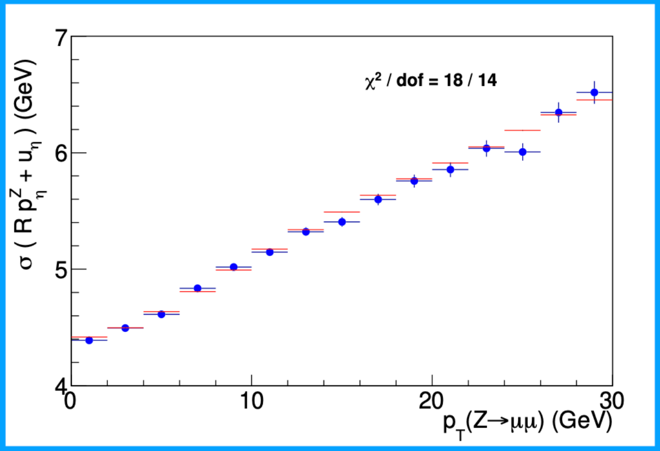

Mass measurement distributions

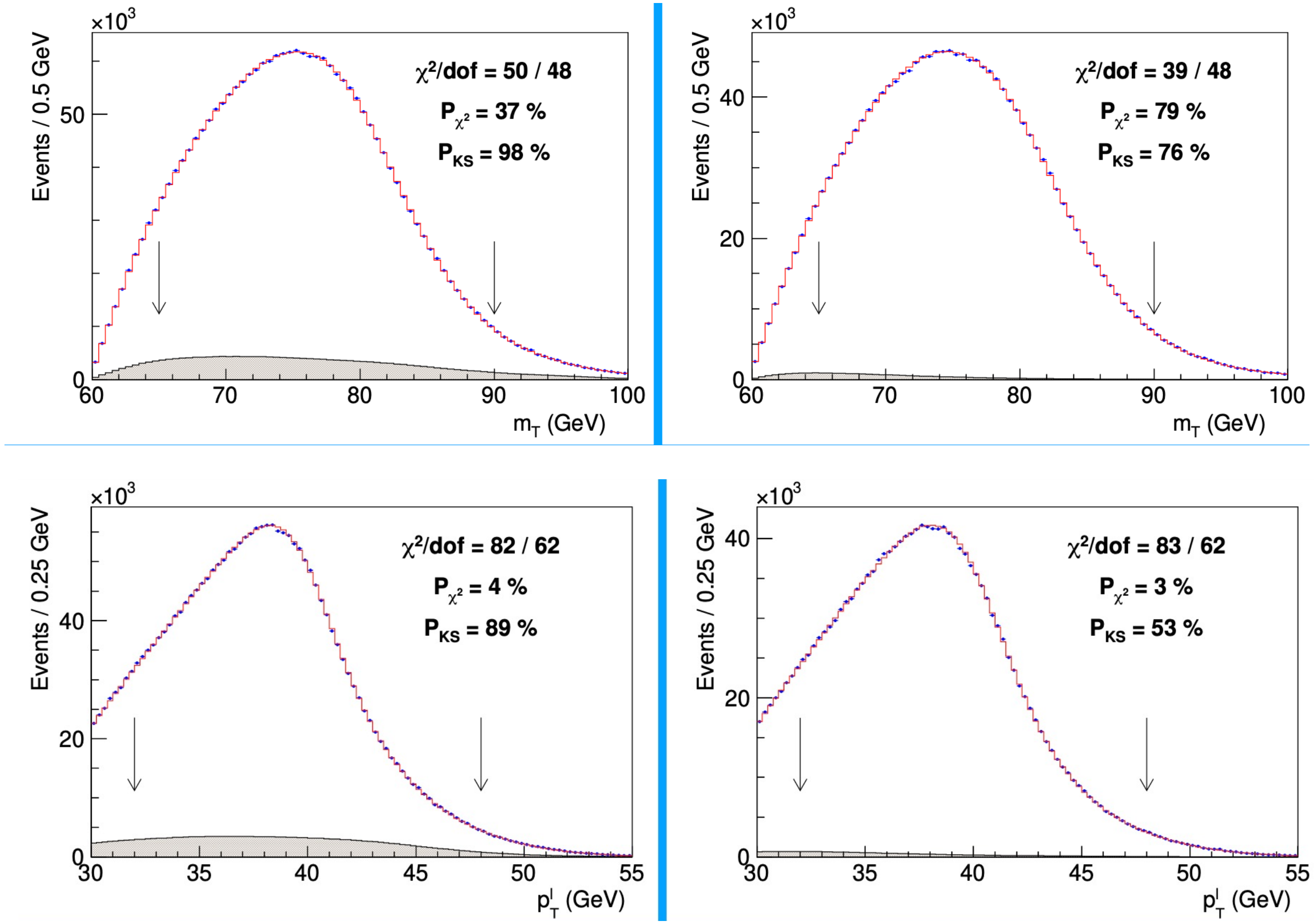

New CDF W boson mass measurement

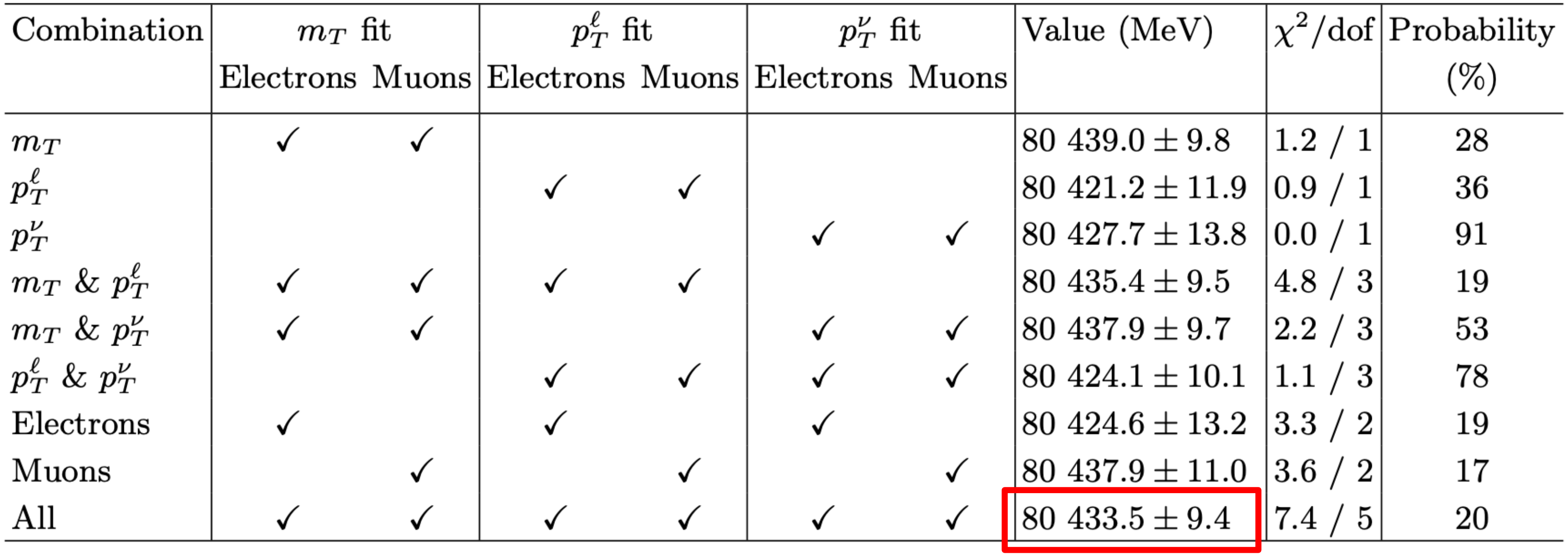

Combination	m_T fit		p_T^ℓ fit		p_T^ν fit		Value (MeV)	χ^2/dof	Probability (%)
	Electrons	Muons	Electrons	Muons	Electrons	Muons			
m_T	✓	✓					$80\,439.0 \pm 9.8$	1.2 / 1	28
p_T^ℓ			✓	✓			$80\,421.2 \pm 11.9$	0.9 / 1	36
p_T^ν					✓	✓	$80\,427.7 \pm 13.8$	0.0 / 1	91
m_T & p_T^ℓ	✓	✓	✓	✓			$80\,435.4 \pm 9.5$	4.8 / 3	19
m_T & p_T^ν	✓	✓			✓	✓	$80\,437.9 \pm 9.7$	2.2 / 3	53
p_T^ℓ & p_T^ν			✓	✓	✓	✓	$80\,424.1 \pm 10.1$	1.1 / 3	78
Electrons	✓		✓		✓		$80\,424.6 \pm 13.2$	3.3 / 2	19
Muons		✓		✓		✓	$80\,437.9 \pm 11.0$	3.6 / 2	17
All	✓	✓	✓	✓	✓	✓	$80\,433.5 \pm 9.4$	7.4 / 5	20

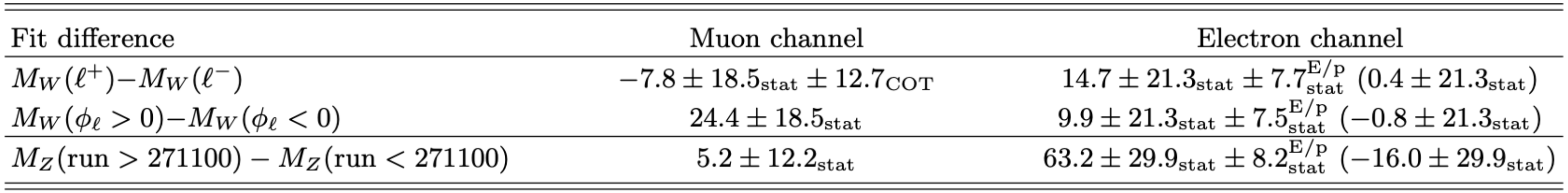

Fit difference	Muon channel	Electron channel
$M_W(\ell^+) - M_W(\ell^-)$	$-7.8 \pm 18.5_{\text{stat}} \pm 12.7_{\text{COT}}$	$14.7 \pm 21.3_{\text{stat}} \pm 7.7^{\text{E/p}}_{\text{stat}}$ $(0.4 \pm 21.3_{\text{stat}})$
$M_W(\phi_\ell > 0) - M_W(\phi_\ell < 0)$	$24.4 \pm 18.5_{\text{stat}}$	$9.9 \pm 21.3_{\text{stat}} \pm 7.5^{\text{E/p}}_{\text{stat}}$ $(-0.8 \pm 21.3_{\text{stat}})$
$M_Z(\text{run} > 271100) - M_Z(\text{run} < 271100)$	$5.2 \pm 12.2_{\text{stat}}$	$63.2 \pm 29.9_{\text{stat}} \pm 8.2^{\text{E/p}}_{\text{stat}}$ $(-16.0 \pm 29.9_{\text{stat}})$

CDF M_W: comparison with the SM

The W boson mass is a sensitive quantity to high-scale physics

A measurement of m_W with <10 MeV precision has been achieved with the complete CDF data set
The result of >20 years of experience with the CDF II detector

Measured mass deviates from the SM by ~0.1% with high significance

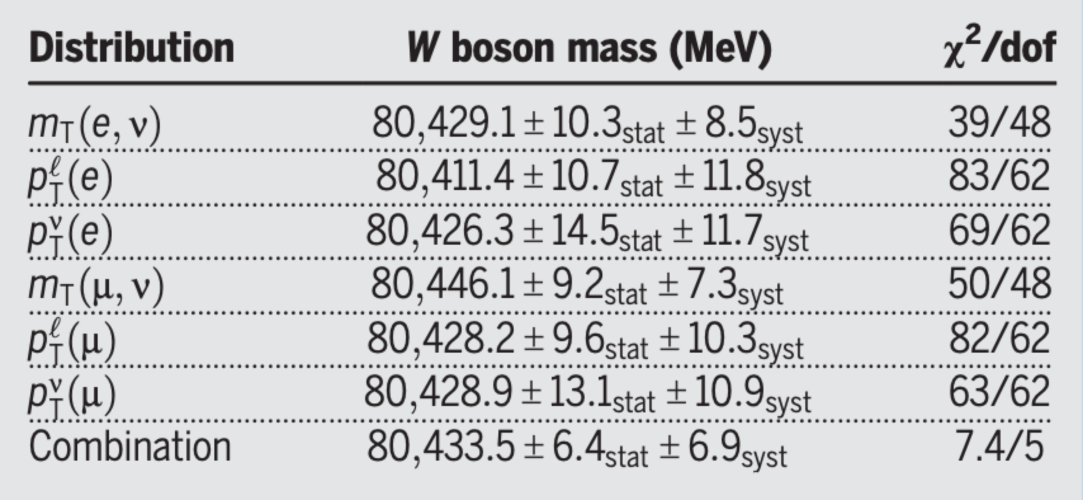

Distribution	***W* boson mass (MeV)**	**χ^2/dof**
$m_T(e,\nu)$	$80{,}429.1 \pm 10.3_{stat} \pm 8.5_{syst}$	39/48
$p_T^{\ell}(e)$	$80{,}411.4 \pm 10.7_{stat} \pm 11.8_{syst}$	83/62
$p_T^{\nu}(e)$	$80{,}426.3 \pm 14.5_{stat} \pm 11.7_{syst}$	69/62
$m_T(\mu,\nu)$	$80{,}446.1 \pm 9.2_{stat} \pm 7.3_{syst}$	50/48
$p_T^{\ell}(\mu)$	$80{,}428.2 \pm 9.6_{stat} \pm 10.3_{syst}$	82/62
$p_T^{\nu}(\mu)$	$80{,}428.9 \pm 13.1_{stat} \pm 10.9_{syst}$	63/62
Combination	$80{,}433.5 \pm 6.4_{stat} \pm 6.9_{syst}$	7.4/5

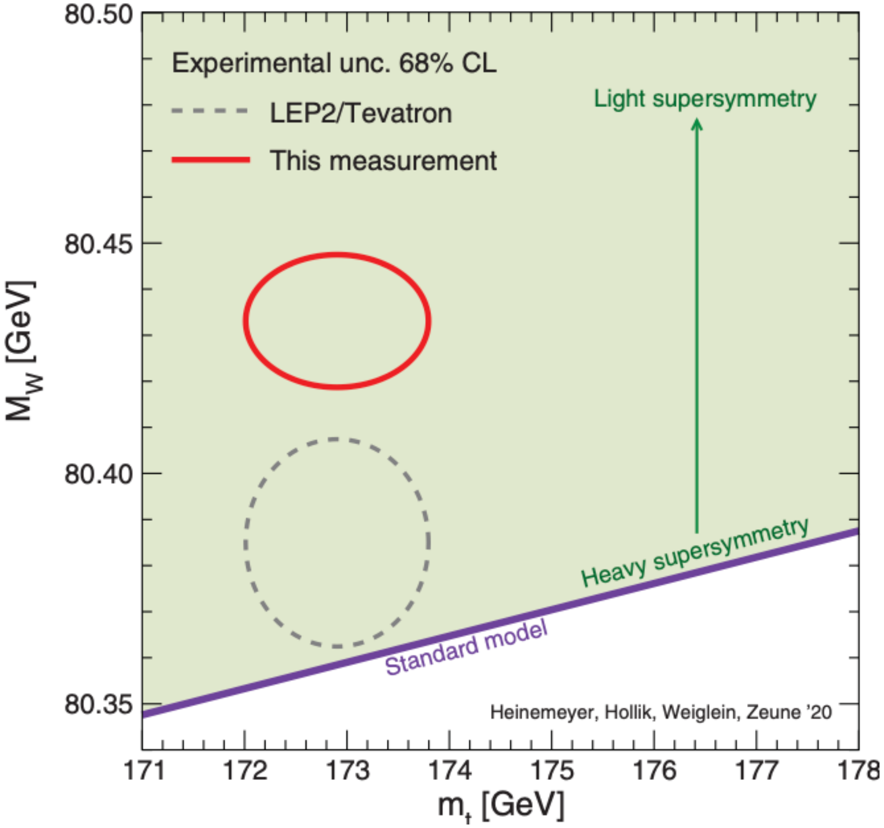

Comparison with SM

Eur. Phys. J. C78, 675 (2018)

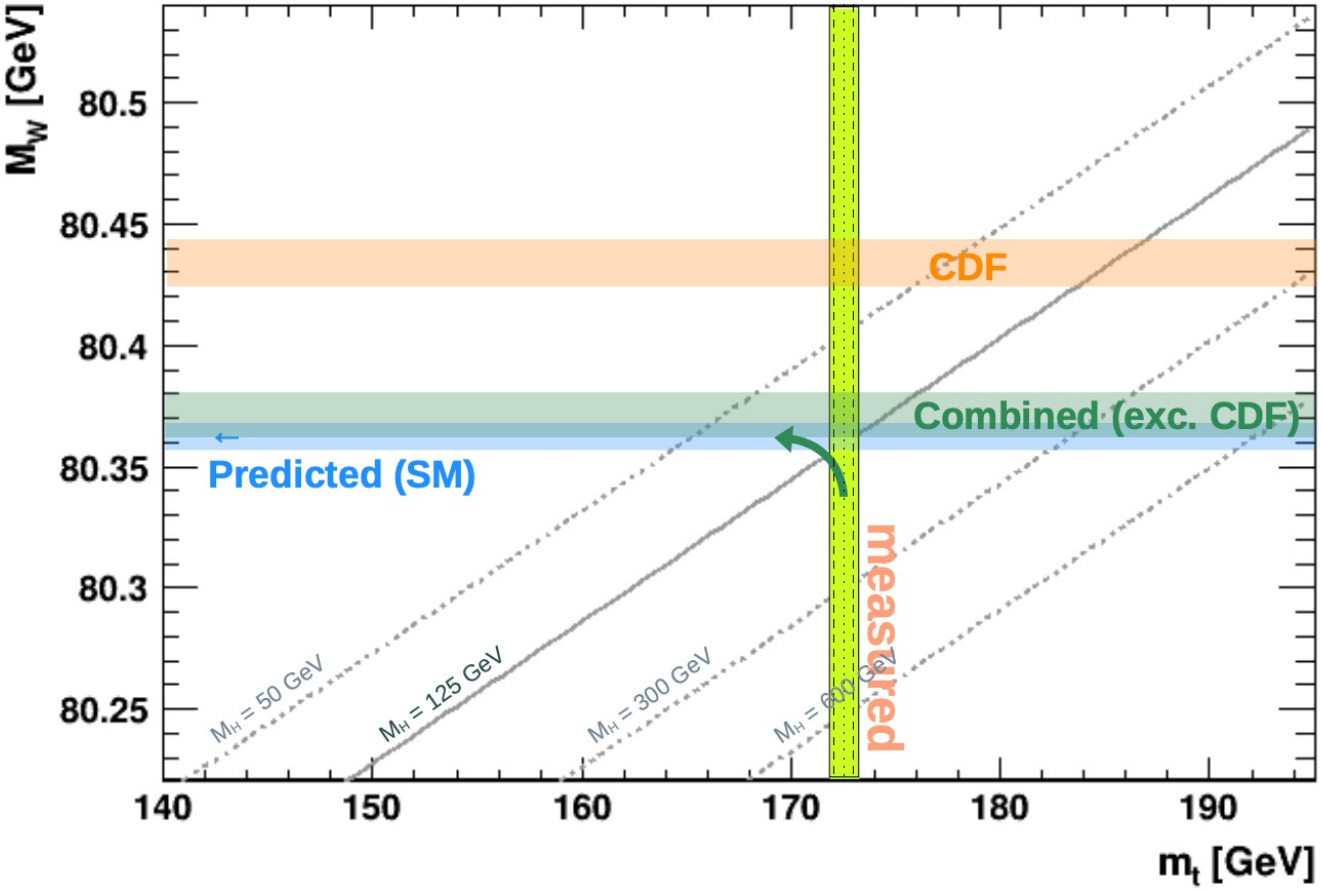

CDF M_W: comparison with the other experiments

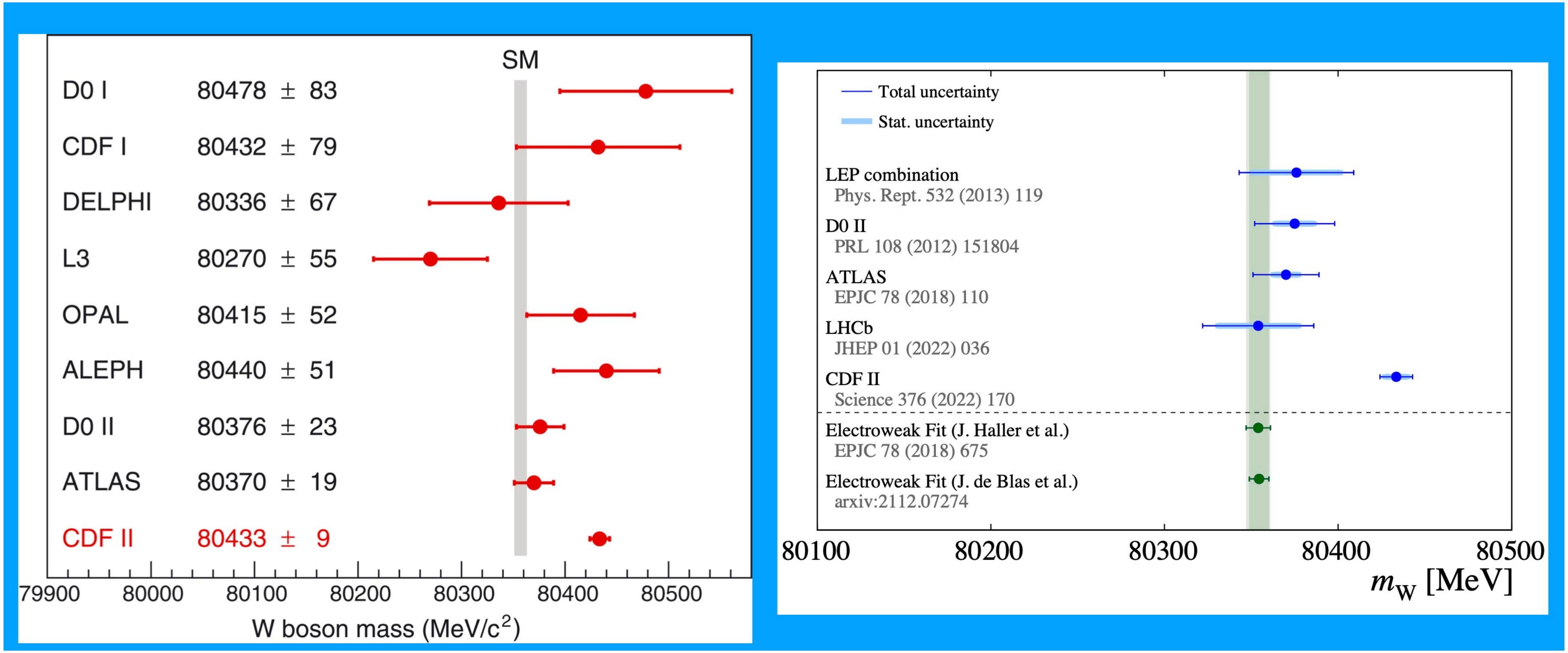

What shall we conclude?

Se sono rose fioriranno?

CMS entered the game

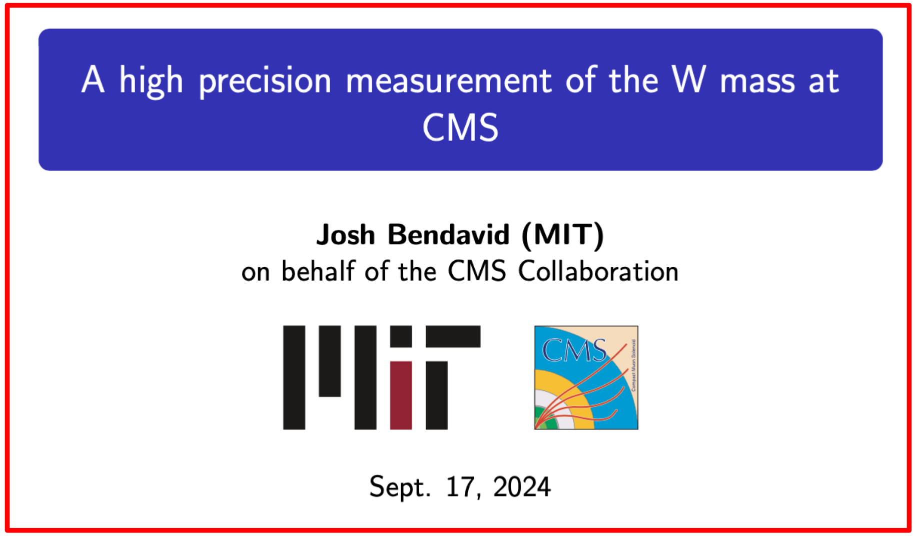

A high precision measurement of the W mass at CMS

Josh Bendavid (MIT)
on behalf of the CMS Collaboration

Sept. 17, 2024

CERN seminar: you can find the full talk on my web page

- Use well-understood subset of 13 TeV data: 16.8 fb^{-1} from later part of 2016 run ($\sim$ 30 mean interactions per crossing)
- Focus on muon channel and kinematics
  - Larger experimental systematics for electrons and hadronic recoil, especially with higher pileup
- **General strategy:** Exploit large dataset, accurate modeling of uncertainties for maximal in-situ contraints on theoretical modeling

○ Reserve Z data as an independent cross-check as much as possible
○ Muon calibration from J/Ψ, validated with Z
○ In-situ constraints on theory modeling from W itself, independent validation with Z.

- m_W extracted from profile likelihood fit to muon (η, p_T, charge)
  - Thousands of bins and systematic variations
  - Optimized Tensorflow-based fitting framework
- Building on experimental techniques, tools, and experience from W-like m_Z measurement (2016) and W rapidity-helicity measurement (2020) which established strong in-situ constraints on PDFs from charged lepton kinematics
- 4B fully simulated MC events, >100M selected W candidates
  - Significant computing/technical challenges for a measurement of this complexity

CMS W mass measurement: event selection

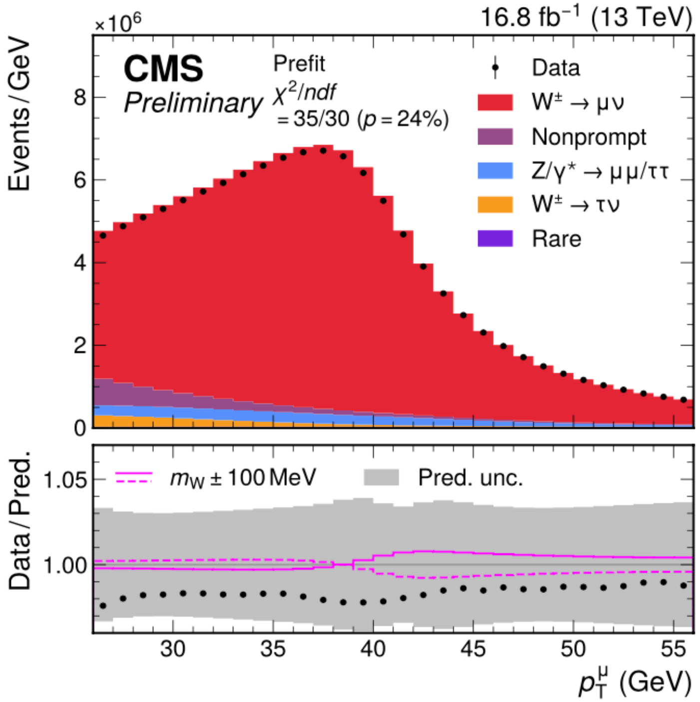

“W-like” selection of Z events

- $Z \to \mu\mu$ events are also selected with very similar selection
- One muon removed and treated as neutrino

- Straightforward single muon selection: track quality criteria, loose transverse impact parameter cut, and isolation
- Selected events are about 90% $W \to \mu\nu$
- Nonprompt background from data-driven estimate
  - Mostly from B and D decays with smaller contribution from π or K decay-in-flight
- Prompt backgrounds from simulation with all relevant corrections/uncertainties
  - $W \to \tau\nu$, $Z \to \mu\mu$ (mostly with one muon out-of-acceptance), $Z \to \tau\tau$, top, diboson

CMS W mass: muon momentum calibration

- **General strategy:** Calibrate with quarkonia, validate with Z
- **Muon chambers are not used for final momentum measurement**, "only" for trigger and identification
- Precise calibration requires accurate simulation track reconstruction, precise modeling of magnetic field, material, and alignment in the inner detector
- **Challenge:** Significant amount of material in the tracking volume

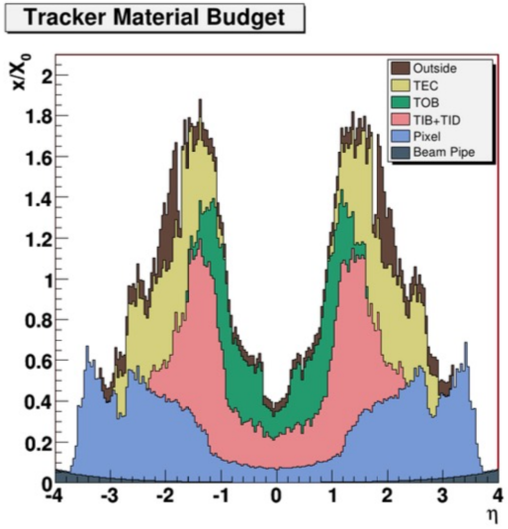

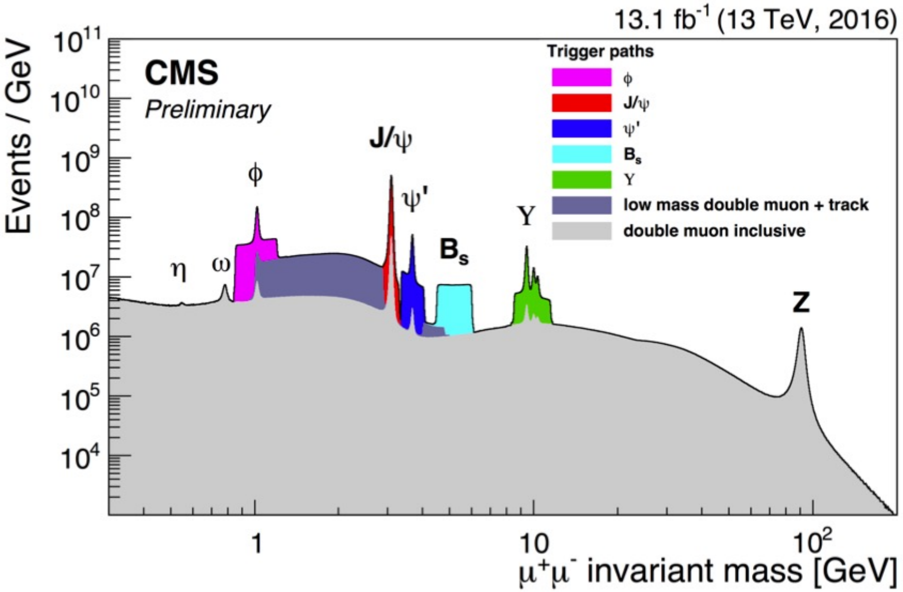

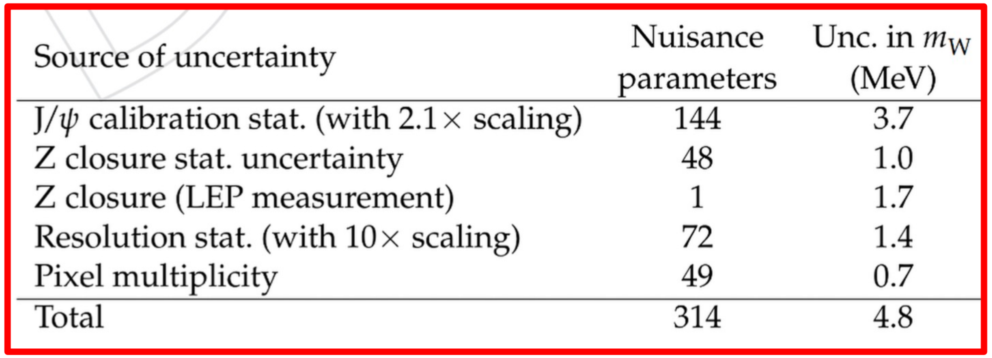

Source of uncertainty	Nuisance parameters	Unc. in m_W (MeV)
J/ψ calibration stat. (with 2.1× scaling)	144	3.7
Z closure stat. uncertainty	48	1.0
Z closure (LEP measurement)	1	1.7
Resolution stat. (with 10× scaling)	72	1.4
Pixel multiplicity	49	0.7
Total	314	4.8

CMS W mass: result

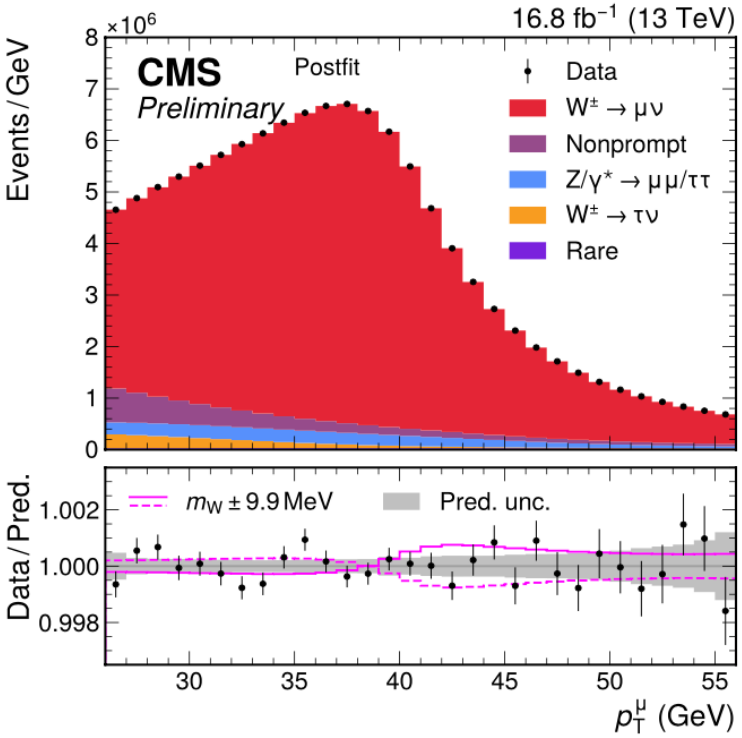

Source of uncertainty	Impact (MeV) Nominal	Impact (MeV) Global
Muon momentum scale	4.8	4.4
Muon reco. efficiency	3.0	2.3
W and Z angular coeffs.	3.3	3.0
Higher-order EW	2.0	1.9
p_T^V modeling	2.0	0.8
PDF	4.4	2.8
Nonprompt background	3.2	1.7
Integrated luminosity	0.1	0.1
MC sample size	1.5	3.8
Data sample size	2.4	6.0
Total uncertainty	9.9	9.9

- For the nominal measurement, total uncertainty is 9.9MeV
- Most precise measurement at the LHC and comparable to CDF precision

Some theory contributions (like PDF) can be evaluated with the data (in a global fit) at the expense of increasing the statistical error (from 2.4 MeV to 6.0 MeV)

CMS W mass: result

$$m_W = 80360.2 \pm 9.9 \mathrm{MeV}$$

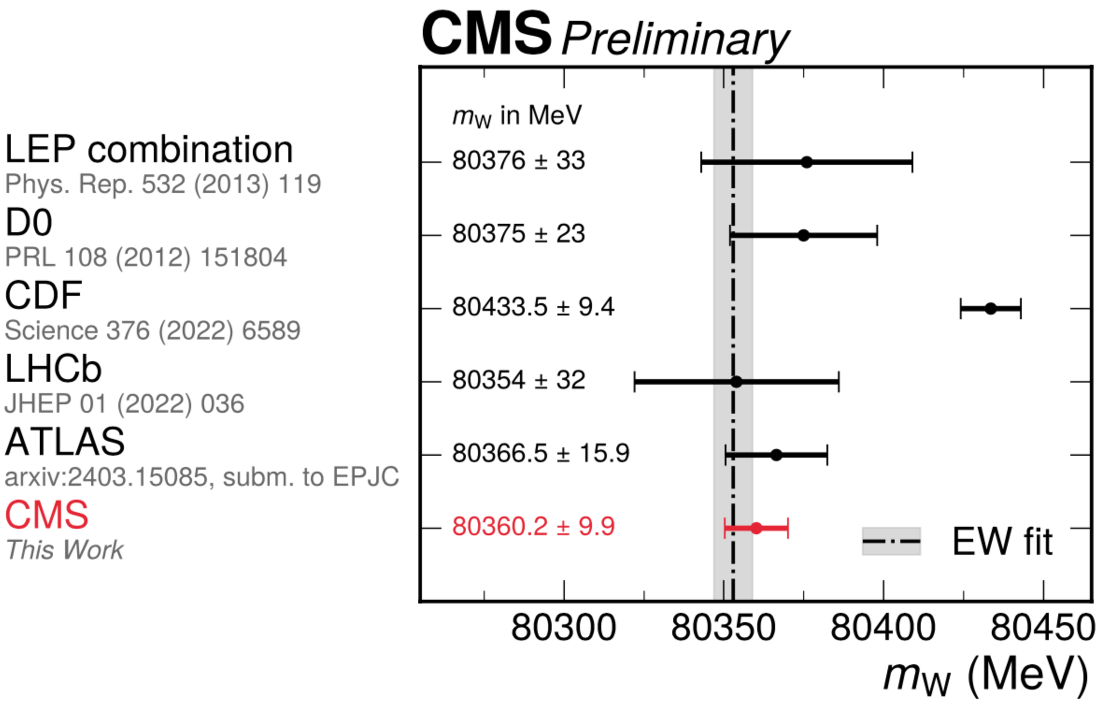

- Compatible with the Standard Model expectation and with other measurements
  - In clear tension with the CDF measurement

$\text{Sin}^2\theta_W$ Measurements

Sin$^2\theta_W$ and the Forward-Backward Asymmetry

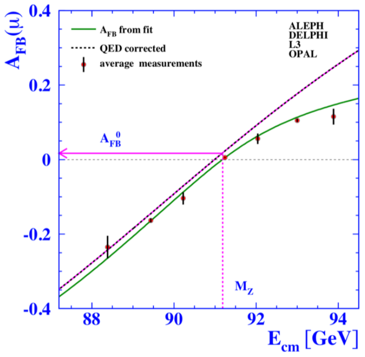

LEP

Forward-Backward asymmetry at LEP

On peak, effect is very small, off peak measurement are also extremely crucial.

At the Z pole: $\mathcal{A}_{FB}^0 = 3\mathcal{A}^e\mathcal{A}^f$

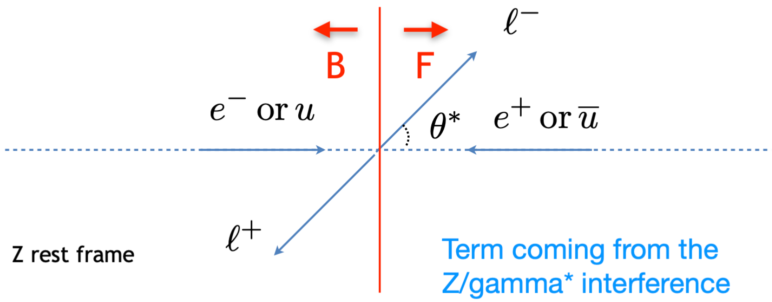

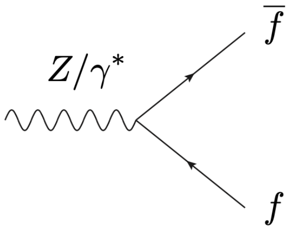

Term coming from the Z/gamma* interference

$$\frac{d\sigma}{d\cos\theta^*} = \frac{4\pi\alpha^2}{3\hat{s}}\left[\frac{3}{8}A(1+\cos^2\theta^*) + \boxed{B\cos\theta^*}\right]$$

$$B \propto \quad A_{FB} = \frac{\sigma_F - \sigma_B}{\sigma_F + \sigma_B}$$

$$\frac{d\sigma}{d\cos\theta^*} \propto \left((g_{ve}^2 + g_{ae}^2)(g_{vf}^2 + g_{af}^2)(1+\cos^2\theta^*) + 8g_{ve}g_{ae}g_{vf}g_{af}\cos\theta^*\right)$$

$$\begin{aligned} g_{a_f} &= \sqrt{\rho}T_f^3 \\ g_{v_f} &= \sqrt{\rho}(T_f^3 - 2Q_f\sin^2\theta_W^{eff}) \end{aligned}$$

$$\Rightarrow$$

$$\mathcal{A}_f \equiv 2\frac{g_{v_f}/g_{a_f}}{1+(g_{v_f}/g_{a_f})^2}$$

$$\Rightarrow$$

$$(\sin^2\theta_W^{\text{eff}})^f = \frac{1}{4|Q_f|}(1 - g_{vf}/g_{af})$$

Measurement Strategy at LHC

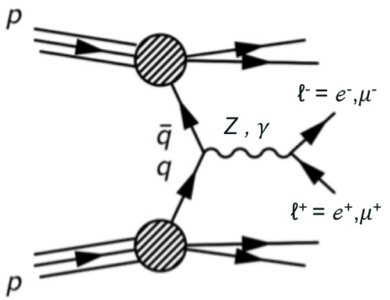

2012 data set: E_{CM}=8 TeV; $\mathcal{L} \approx 20\ fb^{-1}$

Measurement is based on the cos(theta) dependence of the Drell-Yan cross-section (using **ee/μμ** events)

At LO SM

$$\frac{d\sigma}{d\cos\theta^*} = A\left(1+\cos^2\theta^*\right) + B\cos\theta^*$$

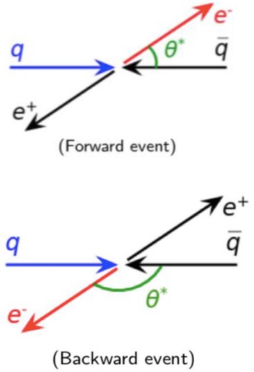

ATLAS: 7.5 x 10^6 di-muons and 7.5 x 10^6 di-electrons
CMS: 8.2 x 10^6 di-muons and 4.9 x 10^6 di-electrons

A_{FB}= Forward-Backward asymmetry

$$A_{FB} = \frac{\sigma(\cos\theta^* > 0) - \sigma(\cos\theta^* < 0)}{\sigma(\cos\theta^* > 0) + \sigma(\cos\theta^* < 0)}$$

PROBLEM: how do we distinguish a quark from an antiquark in the initial state?

a) The antiquark is picked up from the sea; b) at high rapidity is more likely that the Z follows the quark direction.

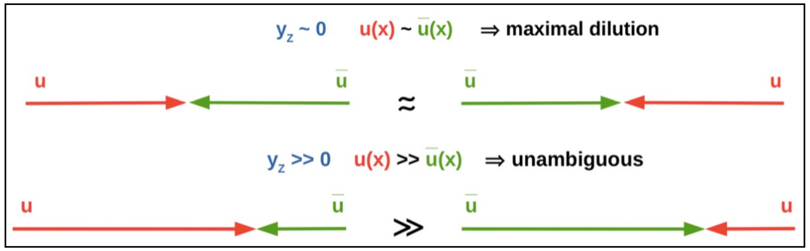

… **Moreover** …

- The measurement must be done in the Z reference frame
- Gluon emission from initial quark leg will give a transvers momentum to the Z

⇨ This measurement is best done in the high rapidity region of the detector

PDF effects on the A_{FB} Measurement

❑ **A_{FB} is sensitive to PDF for two reasons:**

- **different couplings of u- and d-type quarks**
- **y_{ll} direction depends on the relative content of valence and sea quarks**

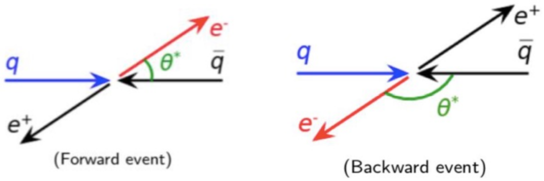

$$v_f = T_3^f - 2Q_f \sin^2\theta_W$$
$$a_f = T_3^f$$

$$A_{FB} = \frac{\sigma(\cos\theta^* > 0) - \sigma(\cos\theta^* < 0)}{\sigma(\cos\theta^* > 0) + \sigma(\cos\theta^* < 0)}$$

MC study on A_{FB}

Using quark direction

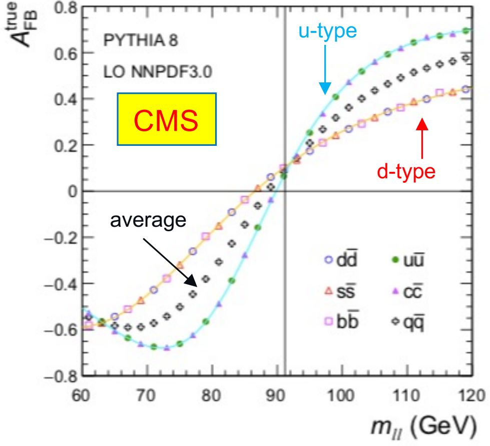

Using di-lepton direction

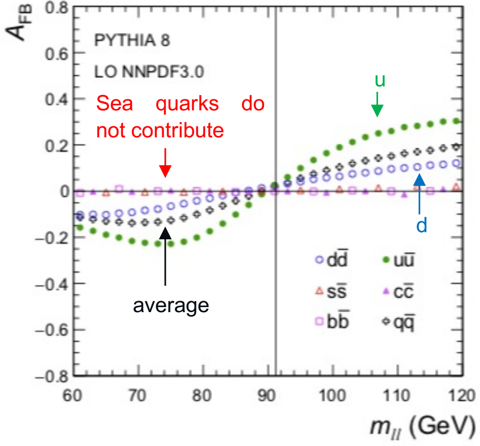

A_{FB} for different rapidity bin

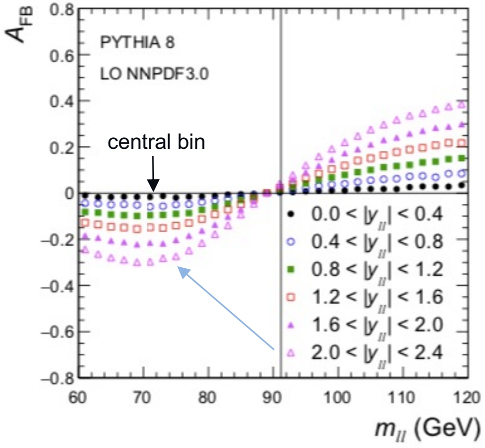

PDF uncertainty is the major source of systematic error and require particular care in the $\sin^2\theta_W$ extraction

CMS: AFB methodology (Eur. Phys. J. C 78: 701)

❑ **Measure A_{FB} asymmetry in Collin-Soper frame in reconstructed m_{ll}, y_{ll} bins**

❑**$\sin^2\theta_{eff}$ extracted from template fit to A_{FB} in data using theoretical predictions**
(Powheg v2 event generator using NNPDF3.0 PDFs)

$$70 \leq M_{\ell\ell} \leq 110 \text{ GeV}$$

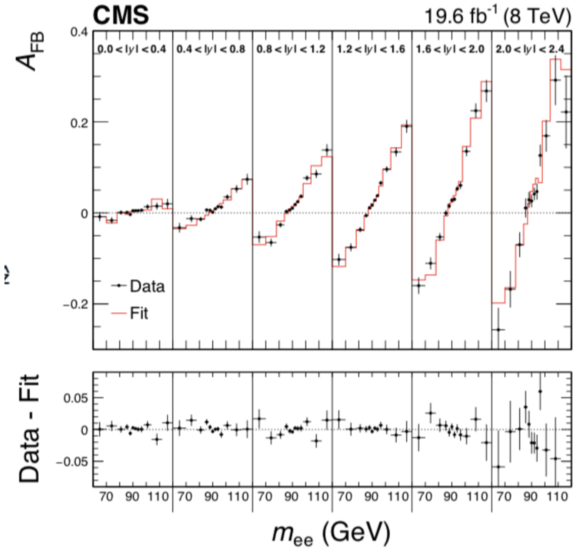

$$0.0 \leq |y| \leq 2.4$$

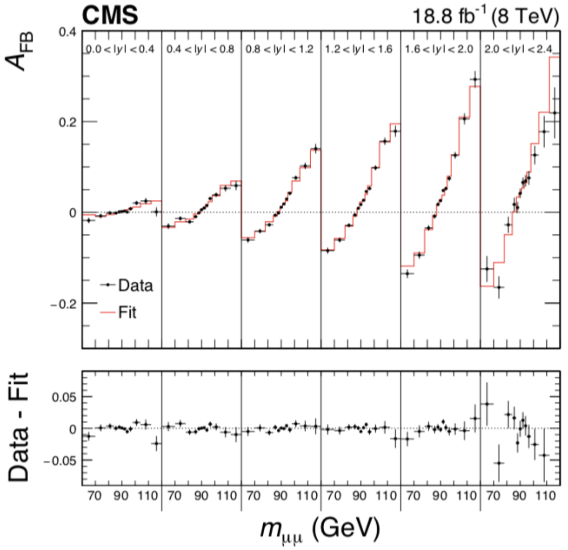

Collins and Soper reference
PhysRevD.16.2219

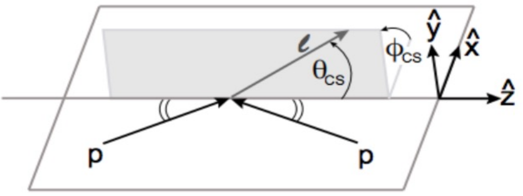

- P are the directions of the two protons in the Z rest frame. They are used to define the z axis.
- l is the direction of the lepton and theta is the angle with respect to the z axis
- Phi is the angle of the plane containing the two leptons with respect to the xz plane

Using quantities measured in the Lab:

$$\cos\theta_{CS} = \frac{2(p_z^{\ell} E^{\overline{\ell'}} - p_z^{\overline{\ell'}} E^{\ell})}{M\sqrt{M^2 + p_T^2}} .$$

ATLAS: A_i methodology (ATLAS-CONF-2018-037)

The differential cross section pp → Z → ℓℓ can be parametrized at EW LO and all order QCD as:

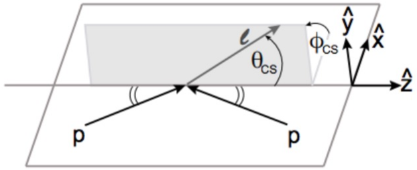

$$\frac{d\sigma}{dp_T^{\ell\ell}\,dy^{\ell\ell}\,dm^{\ell\ell}\,d\cos\theta\,d\phi} = \frac{3}{16\pi}\frac{d\sigma^{U+L}}{dp_T^{\ell\ell}\,dy^{\ell\ell}\,dm^{\ell\ell}}$$
$$\Big\{(1+\cos^2\theta)+\frac{1}{2}A_0(1-3\cos^2\theta)+A_1\,\sin 2\theta\,\cos\phi$$
$$+\frac{1}{2}A_2\,\sin^2\theta\,\cos 2\phi + A_3\,\sin\theta\,\cos\phi + \boxed{A_4}\cos\theta$$
$$+A_5\,\sin^2\theta\,\sin 2\phi + A_6\,\sin 2\theta\,\sin\phi + A_7\,\sin\theta\,\sin\phi\Big\}.$$

$$\boxed{A_{FB}=\frac{3}{8}A_4}$$

- 9 harmonic polynomials $P_i(\cos\theta_{CS},\Phi_{CS})$ describe the lepton angular distribution in the Z rest frame (final state)
- 8 $A_i(m^{\ell\ell}, p_T^{\ell\ell}, y^{\ell\ell})$ coefficients and total unpolarised cross section σ^{U+L} $(m^{\ell\ell}, p_T^{\ell\ell}, y^{\ell\ell})$ describe the Z dynamics (initial state)
- **Parity-violating A_4 term is sensitive to $\sin^2\theta_{eff}$**

(box diagrams give little contribuion near the Z pole)

- A_i obtained from templates binned in $(m^{\ell\ell}, y^{\ell\ell})$
  (method here: J. High Energ. Phys. (2016) 2016: 159)

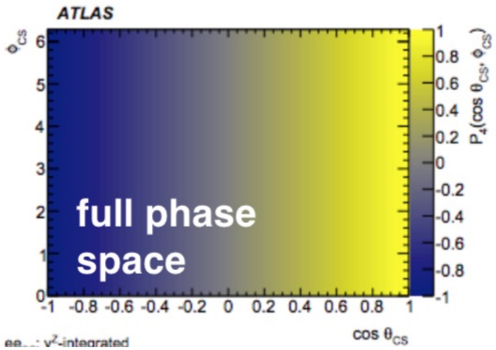

Fold detector acceptance

Fit A_i to the data

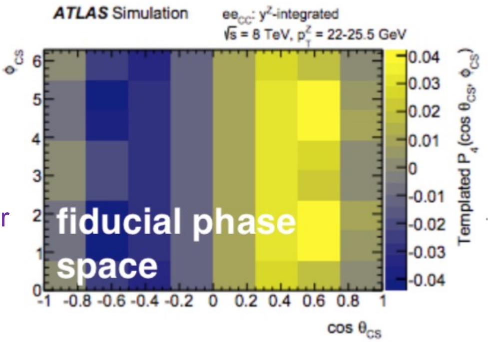

From A_4 we get $\sin^2\theta_{eff}$

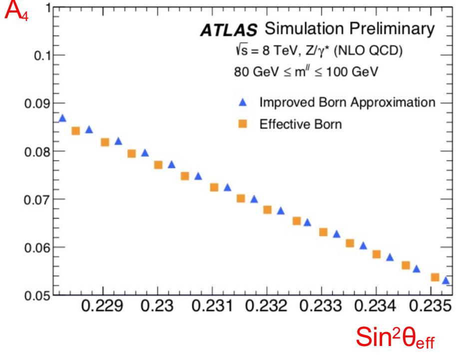

$\mathrm{Sin}^2\theta_{\mathrm{eff}}$: comparison among results

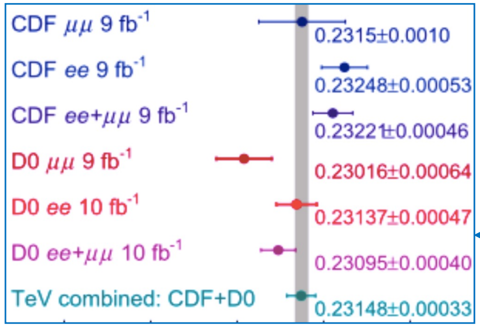

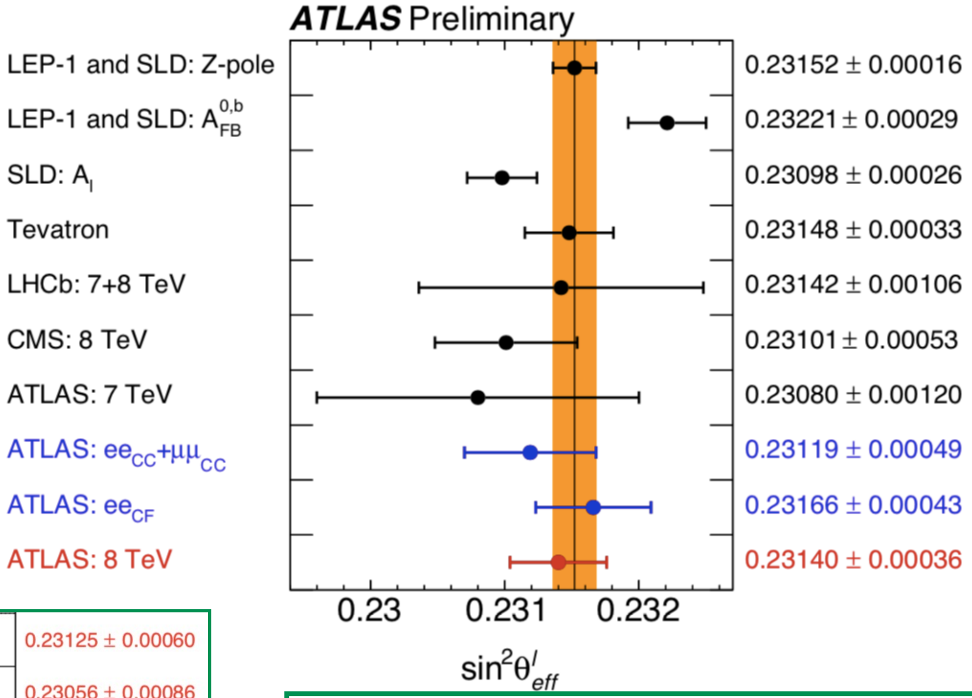

The measurement is still dominated by the ''old'' LEP and SLD done at the Z-pole

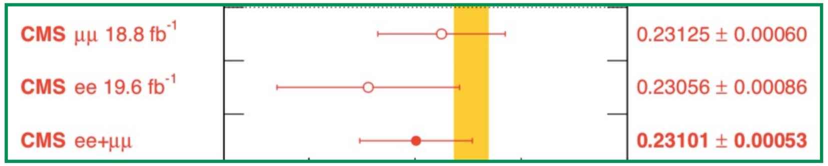

- ATLAS error is similar to the Tevatron one
- ATLAS and CMS errors are comparable in the central region

CMS: $\sin^2\theta^\ell_{\mathrm{eff}} = 0.23101 \pm 0.00036\,(\mathrm{stat}) \pm 0.00018\,(\mathrm{syst}) \pm 0.00016\,(\mathrm{theo}) \pm 0.00031\,(\mathrm{PDF})$

ATLAS: $\sin^2\theta^\ell_{\mathrm{eff}} = 0.23140 \pm 0.00021\,(\mathrm{stat.}) \pm 0.00024\,(\mathrm{PDF}) \pm 0.00016\,(\mathrm{syst.})$

Z invisible width

- Select events where Z recoils against jet
- Measure ratio of Z → invisible to Z → 2l to cancel many systematic uncertainties
- Important test of SM
- **Most precise recoil-based constraint on Γ(Z → inv)** (LEP lineshape result more precise)

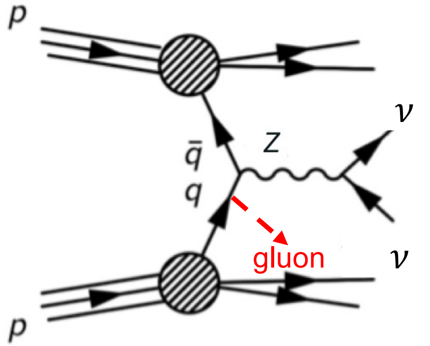

Looking for monojet in the detector

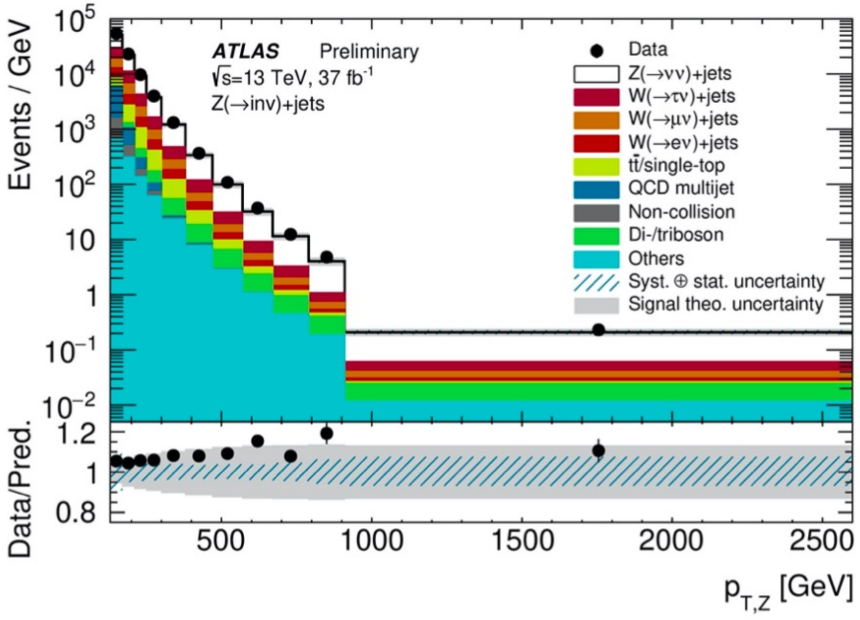

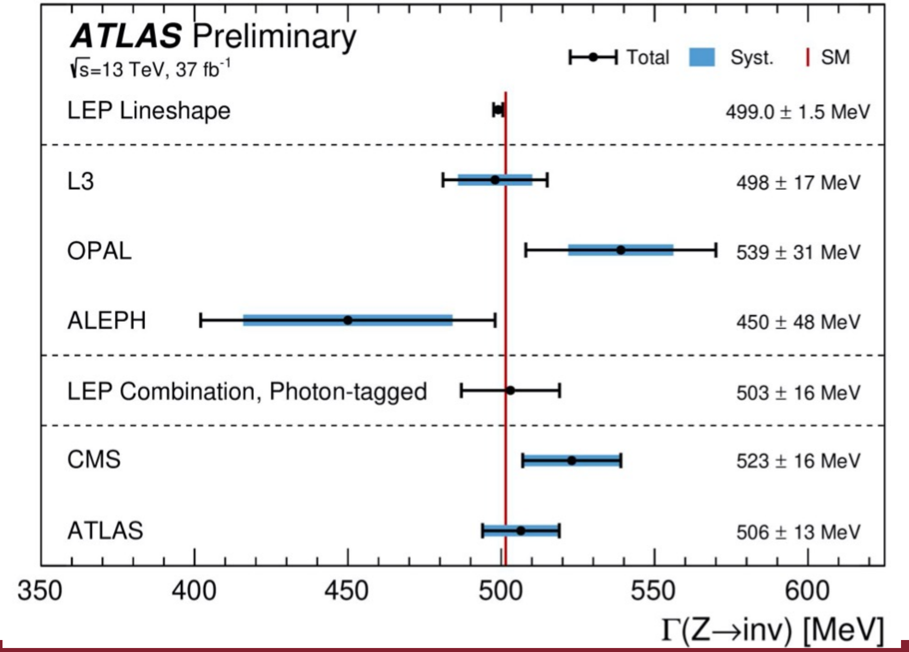

Gauge Boson Couplings

Motivations for the Measurement

- **The non-Abelian gauge nature of the Standard Model predicts, in addition to the trilinear WWZ and WWγ couplings (TGV), also Quartic Gauge Boson Couplings (QGC)**

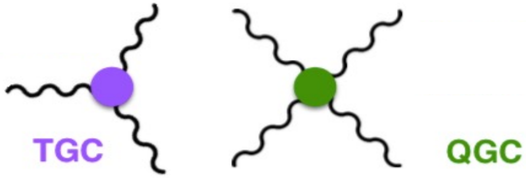

- **TGC and QGC probe different aspects of the weak interactions.**
- **TGC test the non-Abelian gauge structure of the Model; they have been tested at LEP:**

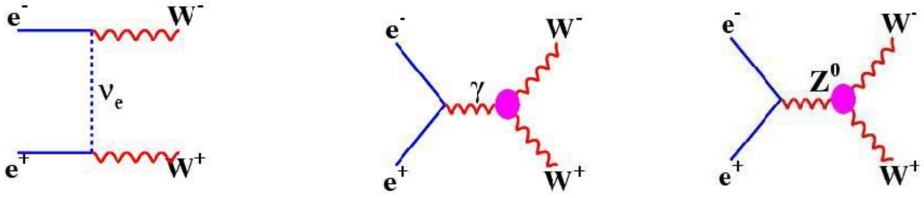

- **QGC are accessible to LHC. They can be regarded as a window on the electroweak symmetry breaking mechanism and they represent a connection to the scalar sector of the theory.**
- **Anomalous couplings are handled by the Effective Field Theory approach:**

$$\mathcal{L}_{EFT} = \mathcal{L}_{SM} + \underbrace{\boxed{\sum_i \frac{c_i}{\Lambda^2} O_i}}_{\text{dim-6}} + \underbrace{\boxed{\sum_j \frac{f_j}{\Lambda^4} O_j}}_{\text{dim-8}} + \cdots$$

Production Cross-Sections

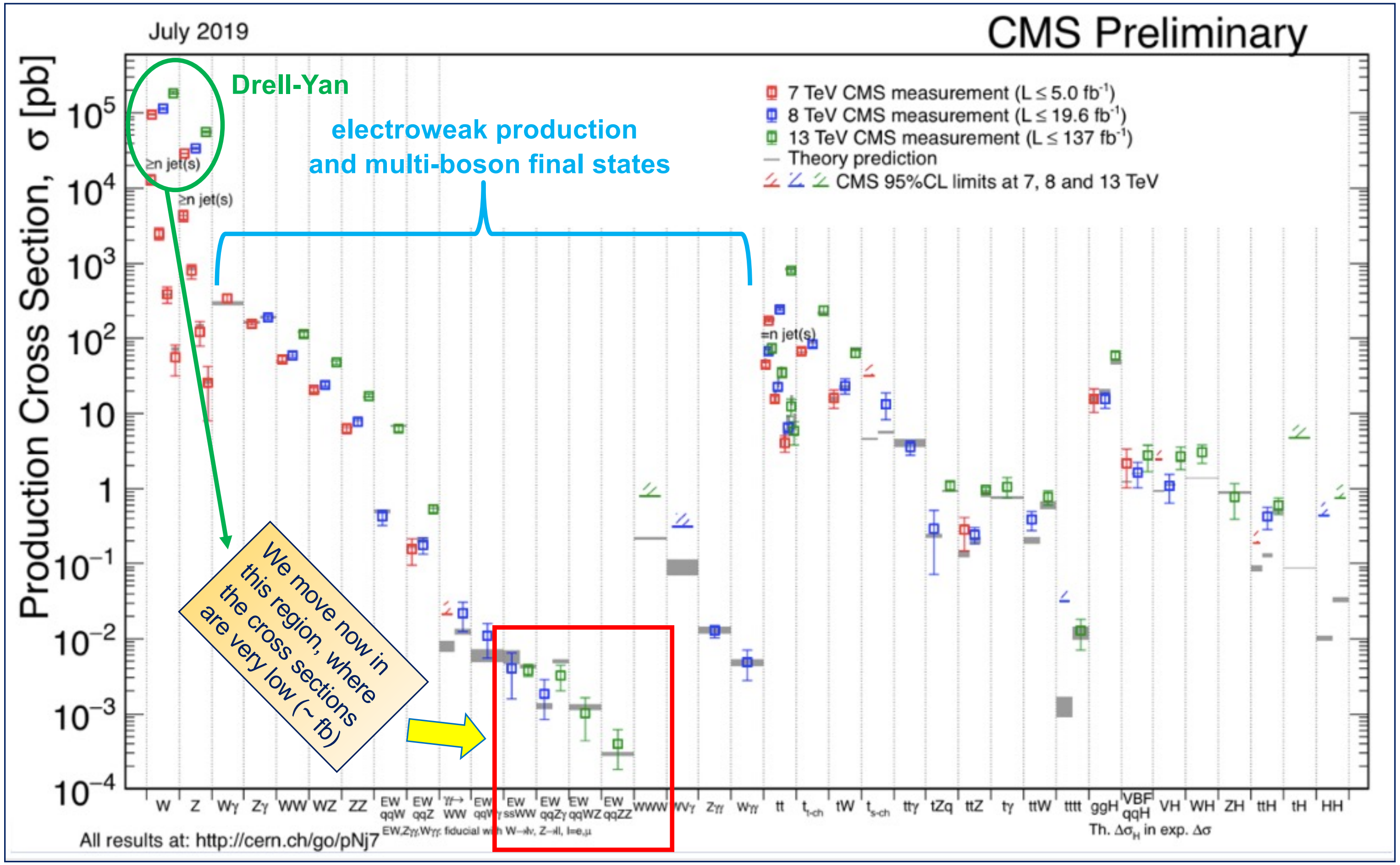

Drell-Yan

electroweak production and multi-boson final states

We move now in this region, where the cross sections are very low (~ fb)

An example:
Vector Boson Scattering (VBS)

VBS: Feynman diagrams

Final state: 2 Vector Bosons + 2 jets

VVjj EWK VBS

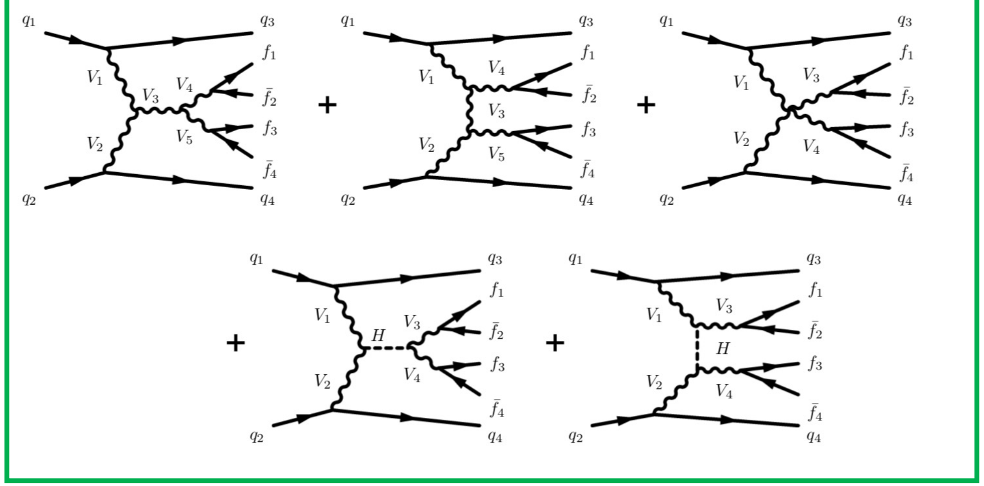

VVjj QCD

$\alpha_S^2\alpha_{EW}^4$

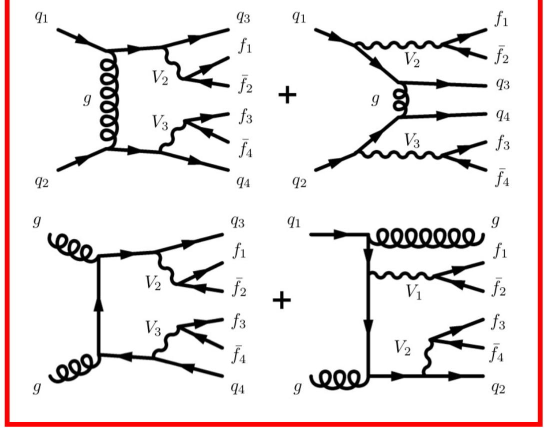

VVjj EWK NON VBS

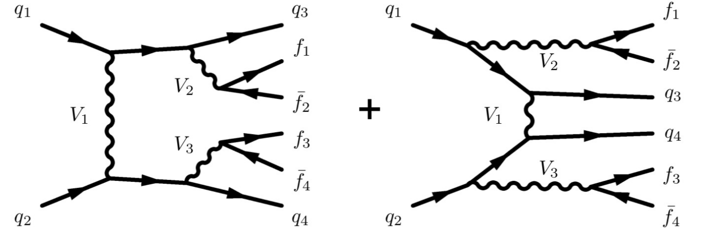

Event topology

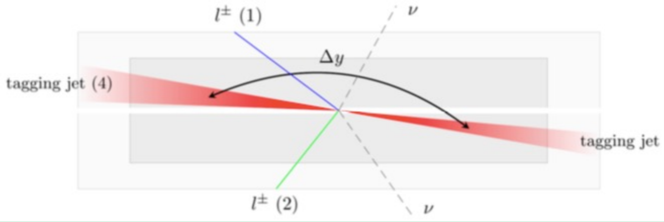

Several final states depending on the nature of the Vector Bosons

VBS: same sign WW

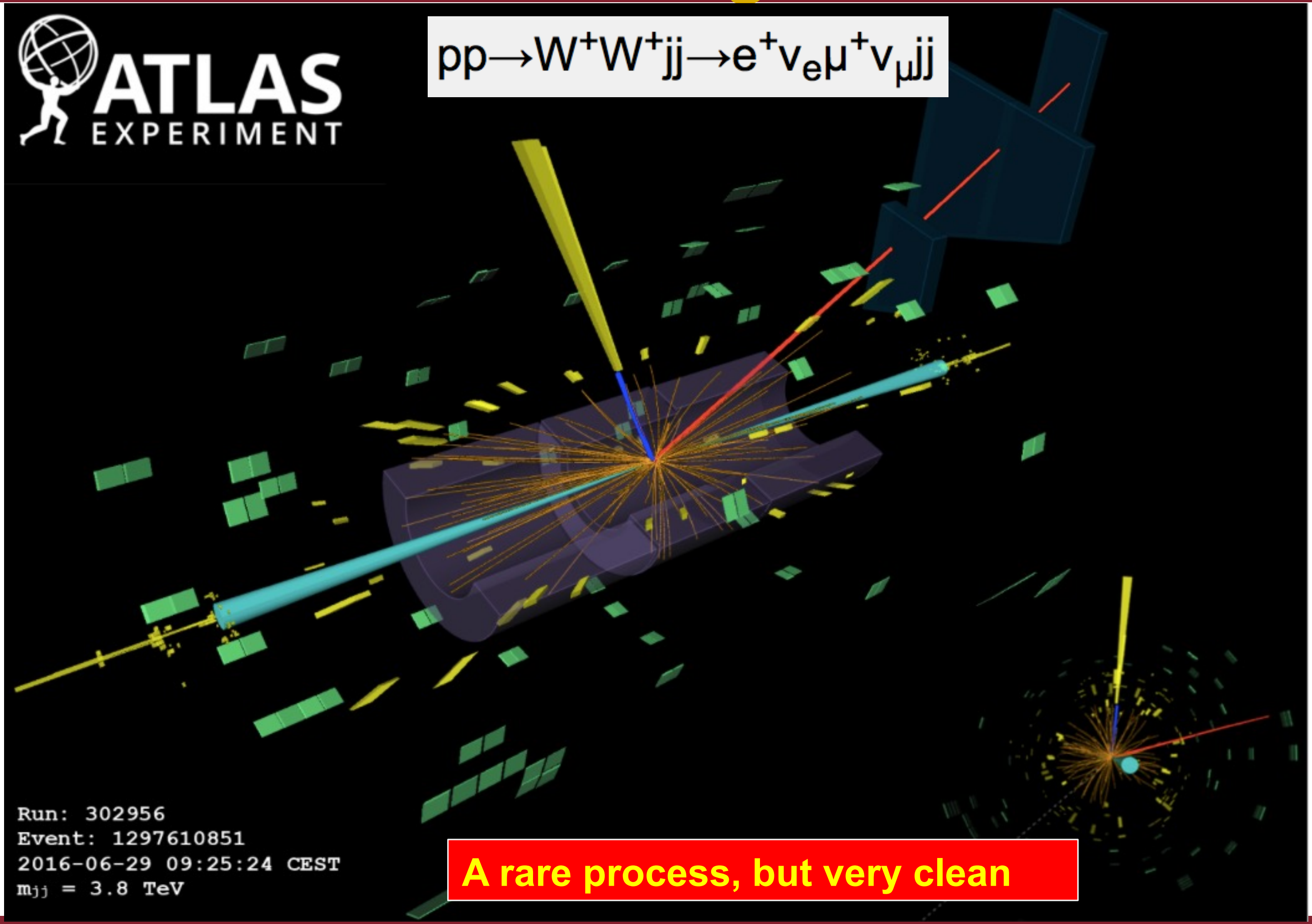

$pp \to W^+W^+jj \to e^+\nu_e\mu^+\nu_\mu jj$

Run: 302956
Event: 1297610851
2016-06-29 09:25:24 CEST
m_{jj} = 3.8 TeV

A rare process, but very clean

Phenomenology Highlights for VBS $W^{\pm}W^{\pm}jj$

- Two hadronics jets in forward and backward regions with high energy (tagging jets)
- Hadronics activity suppressed between the two jets (rapidity gap) due to absence of colour flow between interacting partons
- Boson pair more central than in non-EWK processed

The VBS process involving two same-sign W bosons has the largest signal-to-background ratio of all the VBS processes at LHC.

Di-jet rapidity difference: arxiv:1803.07943

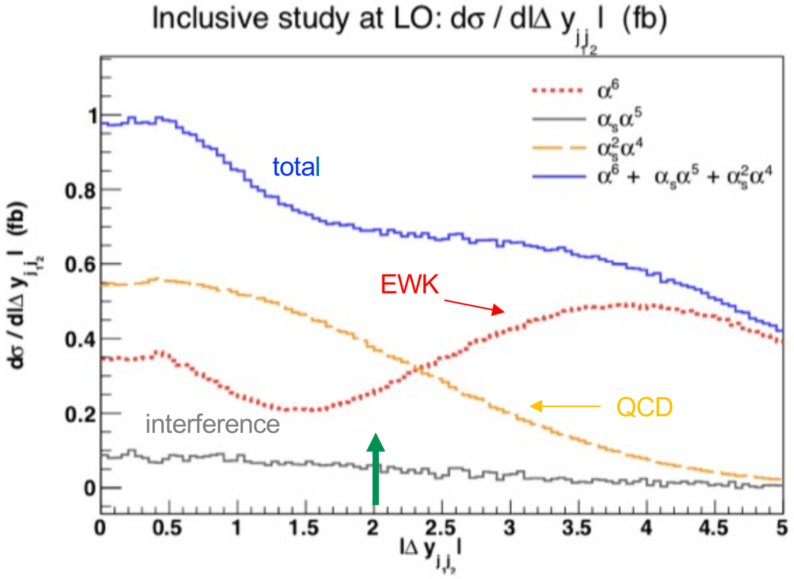

Di-jet invariant mass: arxiv:1803.07943

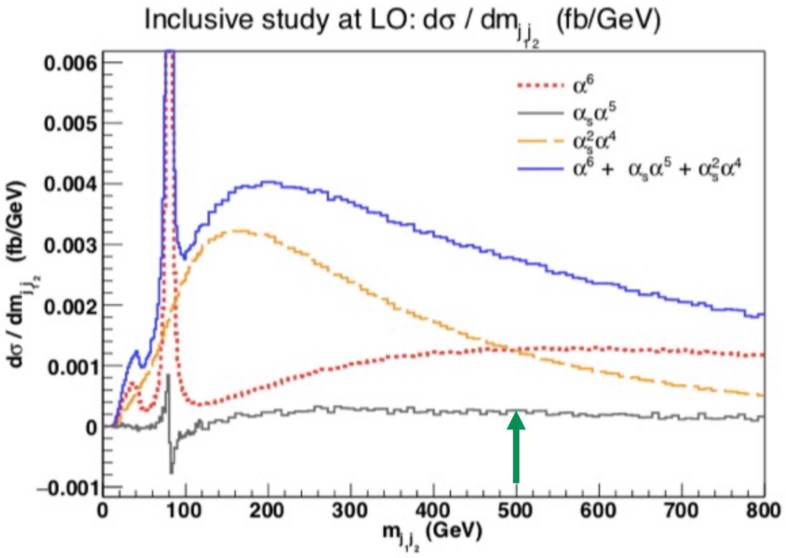

The analysis can be cut flow based

CMS: VBS Same Sign WW (Phys Rev Lett. 120.081801)

2016 data: 35.9 fb^{-1} at 13 TeV

- 2 same sign leptons (e or μ) with: $p_T > 25/20$ GeV and $\eta < 2.5/2.4$
- $M_{jj} > 500$ GeV; $|\Delta\eta_{jj} > 2.5|$

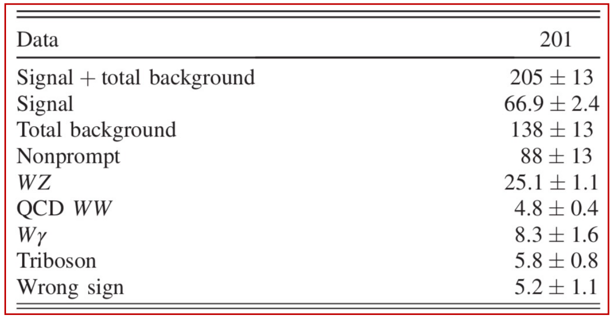

Data	201
Signal + total background	205 ± 13
Signal	66.9 ± 2.4
Total background	138 ± 13
Nonprompt	88 ± 13
WZ	25.1 ± 1.1
QCD *WW*	4.8 ± 0.4
Wγ	8.3 ± 1.6
Triboson	5.8 ± 0.8
Wrong sign	5.2 ± 1.1

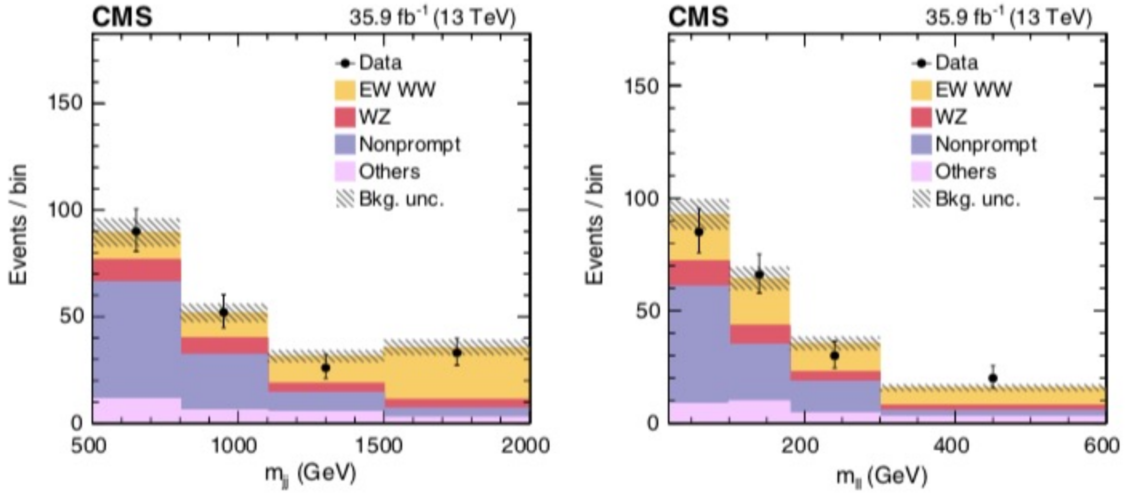

- Significance: 5.5 σ (obs); 5.7 σ (exp.) → **first observation of EWK $W^\pm W^\pm jj$**
- $\sigma_{fid}(W^\pm W^\pm jj) = 3.83 \pm 0.66$ (stat) ± 0.35 (syst) fb (statistically dominated)
- $\sigma^{LO} = 4.25 \pm 0.27$ (scale + PDF) fb

CMS VBS WW: aQGC & limits on $H^{\pm\pm}$

Anomalous gauge couplings

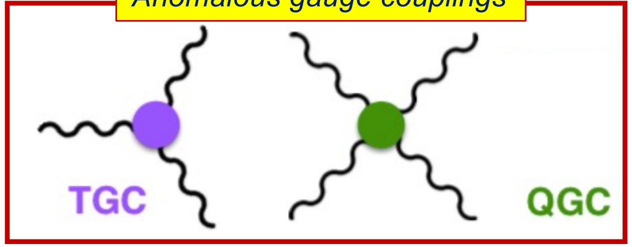

Focus on dim-8 operators for aQGC

	Observed limits (TeV^{-4})	Expected limits (TeV^{-4})
f_{S0}/Λ^4	$[-7.7, 7.7]$	$[-7.0, 7.2]$
f_{S1}/Λ^4	$[-21.6, 21.8]$	$[-19.9, 20.2]$
f_{M0}/Λ^4	$[-6.0, 5.9]$	$[-5.6, 5.5]$
f_{M1}/Λ^4	$[-8.7, 9.1]$	$[-7.9, 8.5]$
f_{M6}/Λ^4	$[-11.9, 11.8]$	$[-11.1, 11.0]$
f_{M7}/Λ^4	$[-13.3, 12.9]$	$[-12.4, 11.8]$
f_{T0}/Λ^4	$[-0.62, 0.65]$	$[-0.58, 0.61]$
f_{T1}/Λ^4	$[-0.28, 0.31]$	$[-0.26, 0.29]$
f_{T2}/Λ^4	$[-0.89, 1.02]$	$[-0.80, 0.95]$

They are all compatible with 0 (SM)

handled by →

Effective Field Theory

$$\mathcal{L}_{EFT} = \mathcal{L}_{SM} + \underbrace{\boxed{\sum_i \frac{c_i}{\Lambda^2} O_i}}_{\text{dim-6}} + \underbrace{\boxed{\sum_j \frac{f_j}{\Lambda^4} O_j}}_{\text{dim-8}} + \cdots$$

You can choose a particular model and set limits on its parameters

Limits on σ x BR for VBF production of $H^{\pm\pm}$

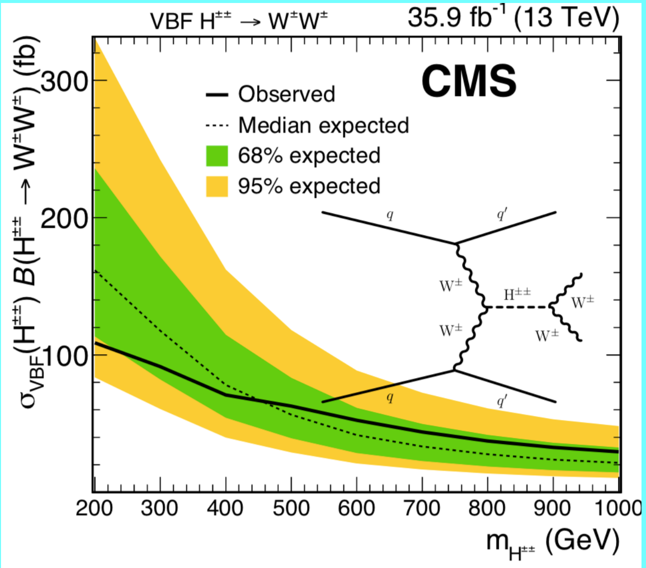

ATLAS: VBS Same Sign WW (arxiv:1906.03203)

2016 data: 36.1 fb^{-1} at 13 TeV

- 2 same sign leptons (e or μ) with: $p_T > 27$ GeV and $\eta < 2.5$
- $M_{jj} > 500$ GeV; $|\Delta\eta_{jj}| > 2.0$

	Combined
WZ	30 ± 4
Non-prompt	15 ± 5
e/γ conversions	13.9 ± 2.9
Other prompt	2.4 ± 0.5
$W^{\pm}W^{\pm}jj$ strong	7.2 ± 2.3
Expected background	69 ± 7
$W^{\pm}W^{\pm}jj$ electroweak	60 ± 11
Data	122

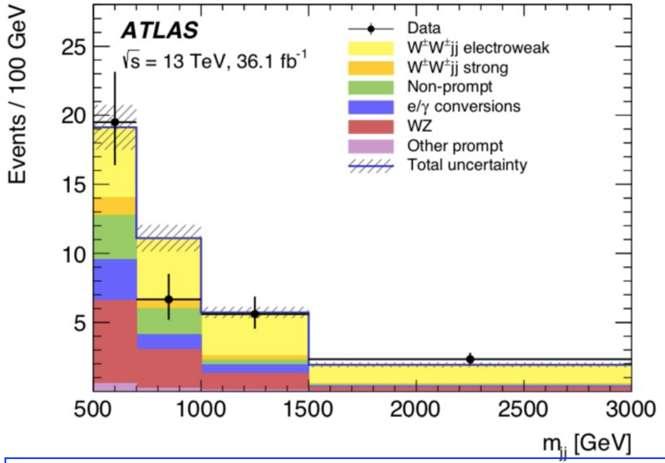

Sherpa v2.2: non-optimal setting of colour flow for the parton shower → excess of central emissions

Comparison with MC predictions

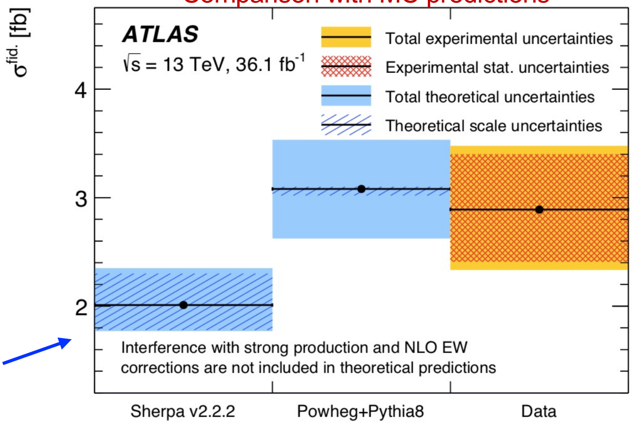

Interference with strong production and NLO EW corrections are not included in theoretical predictions

$$\sigma^{\text{fid.}} = 2.89^{+0.51}_{-0.48}\,(\text{stat.})\,^{+0.24}_{-0.22}\,(\text{exp. syst.})\,^{+0.14}_{-0.16}\,(\text{mod. syst.})\,^{+0.08}_{-0.06}\,(\text{lumi.})\ \text{fb}$$

Significance: 6.5 σ (obs); 4.4 σ (exp. from Sherpa) and 6.5 σ (exp. from Powheg+Pythia8)

Three Bosons Final State (VVV)

Representative tree level Feynman diagrams

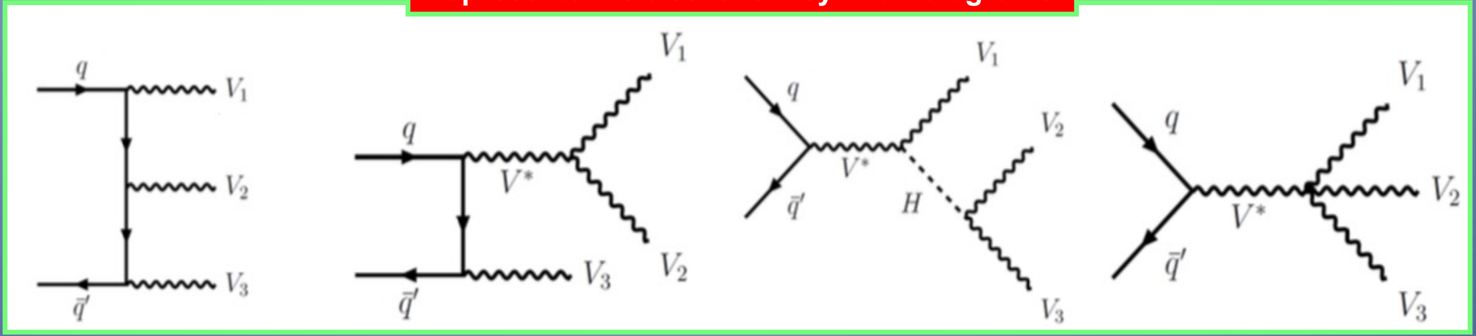

Process never observed at previous colliders

Process sensitive to TGC and QGC

Summary on multi boson cross sections

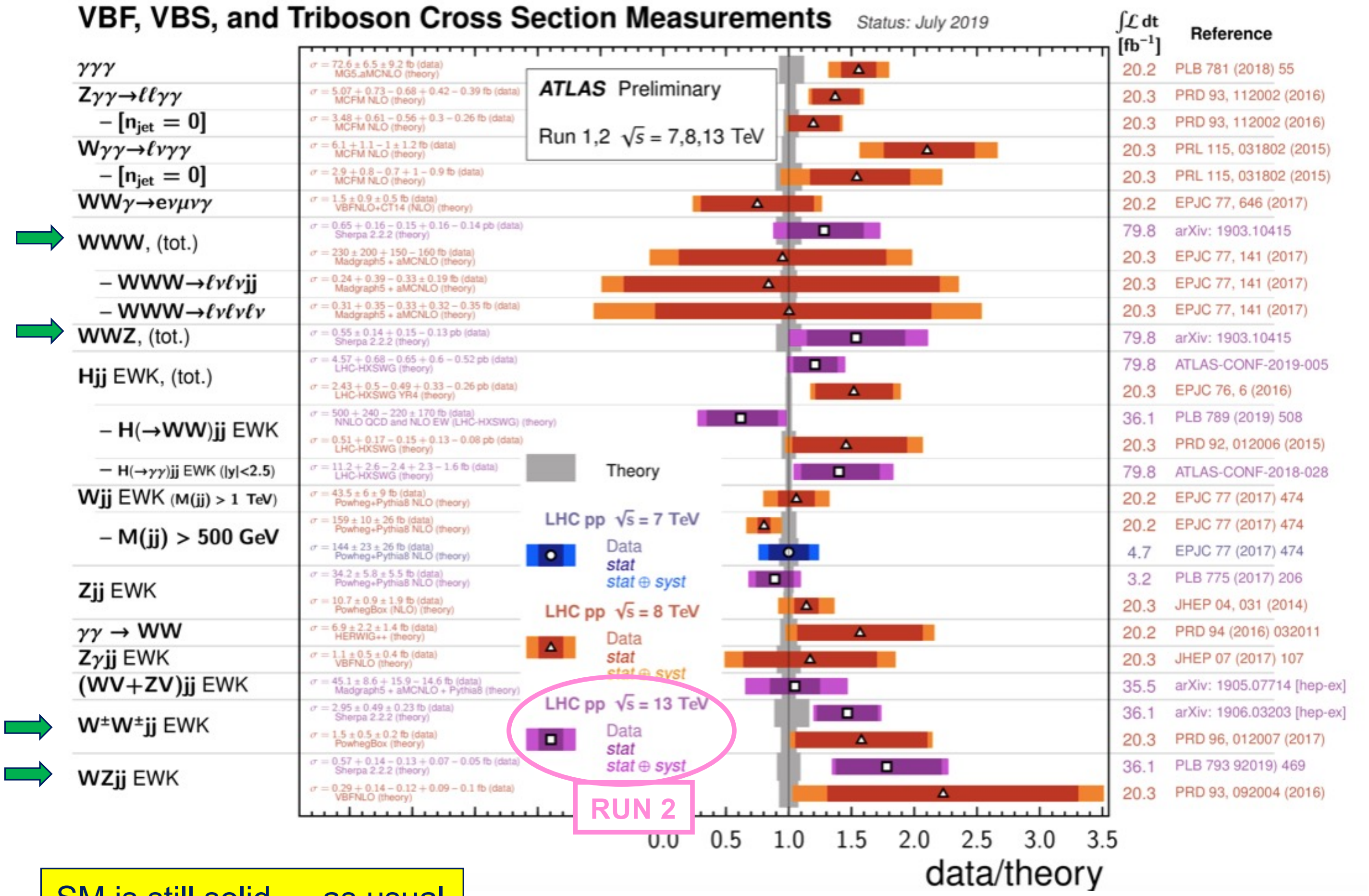

SM is still solid … as usual

Higgs discovery at LHC (Run1)

The Higgs Boson

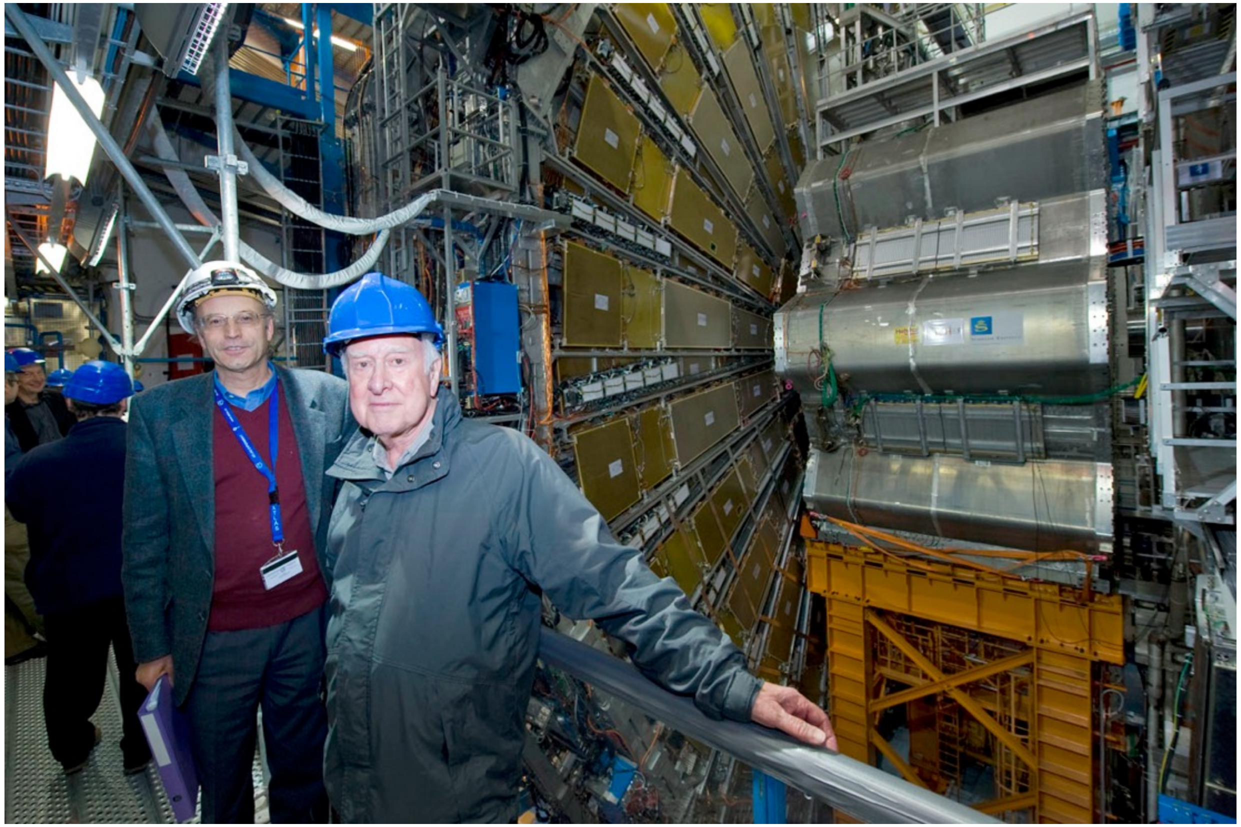

The first Higgs seen in the ATLAS Experiment

$H \rightarrow ZZ^* \rightarrow \mu^+\mu^- \; \mu^+\mu^-$

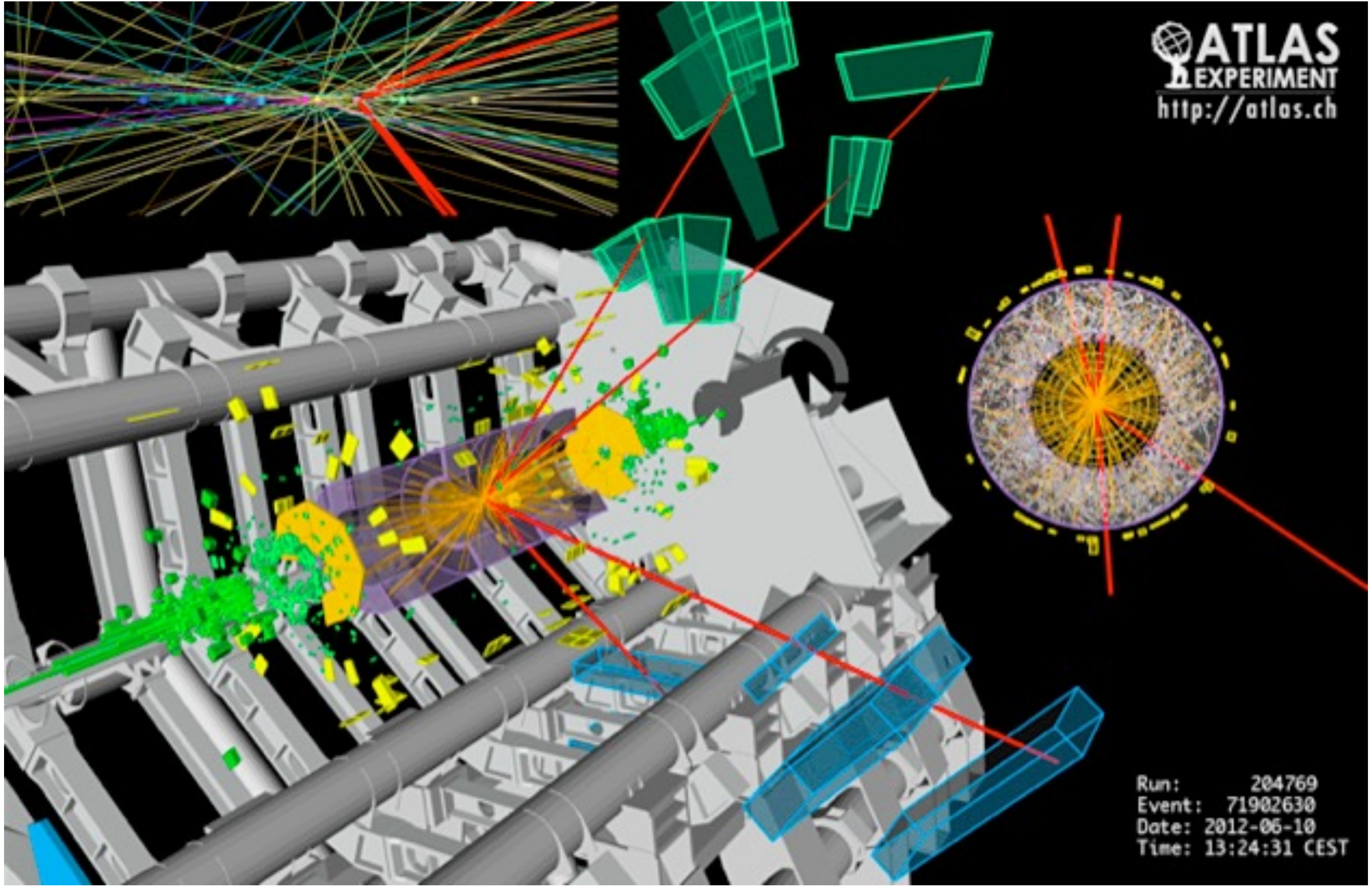

SM Higgs Boson Production

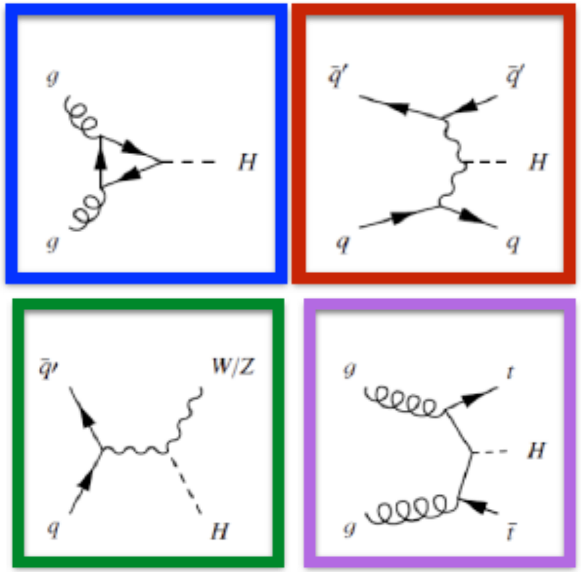

Production	Cross section [pb]	
process	$\sqrt{s} = 7$ TeV	$\sqrt{s} = 8$ TeV
ggF	15.0 ± 1.6	19.2 ± 2.0
VBF	1.22 ± 0.03	1.57 ± 0.04
WH	0.573 ± 0.016	0.698 ± 0.018
ZH	0.332 ± 0.013	0.412 ± 0.013
bbH	0.155 ± 0.021	0.202 ± 0.028
ttH	0.086 ± 0.009	0.128 ± 0.014
tH	0.012 ± 0.001	0.018 ± 0.001
Total	17.4 ± 1.6	22.3 ± 2.0

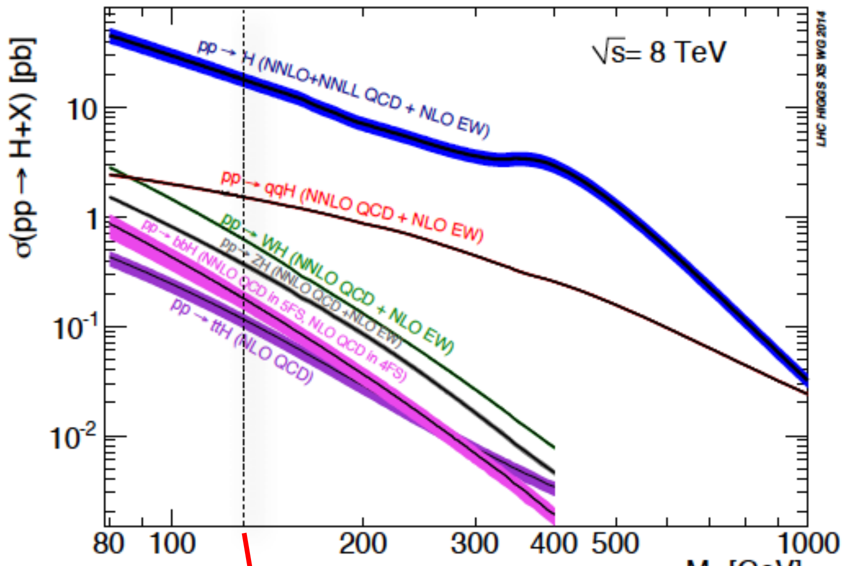

arxiv 1101.0593

ggF	**~86%**	Gluon Fusion
VBF	**~7%**	Vector Boson Fusion
VH	**~5%**	Higgs-strahlung
bbH/ttH	**~1.5%**	ttbar associated production

$\sigma_{tot}(13\text{ TeV}) = \sim 2\sigma_{tot}(8\text{ TeV})$

Higgs Boson decay modes

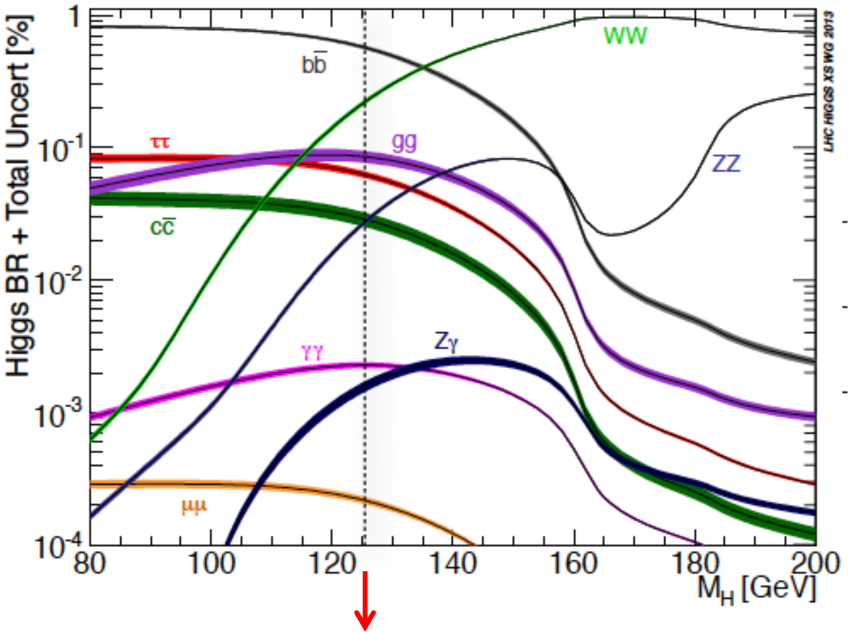

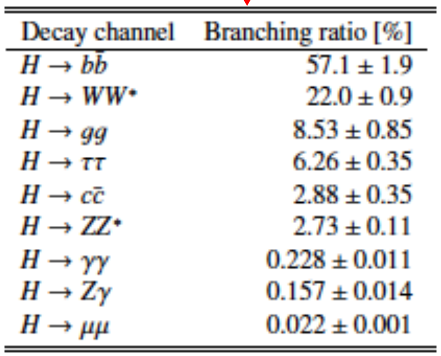

Decay channel	Branching ratio [%]
$H \rightarrow b\bar{b}$	57.1 ± 1.9
$H \rightarrow WW^*$	22.0 ± 0.9
$H \rightarrow gg$	8.53 ± 0.85
$H \rightarrow \tau\tau$	6.26 ± 0.35
$H \rightarrow c\bar{c}$	2.88 ± 0.35
$H \rightarrow ZZ^*$	2.73 ± 0.11
$H \rightarrow \gamma\gamma$	0.228 ± 0.011
$H \rightarrow Z\gamma$	0.157 ± 0.014
$H \rightarrow \mu\mu$	0.022 ± 0.001

Higgs couplings (tree level)

$g_{HWW} = g m_W$

$g_{HZZ} = g \frac{m_Z}{2\cos\theta_W}$

$g_{Hee} = g \frac{m_e}{2m_W}$

They are proportional to the mass

Most used decay modes are built using isolated leptons (e,μ), photons and missing energy

H→ZZ*→4l(e,μ)	**~0.013%**
H→γγ	**~0.23%**
H→ττ	**~6.3%**
H→WW→lνlν	**~1.1%**

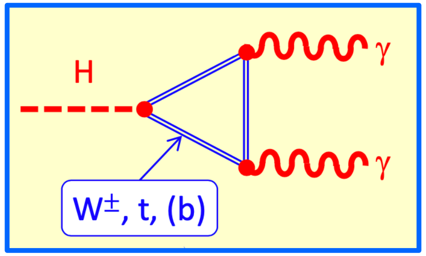

Higgs properties: total width versus M_H

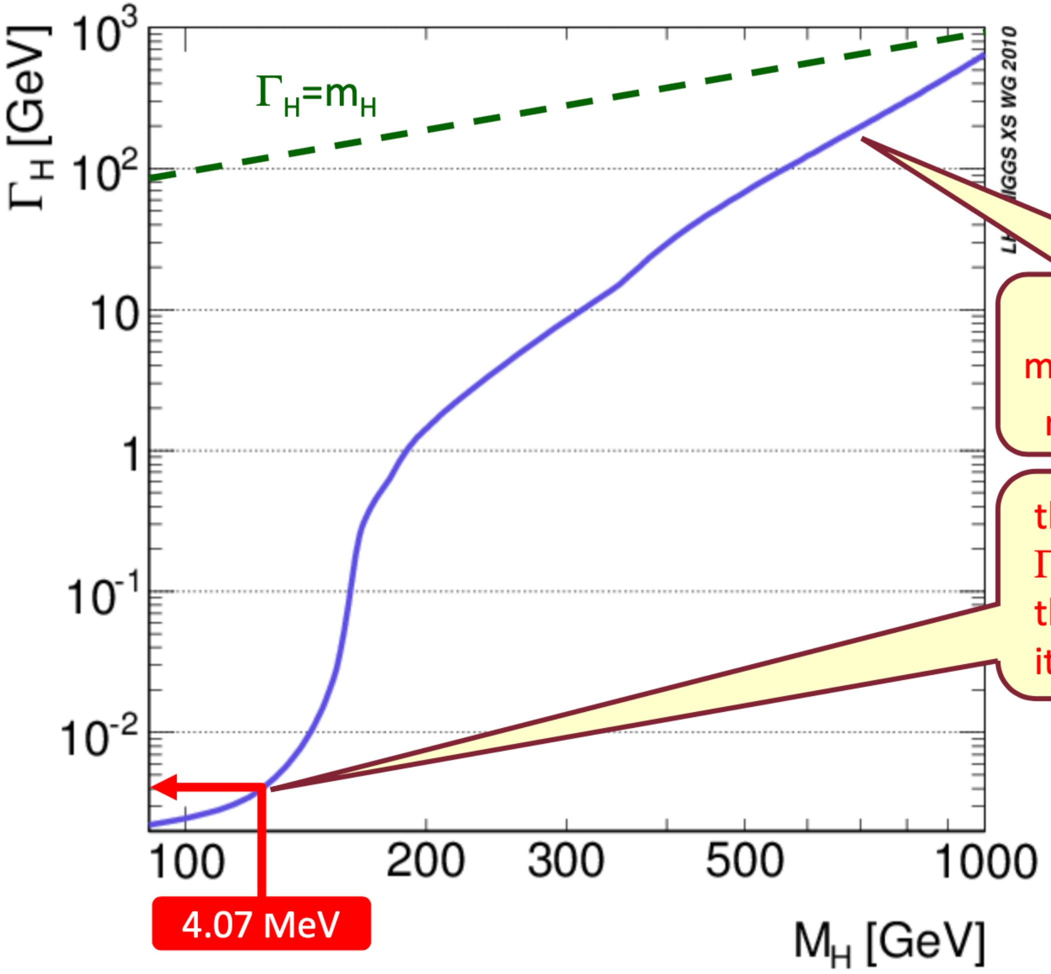

roughly $\propto m_H^3$
$m_H \approx 1.4$ TeV $\rightarrow \Gamma_{tot} \approx m_H$, not anymore a particle

the direct measure of Γ_H is a powerful test of the SM. How measure it ? ideas welcome !

Higgs discovery: H → ZZ* → 4 leptons

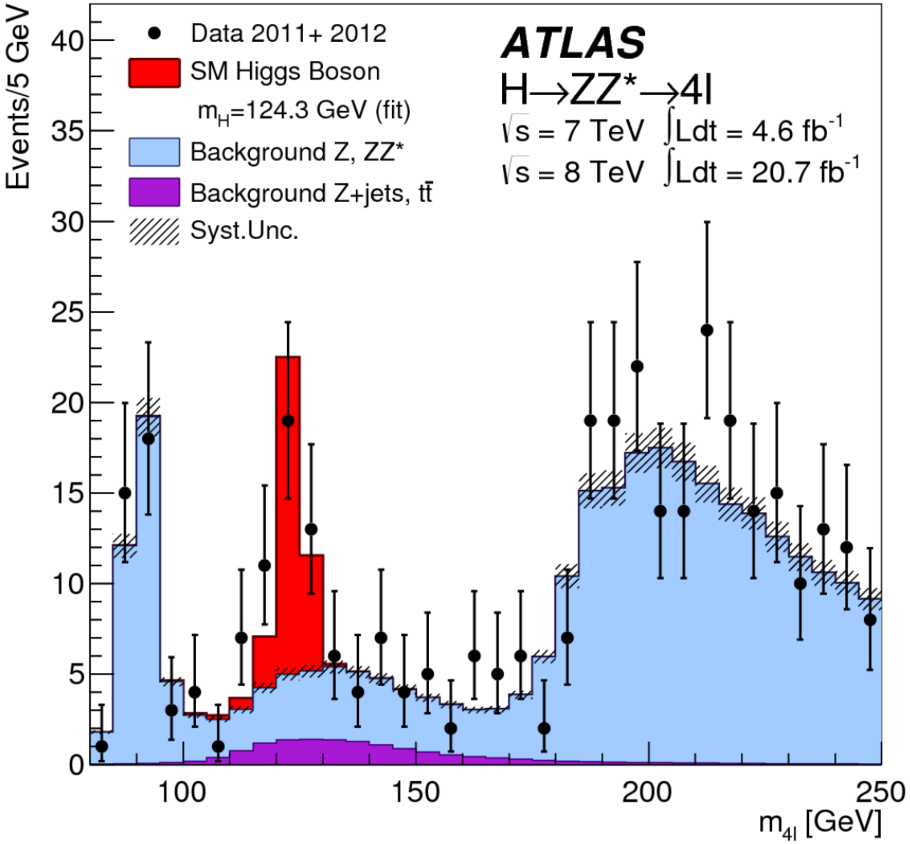

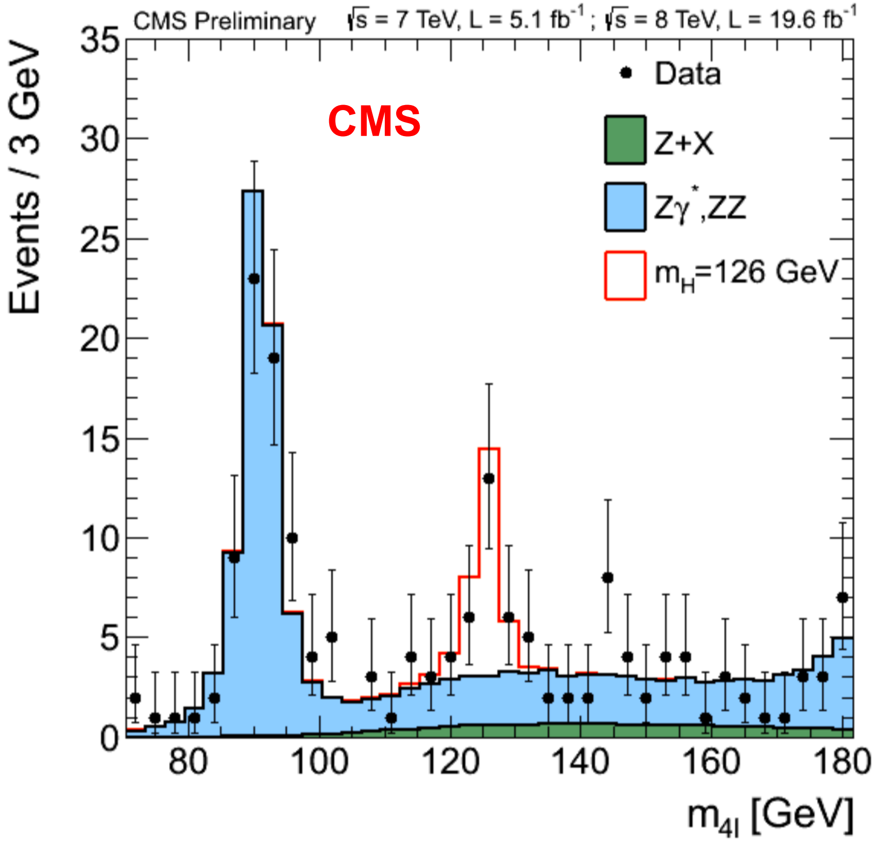

Higgs discovery: H →γγ

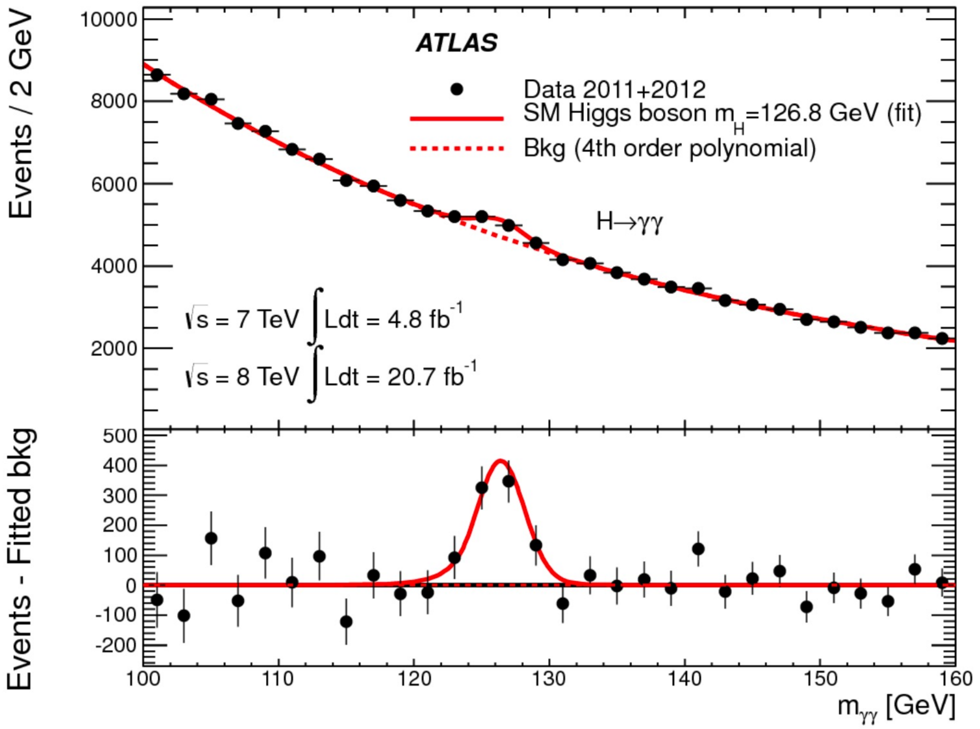

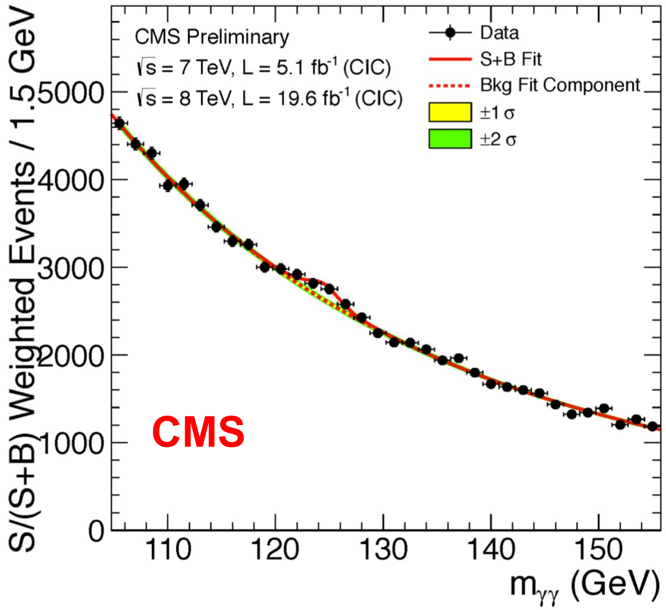

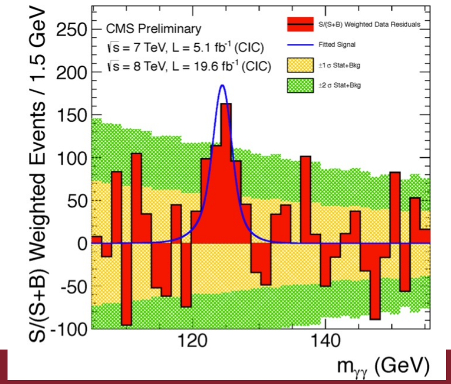

Higgs Boson Mass Measurement

- Precise measurement of m_H from channels with the best mass resolution:
  $H\to\gamma\gamma$ and $H\to ZZ^*\to 4l$ (e,μ) (but B.R.≈0.25% only)
- Dominant uncertainties:
  photon energy scale ($H\to\gamma\gamma$), statistics ($H\to 4l$)

H → ZZ* → 4l (e,μ)

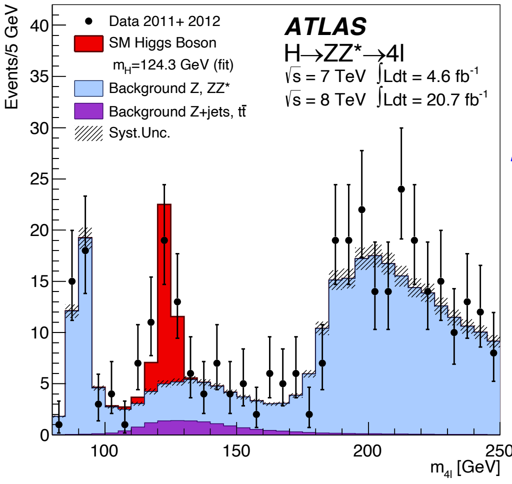

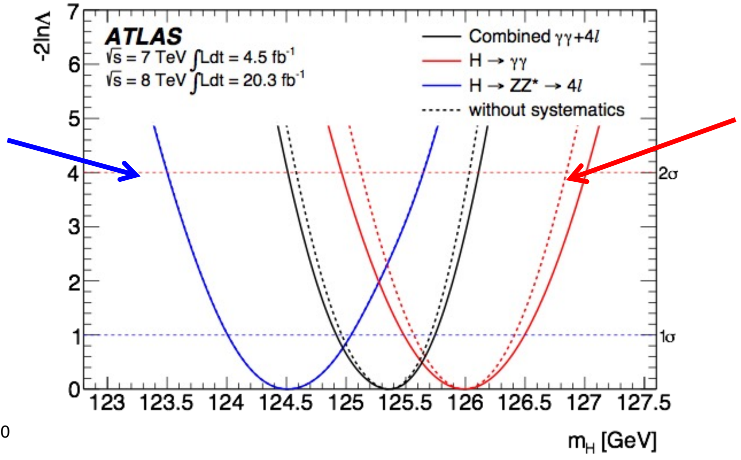

H → γγ

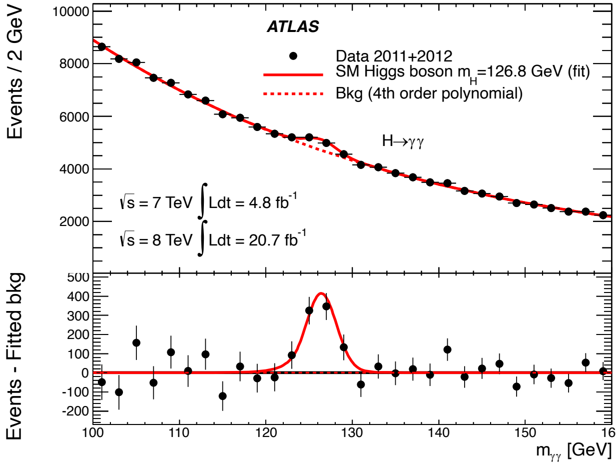

Combined mass: m_H=125.36±0.37 (stat) ±0.18 (syst) GeV

Combined Higgs Boson Mass (Run1)

ATLAS-CMS PRL 114 (2015) 191803

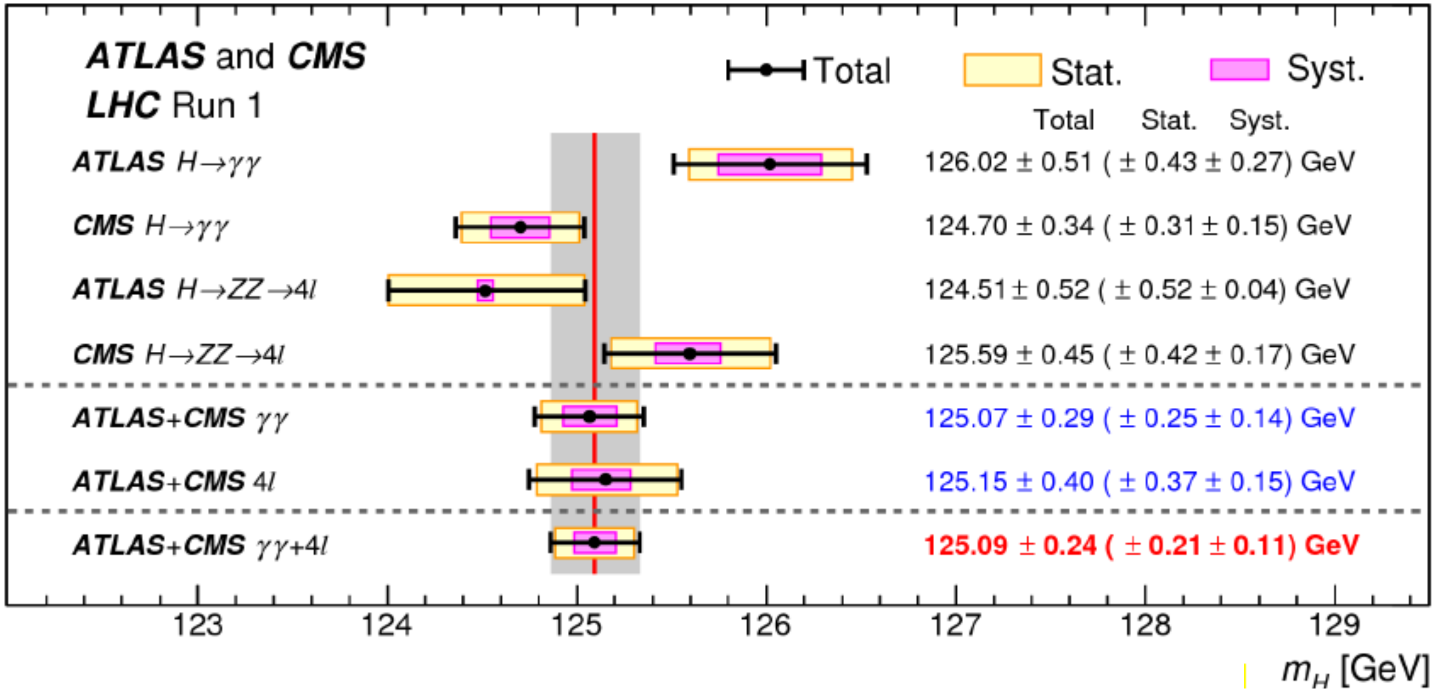

m_H=125.09±0.24 GeV

$$\frac{\Delta m}{m} = 0.2\%$$

Higgs Boson Spin Measurement

- Test SM (0+) against various models
  - Spin-2 Higgs
  - Spin-0 odd (BSM Higgs)
  - (Spin-1 ruled out by observation of H→ γγ decays)

- In all tested cases non-SM models rejected at >99% CL

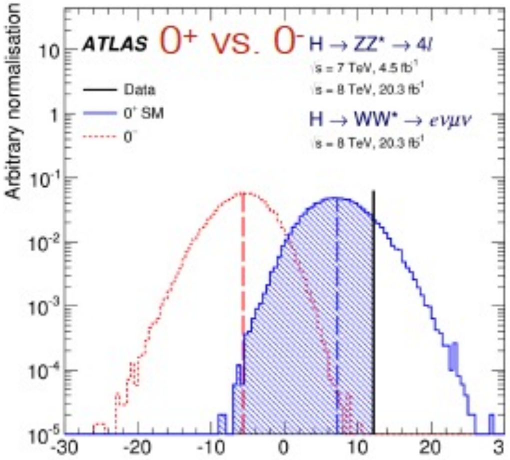

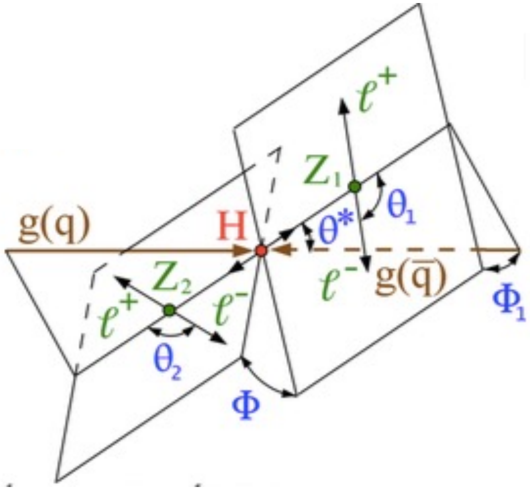

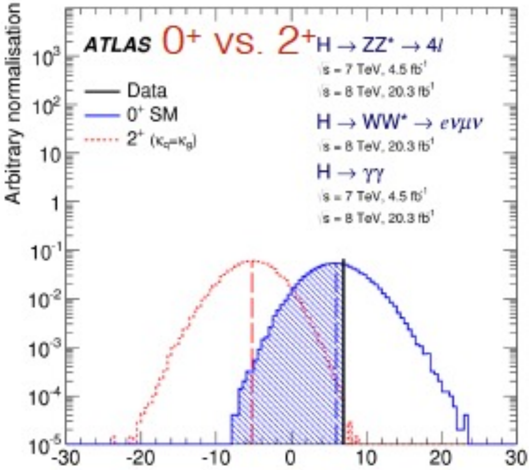

(Multivariate analysis (MVA) based on angular variables)

Comparison with SM expectations

Measure the ratio between observed rate and SM Higgs boson expectation

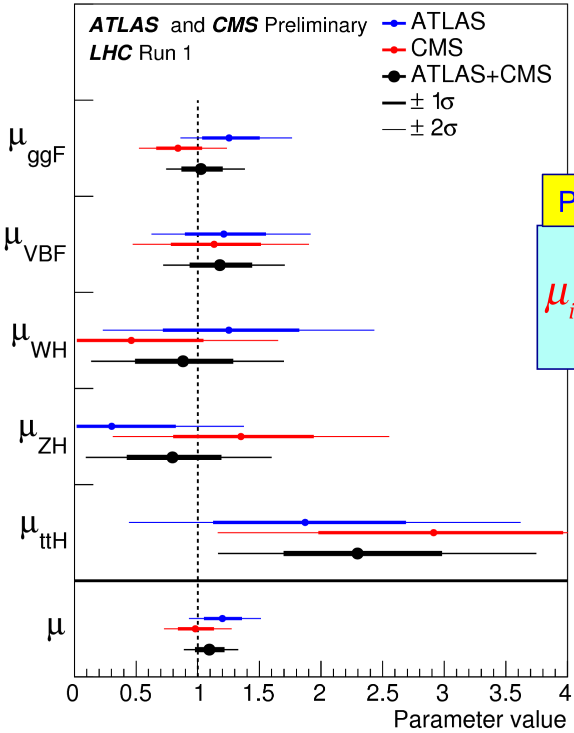

Production

$$\mu_i = \frac{\sigma_i}{(\sigma_i)_{SM}}$$

(μ on production modes have been combined assuming SM BR for the decay)

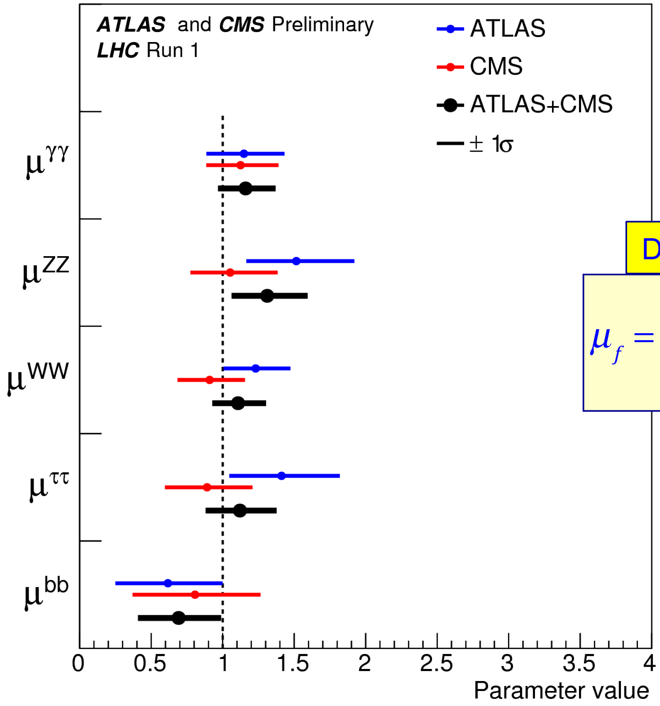

Decay

$$\mu_f = \frac{BR_f}{(BR_f)_{SM}}$$

Results are SM like (all $\mu_s \sim 1$)

Higgs Boson Couplings (Run1)

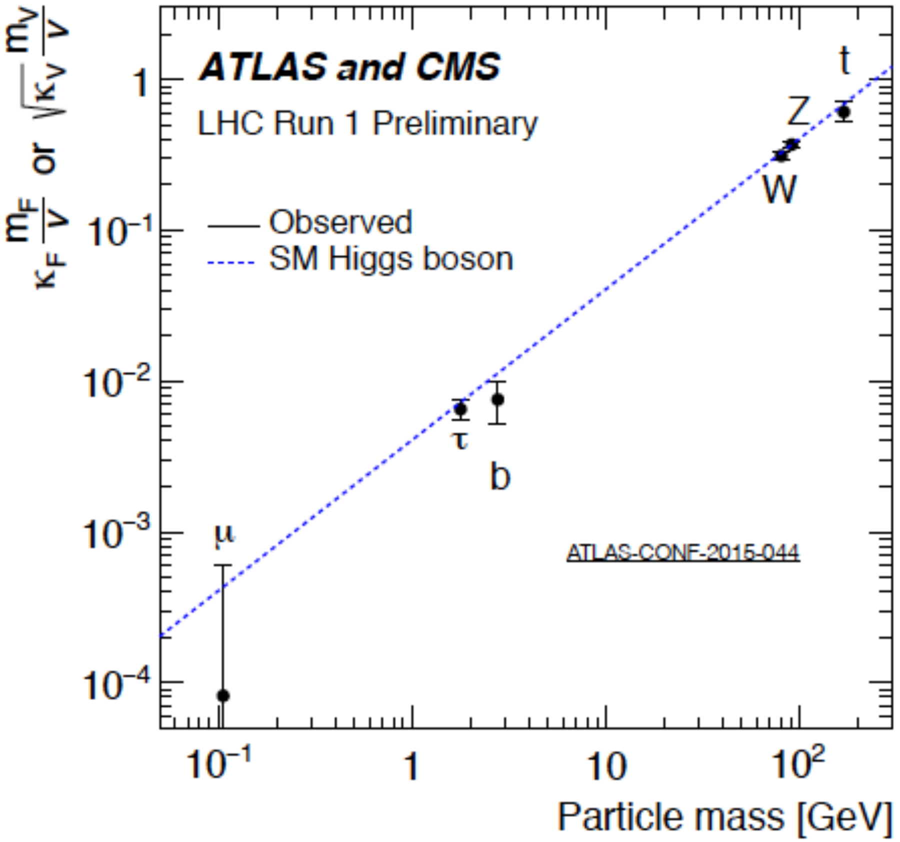

These are not the latest measured couplings

Coupling strengths scale with mass just as predicted by the SM

Higgs Latest Results

- ❑ We will have a dedicated lecture on this subject

Top Physics

The ”needs” for top quark

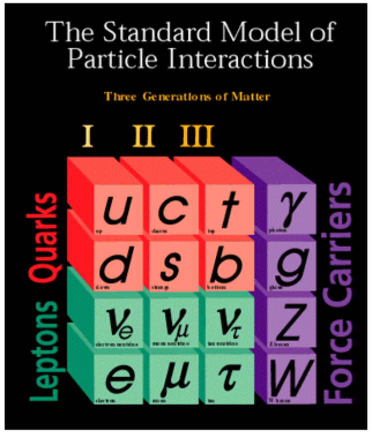

The existence of the Top Quark is predicted by the SM and it is required to explain a number of observations.

Top quark has been discovered at the Tevatron in 1995

Example: absence of the decay $K^0 \rightarrow \mu^+\mu^-$

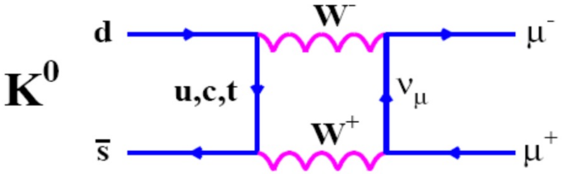

In the Standard Model the top quark cancels the contributions from the u and c quarks

Example: Electro-magnetic anomalies

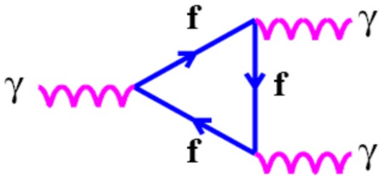

This triangle diagram leads to infinities in the theory unless

$$\sum_f Q_f = 0$$

where the sum is over all fermions (and colours)

$$\sum_f Q_f=[3 \times (-1)]+[3 \times 0]+[3 \times 3 \times \frac{2}{3}]+[3 \times 3 \times (-\frac{1}{3})]=0$$

The Tevatron

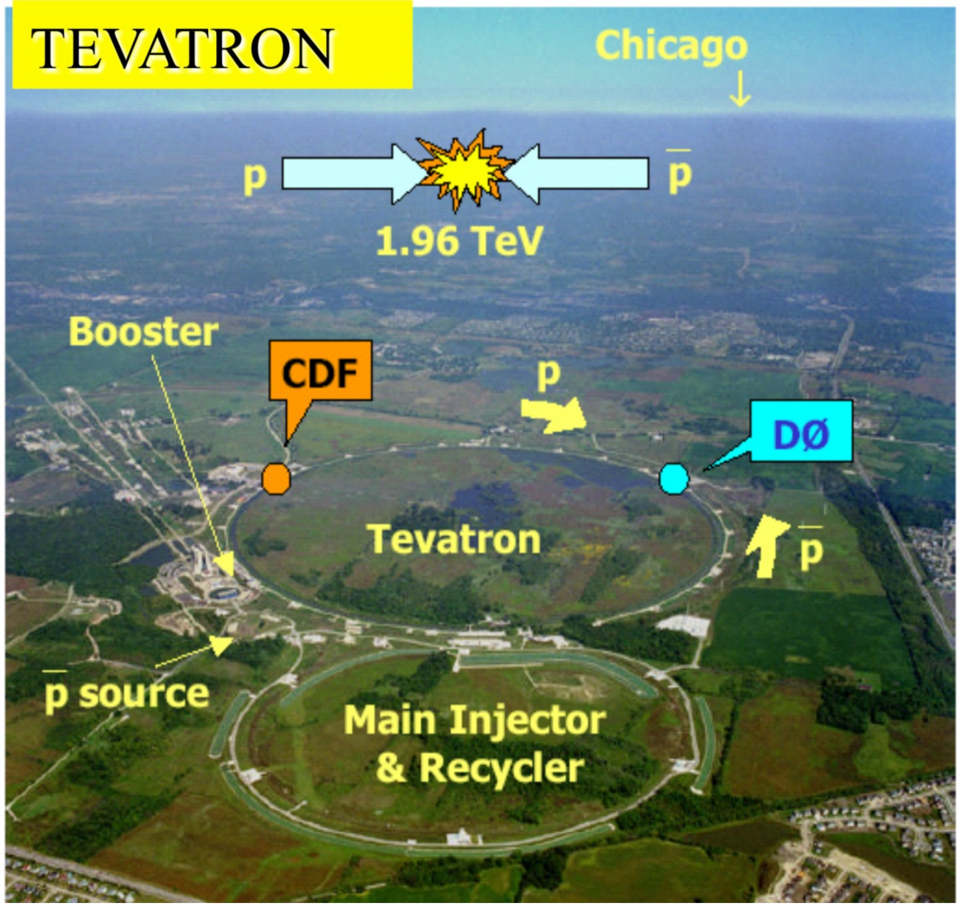

RUN-2 Collider Upgrade

RUN-1 Collider: 1.8 TeV

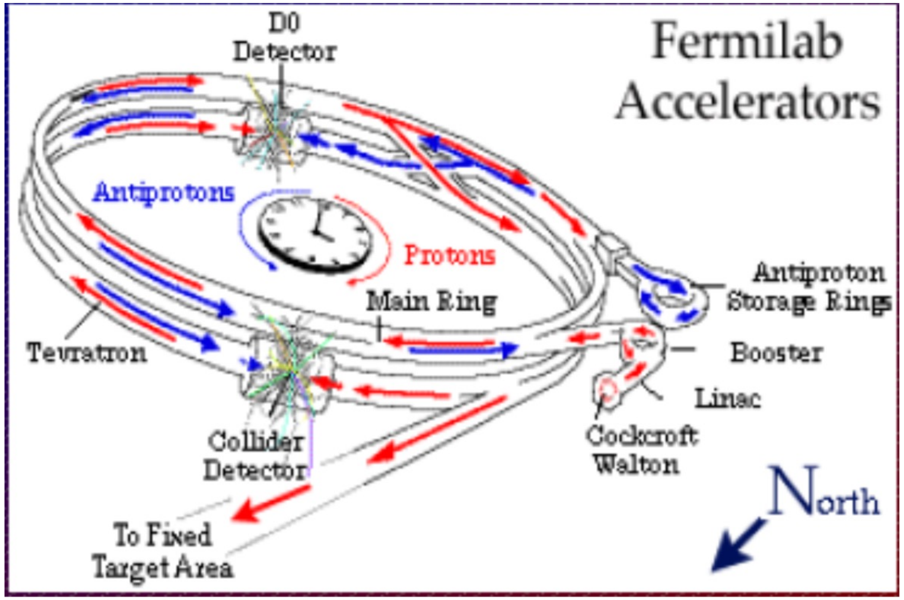

Main Ring and Collider in the same tunnel

Top (pair) production at the hadron colliders

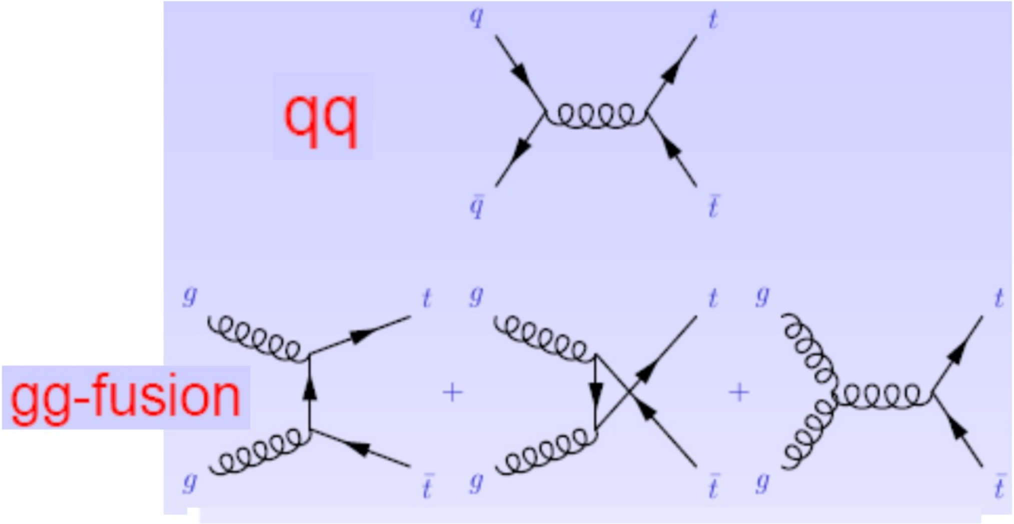

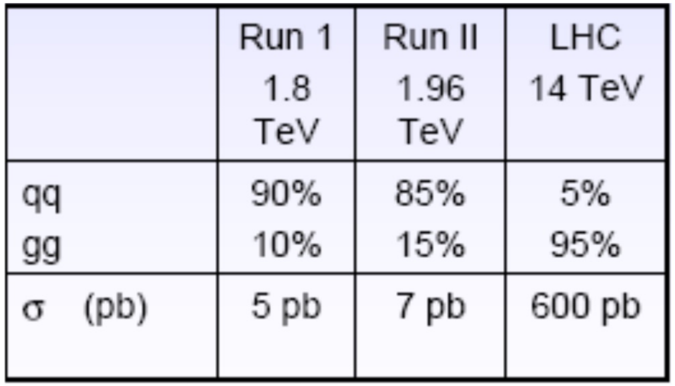

	Run 1 1.8 TeV	Run II 1.96 TeV	LHC 14 TeV
qq	90%	85%	5%
gg	10%	15%	95%
σ (pb)	5 pb	7 pb	600 pb

At LHC the gluon fusion is the dominant channel

Top quark decay

❑ top quark, being heavier than W, decays mostly into a W and a b quark:

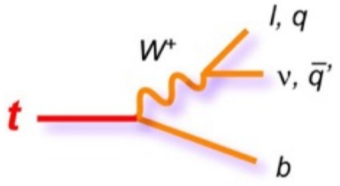

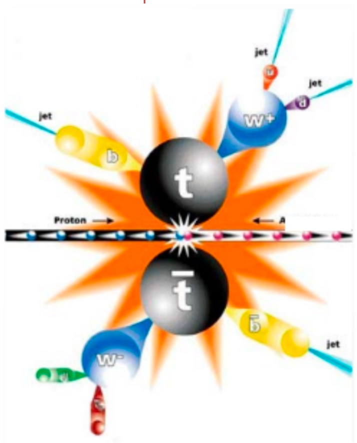

❑ Due to the very high mass, the top quark lifetime is very short: $\tau_{top} \approx 5 \cdot 10^{-25}\ s$

❑ It is shorter than the typical hadronisation timescale: $\tau_{hadr} \approx 10^{-23}\ s$.

❑ Therefore top quark decays before hadronising (no topponium bound state); it offers a unique opportunity to study the properties of a "bare" quark which are transferred to its decays products, e.g. its information.

❑ The final states dipends on the different W decays, but a b quark is always present:

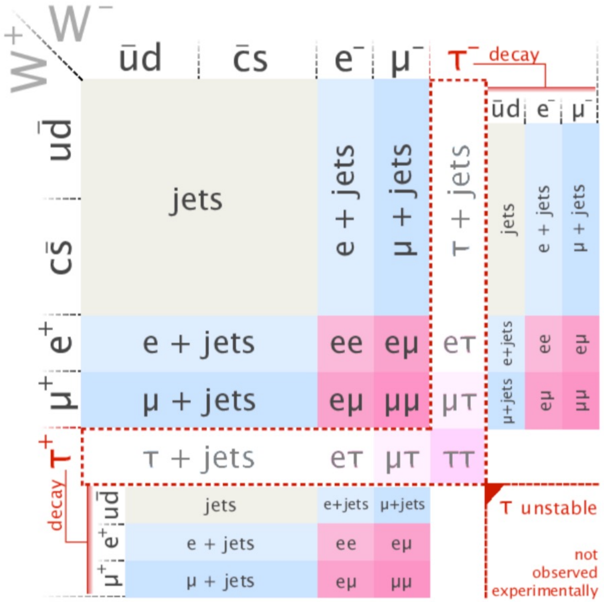

W^+ \ W^-	$\bar{u}d$	$\bar{c}s$	e^-	μ^-	τ^-
$u\bar{d}$	jets		e + jets	μ + jets	τ + jets
$c\bar{s}$					
e^+	e + jets		ee	eμ	eτ
μ^+	μ + jets		eμ	μμ	μτ
τ^+	τ + jets		eτ	μτ	ττ

○ full hadronic
● semileptonic
● dileptonic

$$
\begin{aligned}
Br(W \to \ell\nu) &= 10.9\,\% \\
Br(W \to u\bar{d}, c\bar{s}) &= 67.4\,\%
\end{aligned}
$$

Top quark reconstruction

- A $t\bar{t}$ events contains:
  - ⋆ At least 2 b-quark jets
- and
  - ⋆ Either 2 charged lepton and missing transverse energy (E_{T}^{miss}) (neutrinos)
  - ⋆ Or 1 charged lepton, E_{T}^{miss} and at least 2 more jets
  - ⋆ Or at least 4 more jets
- All detector components used to identify the above leptons (mostly electrons and muons), jets, b-quark jets, E_{T}^{miss}
- Top quarks events can be used to understand the performance of the detector
- Reconstruct $t\bar{t}$ events in data and Monte Carlo (MC) events using e.g. kinematics fits

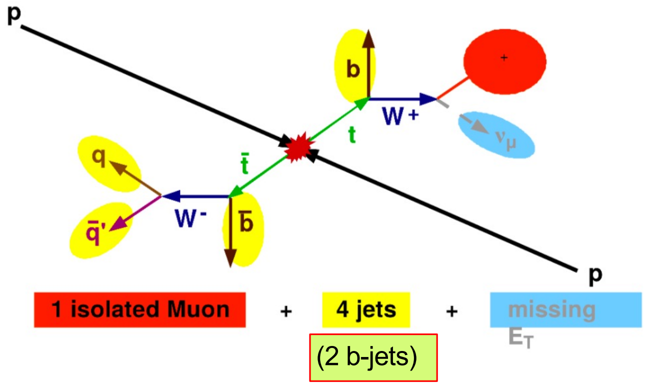

Example: semi-leptonic topology

Example of top-top signature

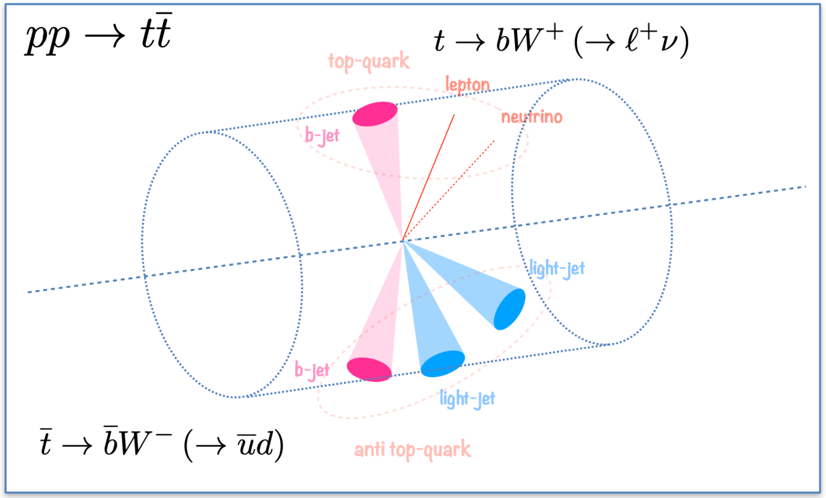

Reconstruction level typical selection

- One identified and isolated lepton (electron or muon) ET/ pT> 25 GeV and with in |eta|<2.5.
- Missing transverse momentum in excess of 20 GeV.
- Four jets wit ET> 35 GeV and |eta|<2.5.
- Two jets tagged as b-jets.

Top Quark Discovery: February 24th 1995

- February 24th, 1995: Simultaneous submission of “top-quark discovery” papers by CDF and D0 @ Tevavtron, Fermilab
  - ⋆ Luminosity collected at $\mathrm{D0}\ 50\,\mathrm{pb}^{-1}$
  - ⋆ $\mathrm{m_{top}} = 199 \pm 30\,\mathrm{GeV}$
  - ⋆ $\sigma_{\mathrm{t\bar{t}}} = 6.4 \pm 2.2\,\mathrm{pb}$
  - ⋆ Background-only hypothesis rejected at $4.6\,\sigma$
  - ⋆ Luminosity collected at $\mathrm{CDF}\ 67\,\mathrm{pb}^{-1}$
  - ⋆ $\mathrm{m_{top}} = 176 \pm 13\,\mathrm{GeV}$
  - ⋆ $\sigma_{\mathrm{t\bar{t}}} = 6.8^{+3.6}_{-2.4}\,\mathrm{pb}$
  - ⋆ Background-only hypothesis rejected at $4.8\,\sigma$

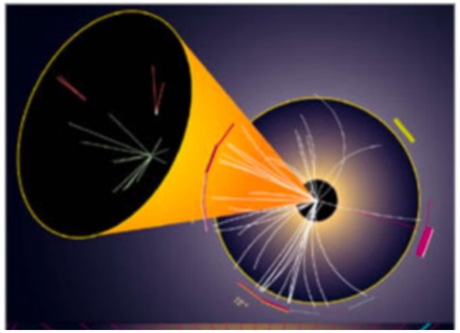

CDF: the big cone is an electron from a W decay.

D0: two muons (in blue, one inside a jet), 4 jets and the neutrino (pink) identified as missing p_T

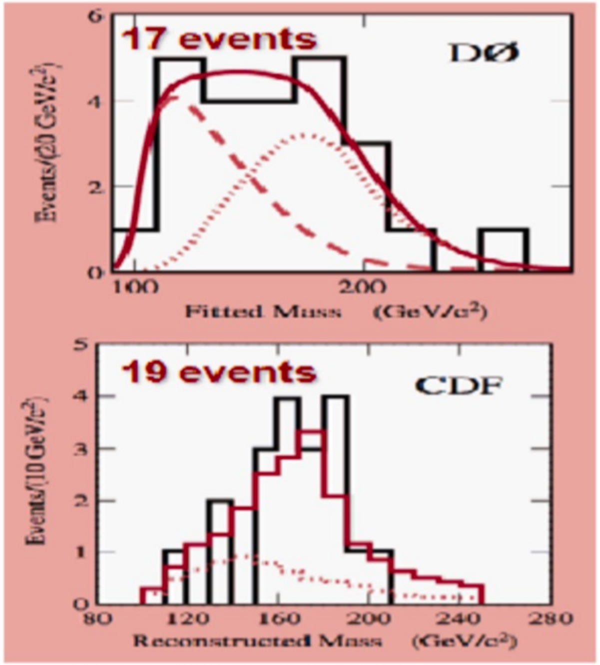

1995, CDF and DØ experiments, Fermilab

Top reconstructed mass

Top quark physics

- **Top proprieties**
  - ⋆ Mass, width, charge, spin, ...
- **Top production**
  - ⋆ $t\bar{t}$ cross-section, production dynamics, spin polarization
- **Top decay**
  - ⋆ V_{tb}, brancing ratios, rare decays, W helicity

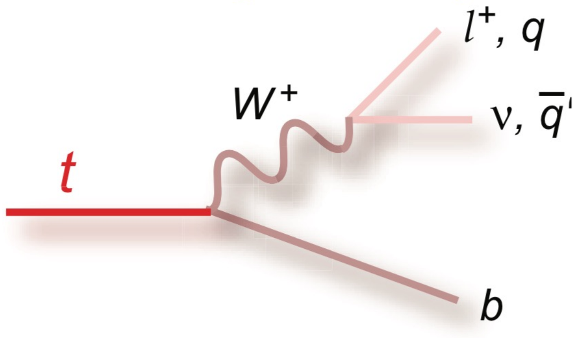

- Top quark allows tests of the participating forces
- Top quark plays an important role in the search for new physics beyond the SM (BSM) (new particles decaying to top quark)
- Top quark events are background to many physics processes

Top pair production cross section at LHC

Main production diagrams
At tree level leading order
$O(\alpha_S^2)$

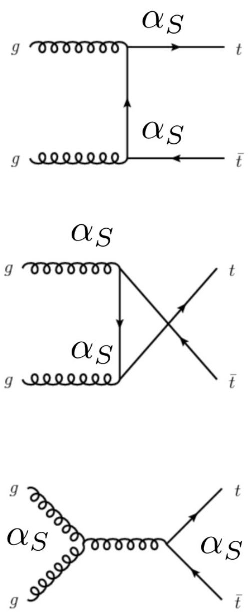

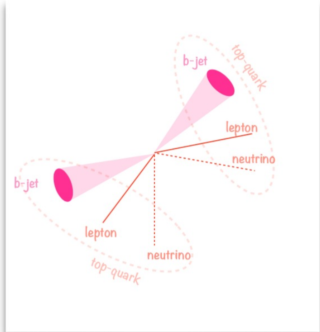

Di-lepton topology:

Precise determination of cross section in the different flavour electron-muon channel in particular. Excellent signal to background ratio. Lower stats (4%).

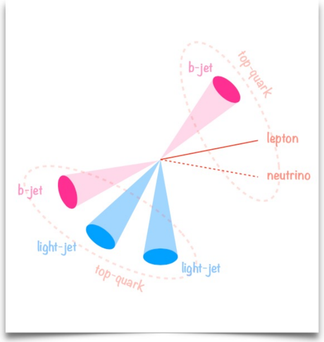

Semi-leptonic topology:

Best compromise between statistics (30%) and signal to background ratio.

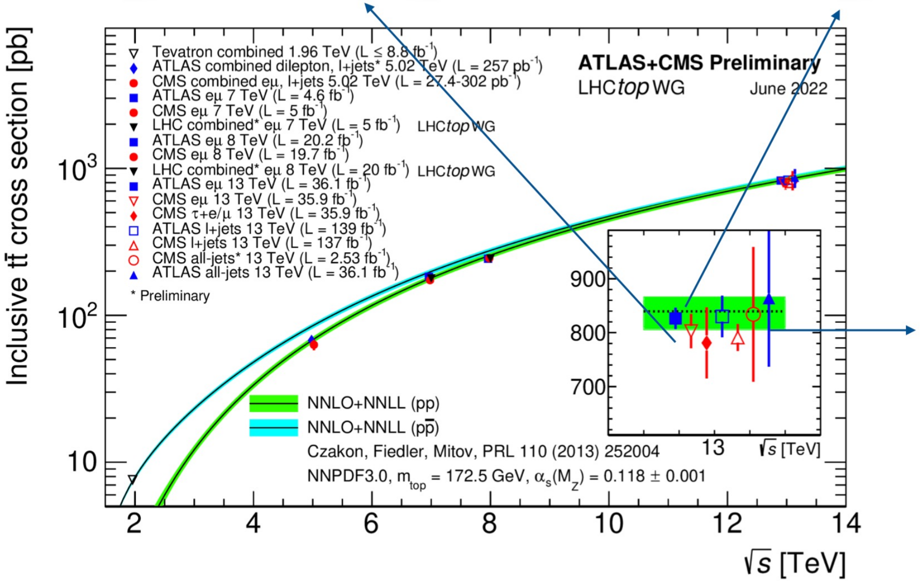

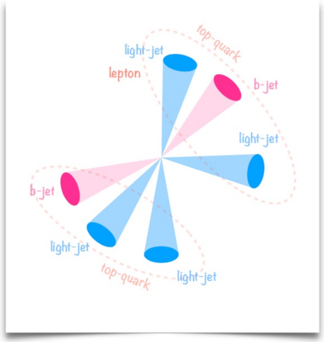

Full hadronic topology:

Largest stats (50%) but larger multi-jet background and large combinatorial.

Single top production cross section

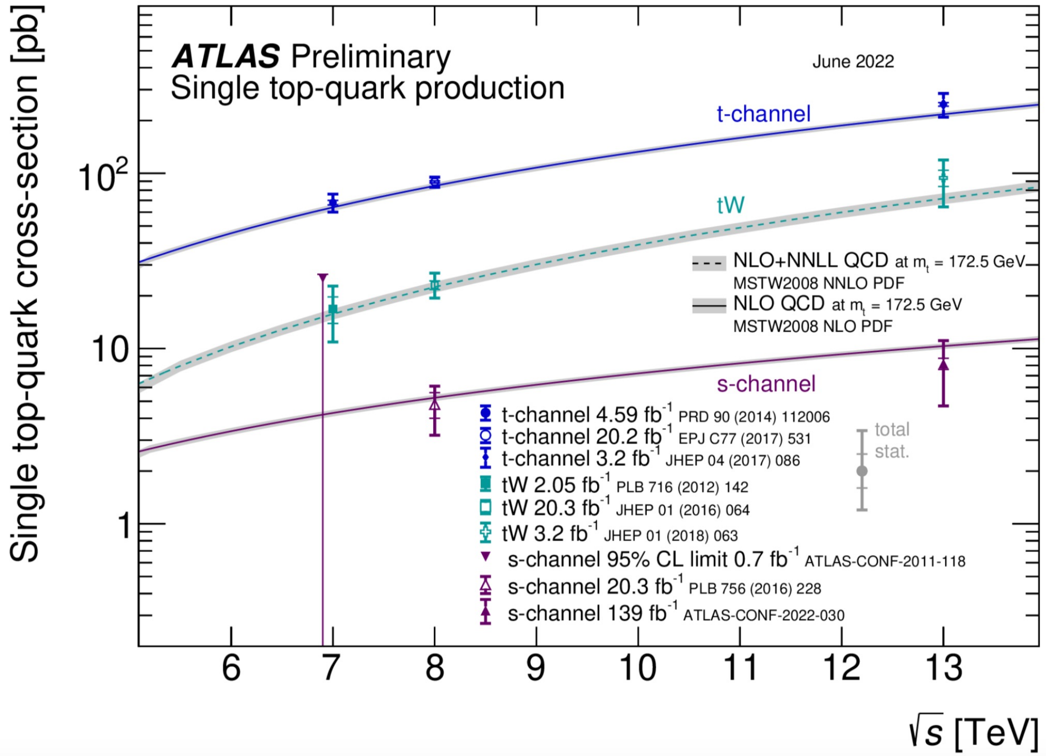

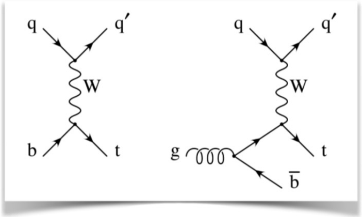

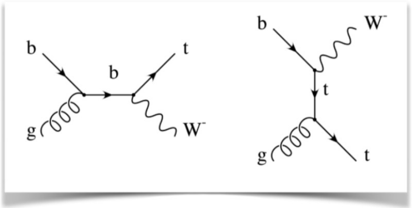

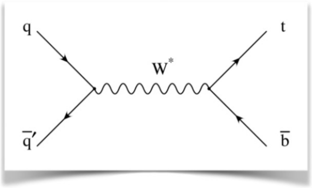

- Can be used to measure $|V_{tb}|$
  - ⋆ Example: $|V_{tb}| = \sqrt{\frac{\sigma_{meas}}{\sigma_{theo.}(V_{tb}=1)}}$
  - ⋆ $|V_{tb}| = 1.02 \pm 0.4(\mathrm{meas.}) \pm 0.02(\mathrm{theo.})$

Top quark mass measurement

- Direct $\mathrm{m_{top}}$ measurements:
  - ⋆ Reconstruct $\mathrm{t\bar{t}}$ events in data and MC
  - ⋆ Reduce backgrounds to obtain a clean sample
  - ⋆ Reconstruct the final state
  - ⋆ Use sophisticated technique to extract the $\mathrm{m_{top}}$, using e.g. a kinematic fit
- Indirect $\mathrm{m_{top}^{pole}}$ measurements
  - ⋆ Instead of fitting to MC distributions "folded" with the detector response unfold the data to e.g parton-level
  - ⋆ Caveat: Larger uncertainties on both theory and experiment
  - ⋆ Measure cross section as function of $\mathrm{m_{top}^{pole}}$ in LO, NLO and NNLO and determine $\mathrm{m_{top}^{pole}}$

Eur. Phys. J. C75 (2015) 330

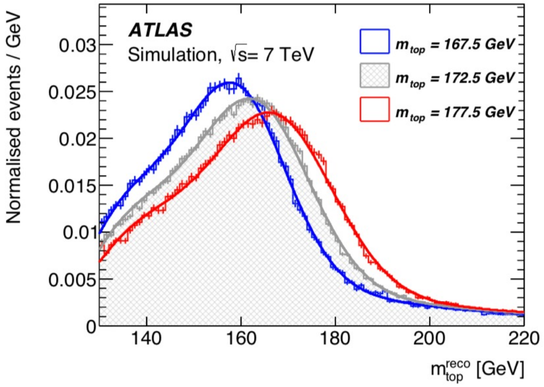

Eur. Phys. J. C74 (2014) 3109

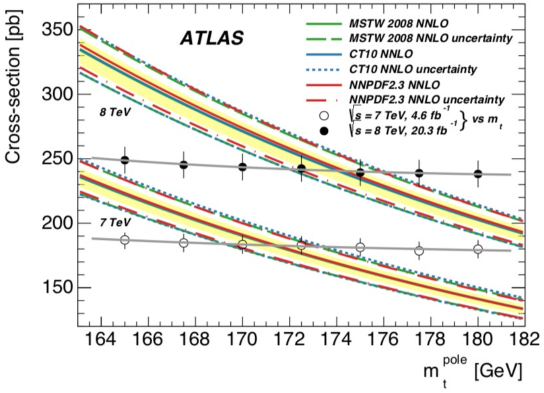

Top quark mass summary

- Direct m_{top} measurements
  - ⋆ Most precise from LHC combinations
  - ⋆ ATLAS: $m_{top} = 172.69 \pm 0.48_{tot}$ GeV
  - ⋆ CMS: $m_{top} = 172.44 \pm 0.48_{tot}$ GeV
- Indirect m_{top} measurements
  - ⋆ Most precise from CMS @ 13 TeV
  - ⋆ CMS: $m_{top}^{pole} = 170.9 \pm 0.8_{tot}$ GeV
  - ⋆ ATLAS: $m_{top}^{pole} = 171.2^{+1.2}_{-1.0}{}_{tot}$ GeV

JHEP 09 (2017) 118

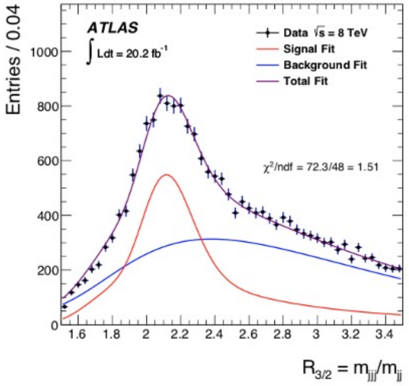

M_{jjj}: top mass
M_{jj}: W mass

Most precise individual top mass from CMS

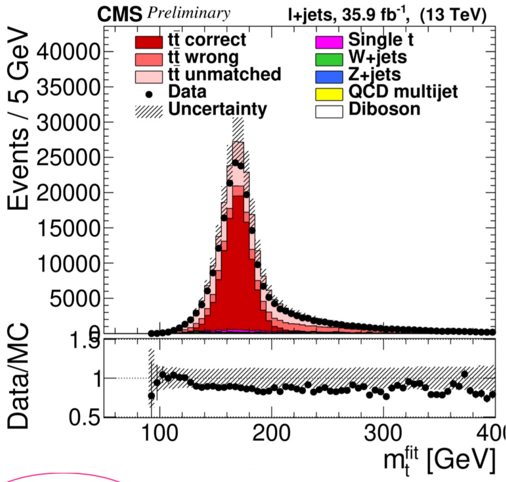

$171.77 \pm 0.04\,(stat) \pm 0.38\,(syst)$ GeV

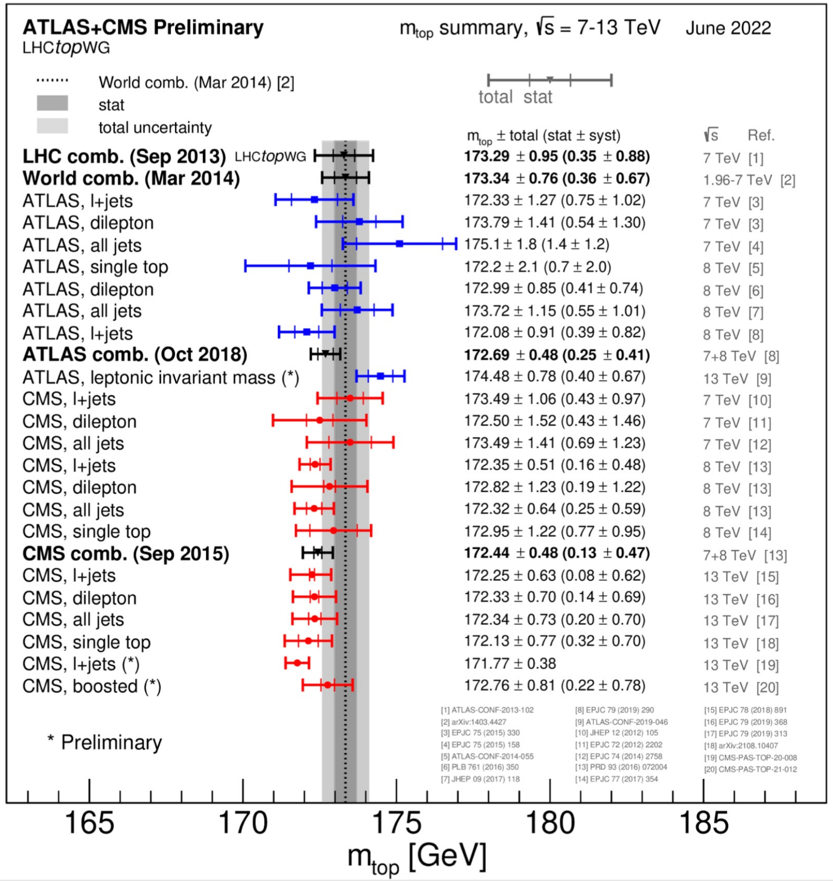

	$m_{top} \pm$ total (stat $\pm$ syst)	$\sqrt{s}$	Ref.
LHC comb. (Sep 2013) LHC*top*WG	**173.29 ± 0.95 (0.35 ± 0.88)**	7 TeV	[1]
World comb. (Mar 2014)	**173.34 ± 0.76 (0.36 ± 0.67)**	1.96-7 TeV	[2]
ATLAS, l+jets	172.33 ± 1.27 (0.75 ± 1.02)	7 TeV	[3]
ATLAS, dilepton	173.79 ± 1.41 (0.54 ± 1.30)	7 TeV	[3]
ATLAS, all jets	175.1 ± 1.8 (1.4 ± 1.2)	7 TeV	[4]
ATLAS, single top	172.2 ± 2.1 (0.7 ± 2.0)	8 TeV	[5]
ATLAS, dilepton	172.99 ± 0.85 (0.41 ± 0.74)	8 TeV	[6]
ATLAS, all jets	173.72 ± 1.15 (0.55 ± 1.01)	8 TeV	[7]
ATLAS, l+jets	172.08 ± 0.91 (0.39 ± 0.82)	8 TeV	[8]
ATLAS comb. (Oct 2018)	**172.69 ± 0.48 (0.25 ± 0.41)**	7+8 TeV	[8]
ATLAS, leptonic invariant mass (*)	174.48 ± 0.78 (0.40 ± 0.67)	13 TeV	[9]
CMS, l+jets	173.49 ± 1.06 (0.43 ± 0.97)	7 TeV	[10]
CMS, dilepton	172.50 ± 1.52 (0.43 ± 1.46)	7 TeV	[11]
CMS, all jets	173.49 ± 1.41 (0.69 ± 1.23)	7 TeV	[12]
CMS, l+jets	172.35 ± 0.51 (0.16 ± 0.48)	8 TeV	[13]
CMS, dilepton	172.82 ± 1.23 (0.19 ± 1.22)	8 TeV	[13]
CMS, all jets	172.32 ± 0.64 (0.25 ± 0.59)	8 TeV	[13]
CMS, single top	172.95 ± 1.22 (0.77 ± 0.95)	8 TeV	[14]
CMS comb. (Sep 2015)	**172.44 ± 0.48 (0.13 ± 0.47)**	7+8 TeV	[13]
CMS, l+jets	172.25 ± 0.63 (0.08 ± 0.62)	13 TeV	[15]
CMS, dilepton	172.33 ± 0.70 (0.14 ± 0.69)	13 TeV	[16]
CMS, all jets	172.34 ± 0.73 (0.20 ± 0.70)	13 TeV	[17]
CMS, single top	172.13 ± 0.77 (0.32 ± 0.70)	13 TeV	[18]
CMS, l+jets (*)	171.77 ± 0.38	13 TeV	[19]
CMS, boosted (*)	172.76 ± 0.81 (0.22 ± 0.78)	13 TeV	[20]

[1] ATLAS-CONF-2013-102
[2] arXiv:1403.4427
[3] EPJC 75 (2015) 330
[4] EPJC 75 (2015) 158
[5] ATLAS-CONF-2014-055
[6] PLB 761 (2016) 350
[7] JHEP 09 (2017) 118
[8] EPJC 79 (2019) 290
[9] ATLAS-CONF-2019-046
[10] JHEP 12 (2012) 105
[11] EPJC 72 (2012) 2202
[12] EPJC 74 (2014) 2758
[13] PRD 93 (2016) 072004
[14] EPJC 77 (2017) 354
[15] EPJC 78 (2018) 891
[16] EPJC 79 (2019) 368
[17] EPJC 79 (2019) 313
[18] arXiv:2108.10407
[19] CMS-PAS-TOP-20-008
[20] CMS-PAS-TOP-21-012

Digression on the mass measurement

The relation between the Monte Carlo template used to fit the mass spectrum and the Field Theoretical parameter of the pole mass is not straightforward.

The top is coloured, so it is impossible to unambiguously associate every object in the final state to it!

These ambiguities lead to an uncertainty on the top mass measurement varying between 1 GeV and 200 MeV.

The pole mass can be measured using observables that are not dependent on the detailed reconstruction of the top system.

e.g. the pole mass can be measured using the top production cross section (at the cost of introducing a dependence on the production prediction).

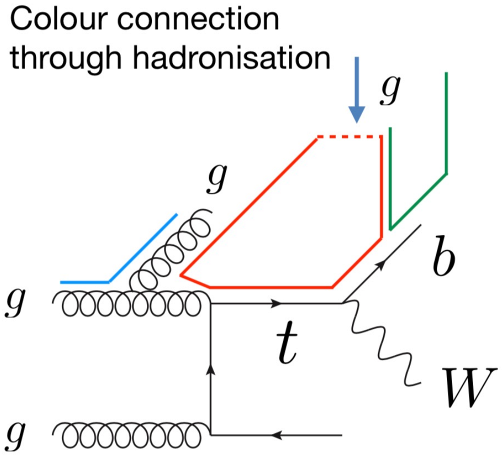
Colour connection through hadronisation

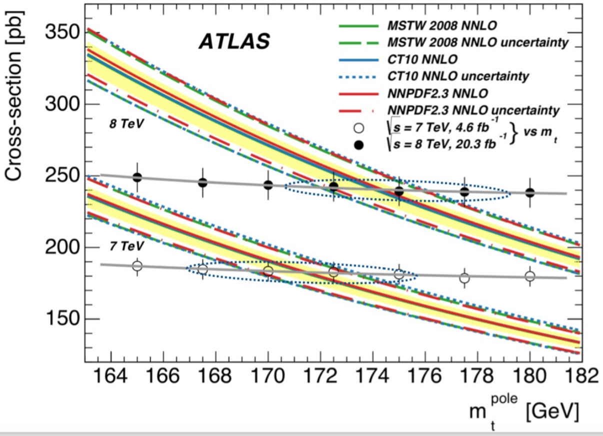

Digression on the mass measurement

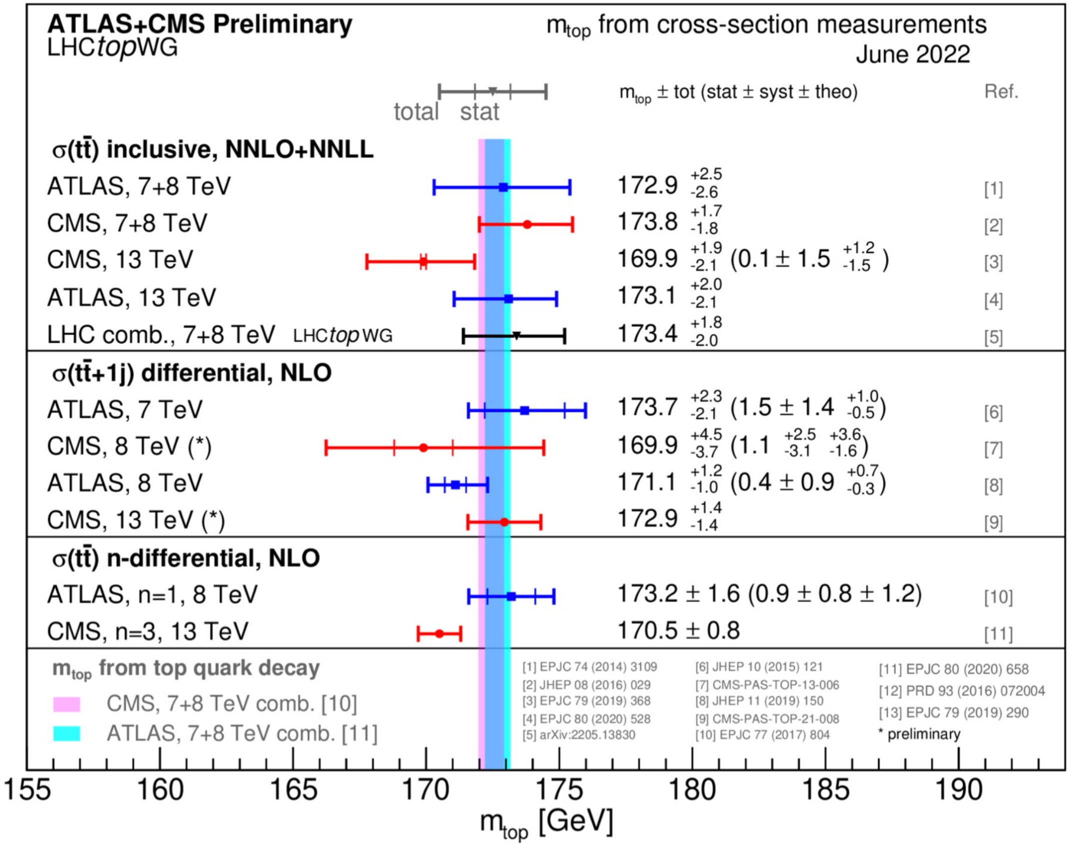

Measurements from cross sections will be limited by prediction uncertainties and luminosity.

Study of the reach in precision at HL-LHC

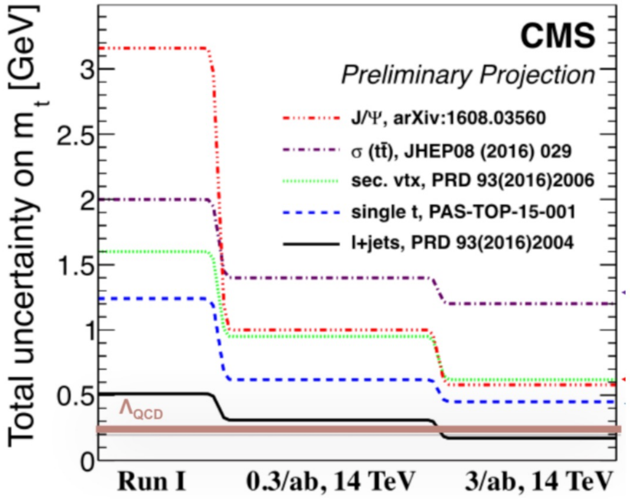

Reaching a floor in the precision on the top mass at around HL-LHC Lambda QCD ~180 MeV

Top quark mass … and the Universe

- The top-quark mass, $\mathrm{m_{top}}$, is a fundamental parameter of the Standard Model (SM)
- Precise determinations of the SM parameters ($\mathrm{m_{top}}, \mathrm{m_W}, \mathrm{m_H}, \ldots$) allow to challenge consistency tests of the SM and to look for signs of new physics beyond the SM (BSM)
- Plots show: (left) Regions of absolute stability, meta-stability and instability of the SM vacuum in the top-quark pole mass and the Higgs mass, $\mathrm{m_{top}^{pole}} - \mathrm{m_H}$, plane; (right) ellipses for the $1\,\sigma$ uncertainties in the $\mathrm{m_{top}^{pole}} - \mathrm{m_H}$ plane confronted with the SM vacuum expectations;

arXiv:1205.6497v2

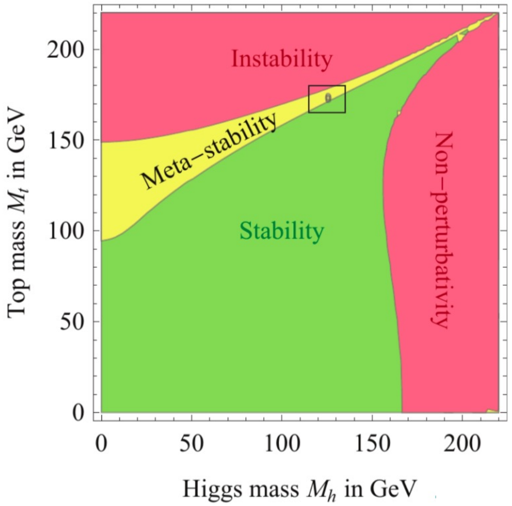

arXiv.1207.0980v3

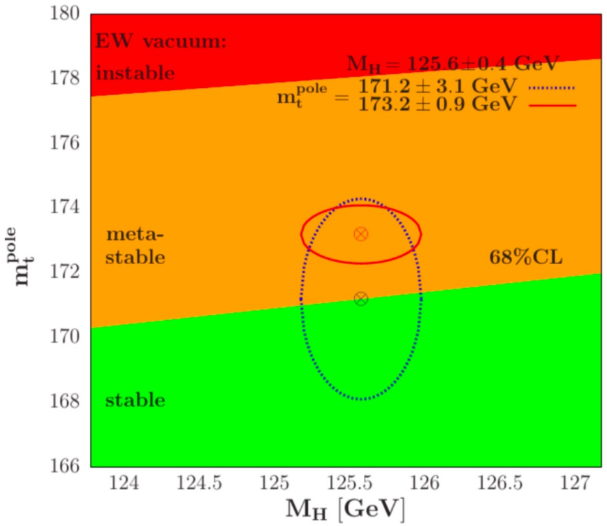

Electroweak fits

- Plot show: electroweak fits at NNLO: contours at 68% and 95% CL obtained from scans of mass of the W, m_W, versus m_{top}

arXiv:1407.3792v1

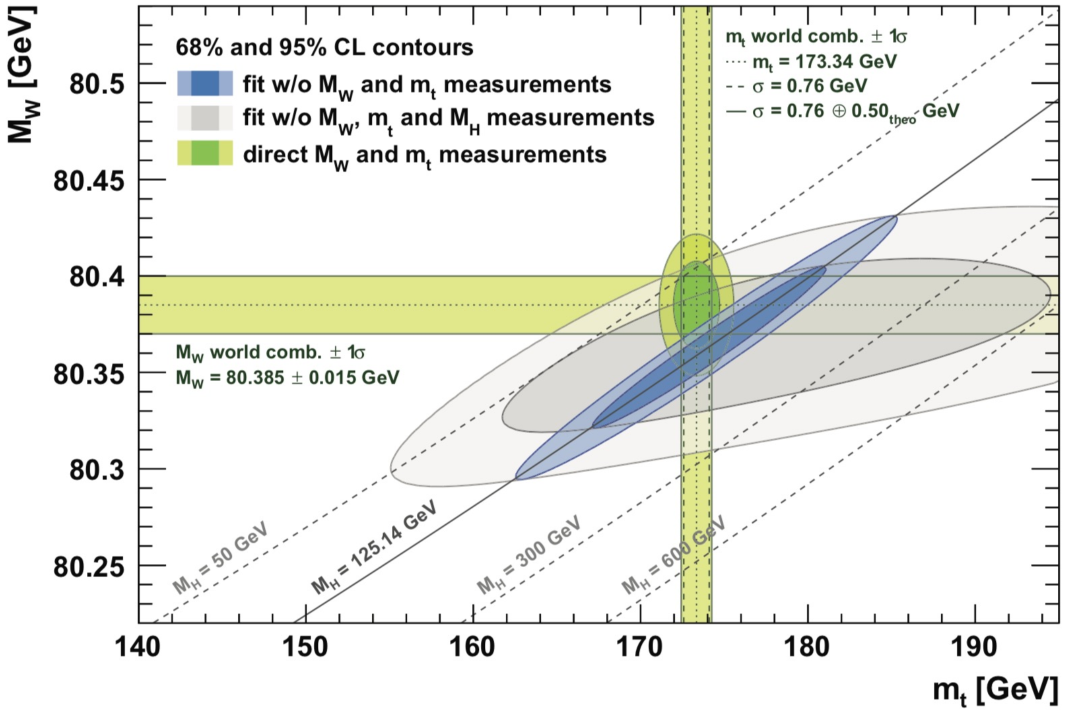

Dark Matter at LHC

Evidence for Dark Matter

*Comprises **majority** of **mass** in Galaxies*
Missing mass on Galaxy Cluster scale Zwicky (1937)

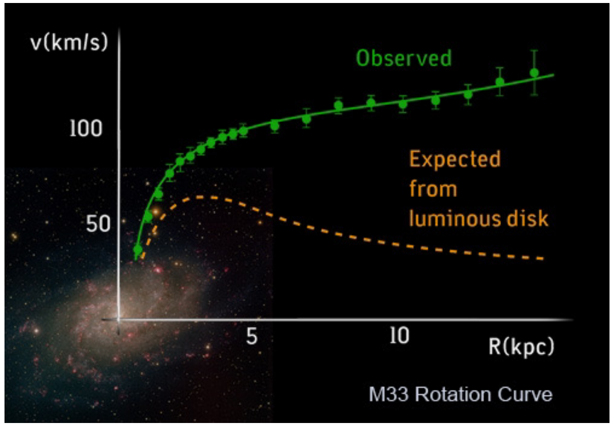

*Large **halos** around Galaxies*
Rotation Curves Rubin+(1980)

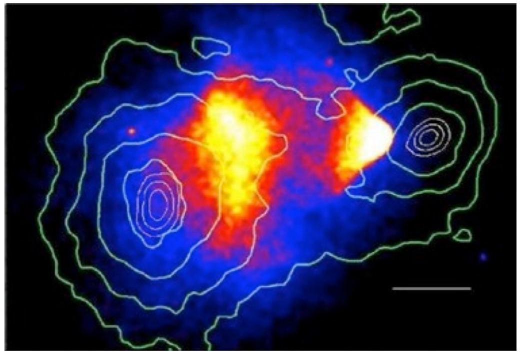

*Almost **collisionless***
Bullet Cluster Clowe+(2006)

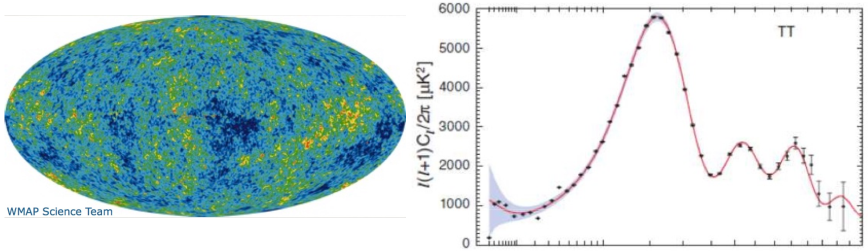

Non-Baryonic Big-Bang Nucleosynthesis,
CMB Acoustic Oscillations
WMAP(2010),*Planck*(2015)

Detecting Dark Matter

Assumption: non-gravitational interaction with ordinary matter

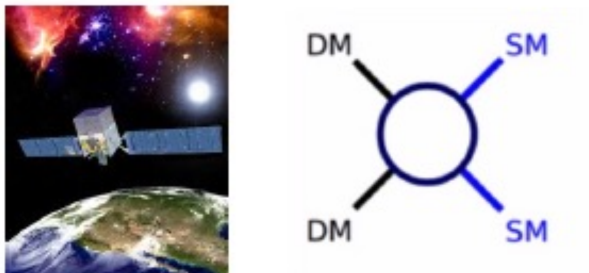

Indirect Detection

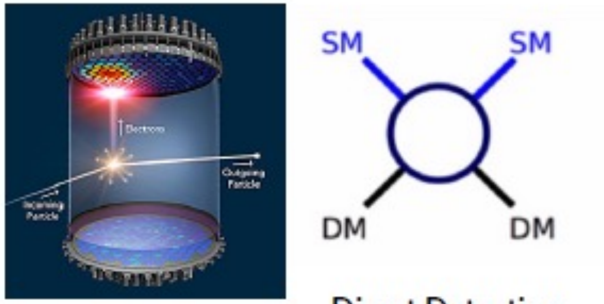

Direct Detection

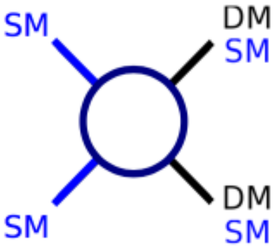

Colliders
(Contact interaction)

Contact interaction (EFT)
“works” if the scale $\Lambda >> Q^2$
(like Fermi theory).
otherwise we need a Simplified Model with (at least) a Mediator

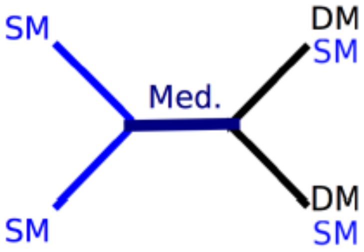

Colliders
(Simplified Models)

Detecting Dark Matter at LHC

Non-interacting DM particles
→ Missing transverse energy (MET)

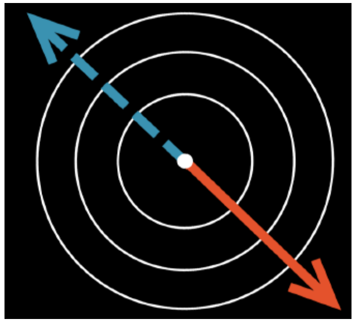

X (jet, photon, etc..)

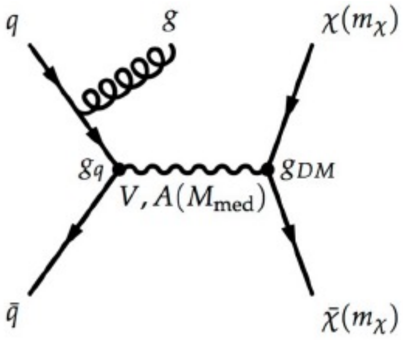

(similar to the single photon analysis at LEP)

General analysis strategy

- Require MET
- Select for X
- Veto other objects
- Additional cuts to suppress background
- Data-driven techniques to estimate background → invert vetoes

Results are interpreted in the Simplified Model framework to allow comparison with Direct Detection

- Mediator particle connects the SM quarks to DM particles:
  - Axial Vector, Pseudoscalar, etc…
- Model depends on four parameters:
  - DM mass, Mediator mass, SM-mediator coupling, DM-mediator coupling

DM at ATLAS, one example: monojet

Backgrounds

- ☐ Main backgrounds are EW processes with intrinsic E_T^{miss} , accompanied by jets:
  - ➢ Z(νν)+jets: irreducible background
  - ➢ W(lν)+jets: with unrecostructed or misidentified lepton
- ☐ Both estimated from data using leptonic Z or W control regions

- ☐ **Other backgrounds:**
  - ➢ Non-collision background (data)
  - ➢ Multijet background (data)
  - ➢ Z→ee, top, diboson (MC)

Signal Region MET

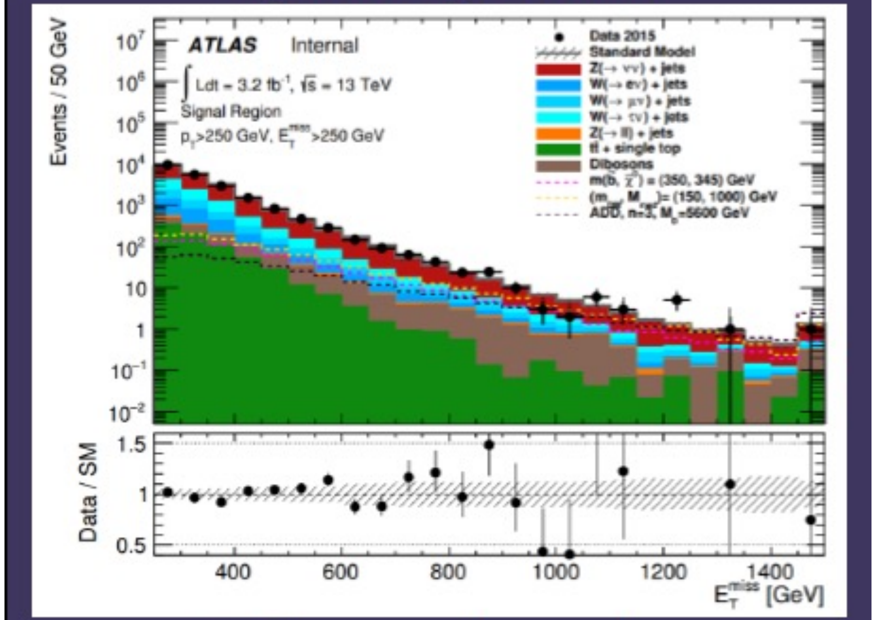

➡ No excess observed

Dominant uncertainties:

Statistical (3-10%), top (~3%), boson+jet modeling (2-4%)

DM at ATLAS, one example: monojet

Results

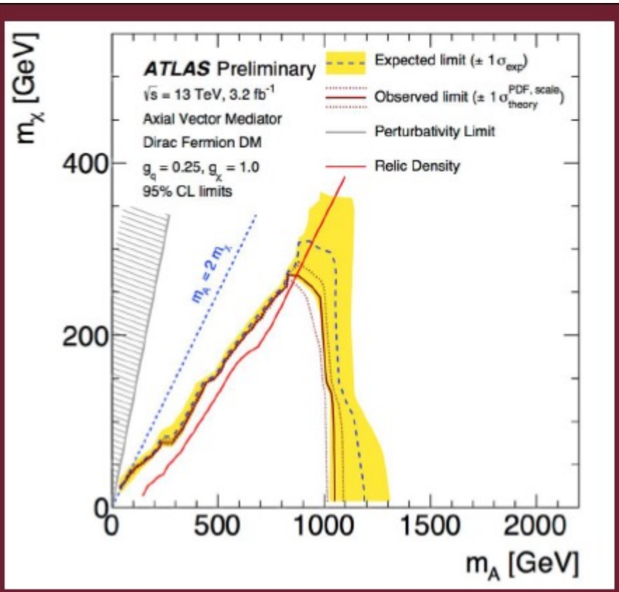

Limits as a function of DM & mediator mass

➥ Axial vector mediator, fixed values of g_{DM} & g_{SM}

DM excluded up to 250GeV for 1 TeV mediator

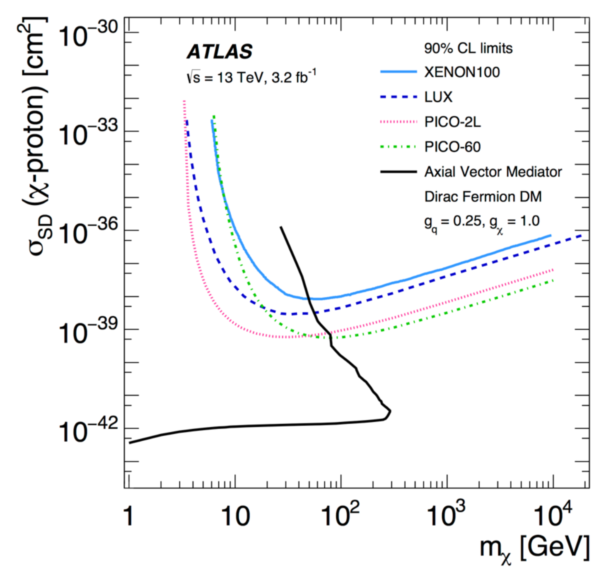

LHC limits reinterpreted as limit on DM-proton scattering cross-section

➥ LHC complementary at low m_{DM}

Parameter values & limit interpretation as recommended by the LHC Dark Matter Working Group [ArXiv:1603.04156]

SuperSymmetry

A brief introduction to SuperSymmetry

- ☐ **SuSy is a generalization of the SM: symmetry between fermions and bosons**
  - **Introduces sfermions and gauginos**
    → doubles particles content with respect to SM
  - **Extended Higgs sector: h, H, A, H^+, H^-**
- ☐ **PRO:**
  - **Alleviates hierarchy problem ($m_h << m_P$)**
  - **has a good Dark Matter candidate (neutralino)**
  - **Allows for gauge coupling unification**
- ☐ **CONS:**
  - **Over 100 free parameters (although with some ad hoc assumptions we can reduce the number of parameters)**
  - **wide range of possible experimental signatures**

It was expected ''something'' at the TeV scale

Search for SuSy particles

A few diagrams with susy particles in the final state, with the decay chain

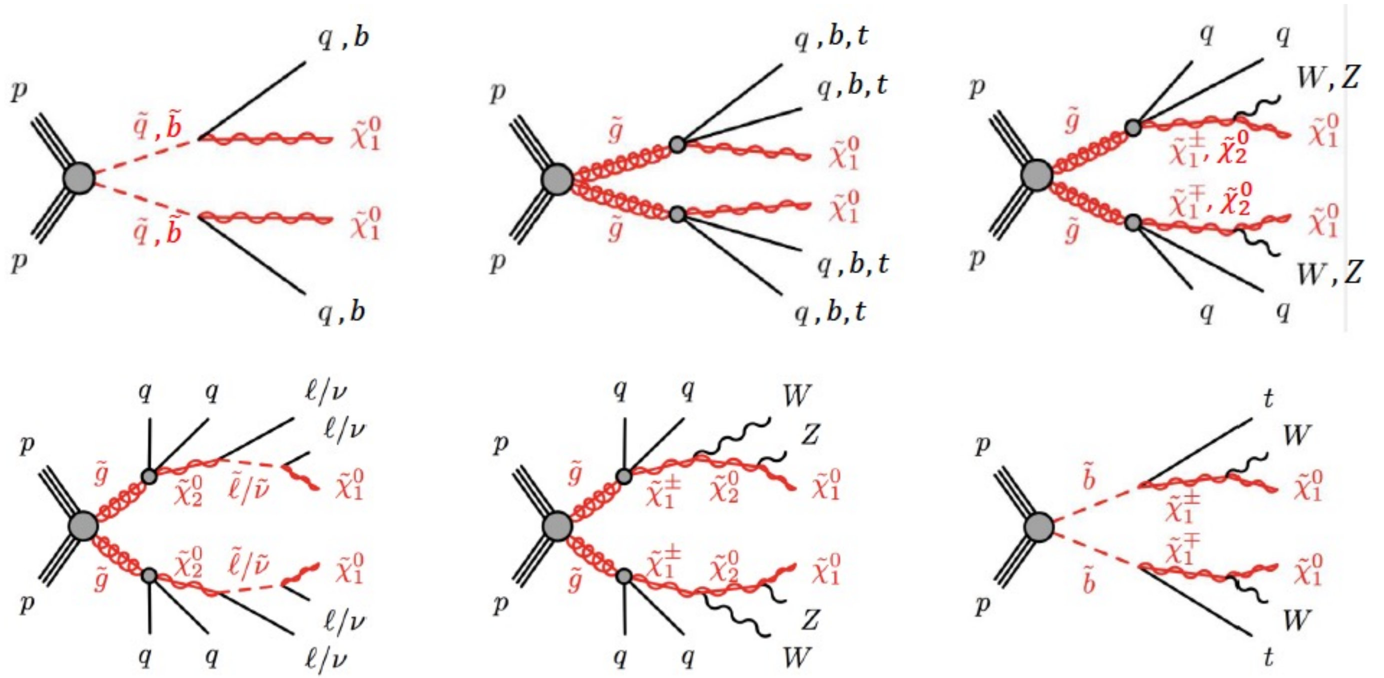

(R-parity conservation)

- **Lightest susy particle ($\tilde{\chi}_1^0$) escapes detection → Missing Transverse Momentum and Missing Energy**

- **Different analysis strategies according to many different final states**

Example: gaugino and neutralino mass limits

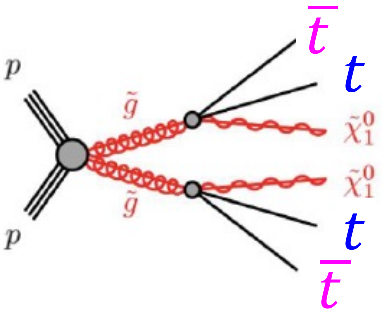

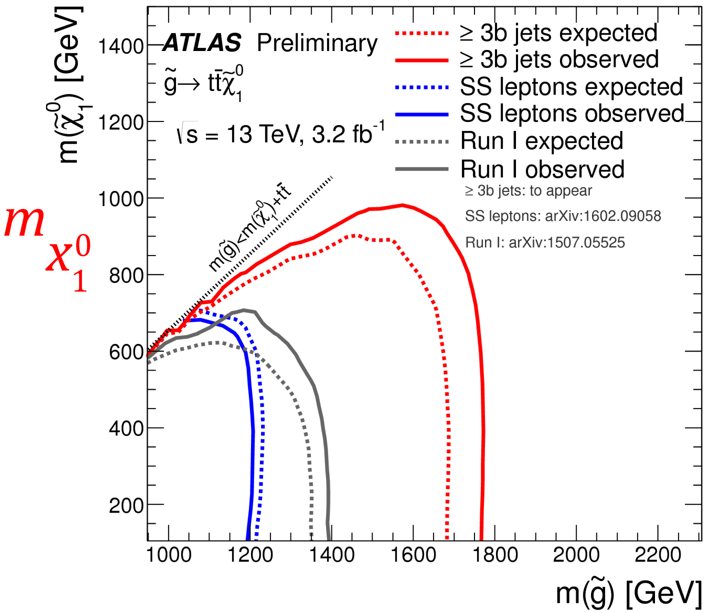

No signal has been found (yet)!

exclusion plot

From other susy searches many exclusions limits on the parameters phase space

now there is less and less room to “manouver”.

Particles masses higher and higher; cross-sections lower and lower

ATLAS SuSy particles: Run2 results

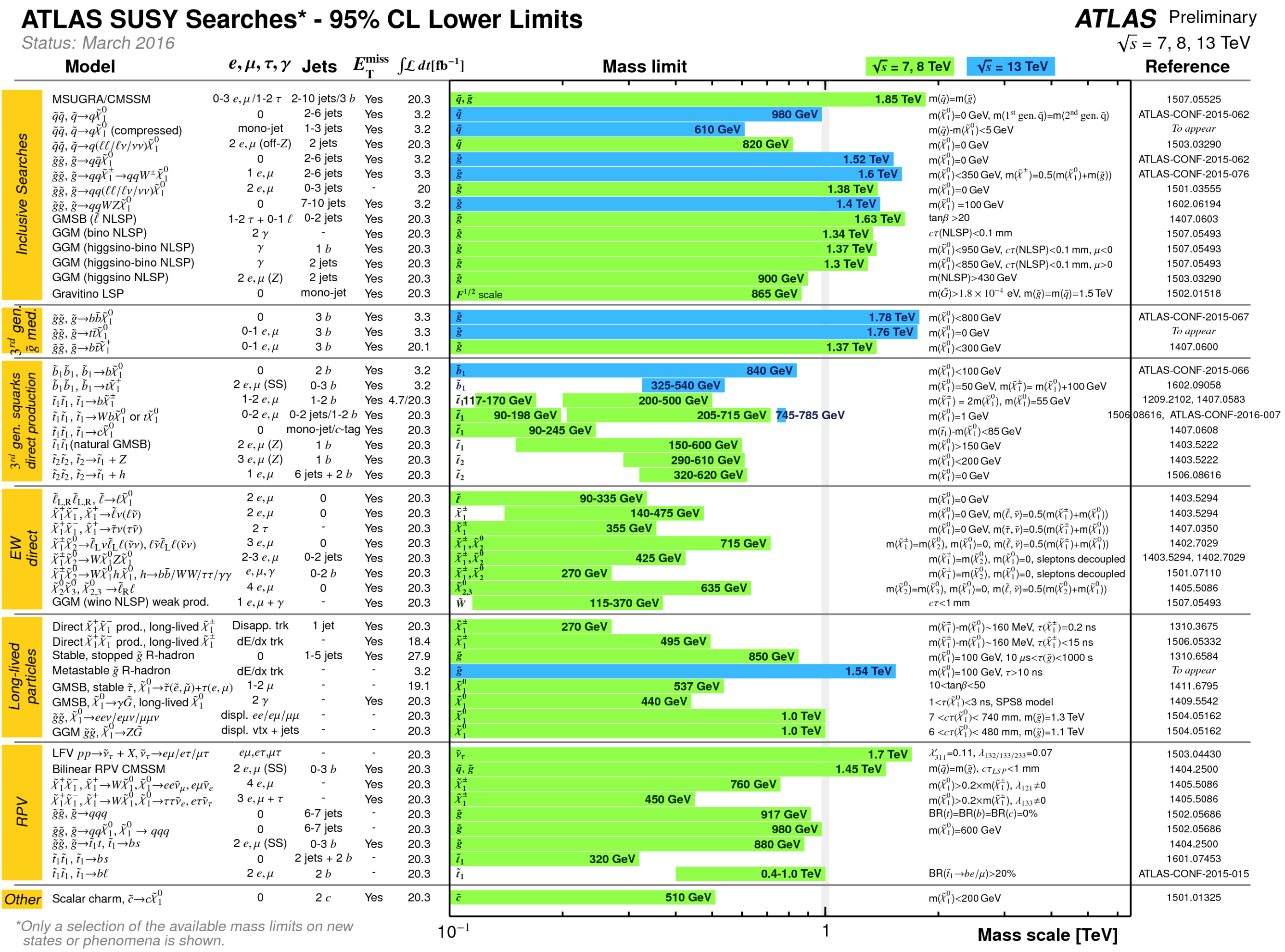

ATLAS SUSY Searches* - 95% CL Lower Limits

Status: March 2016

ATLAS Preliminary

$\sqrt{s}$ = 7, 8, 13 TeV

🟩 $\sqrt{s}$ = 7, 8 TeV 🟦 $\sqrt{s}$ = 13 TeV

	Model	e,μ,τ,γ	Jets	E_T^{miss}	$\int\mathcal{L}\,dt[\mathrm{fb}^{-1}]$	Mass limit		Reference
Inclusive Searches	MSUGRA/CMSSM	0-3 e,μ/1-2 τ	2-10 jets/3 b	Yes	20.3	$\tilde{q},\tilde{g}$ 🟩 1.85 TeV	m($\tilde{q}$)=m($\tilde{g}$)	1507.05525
	$\tilde{q}\tilde{q}$, $\tilde{q}\to q\tilde{\chi}^0_1$	0	2-6 jets	Yes	3.2	$\tilde{q}$ 🟦 980 GeV	m($\tilde{\chi}^0_1$)=0 GeV, m(1st gen. $\tilde{q}$)=m(2nd gen. $\tilde{q}$)	ATLAS-CONF-2015-062
	$\tilde{q}\tilde{q}$, $\tilde{q}\to q\tilde{\chi}^0_1$ (compressed)	mono-jet	1-3 jets	Yes	3.2	$\tilde{q}$ 🟦 610 GeV	m($\tilde{q}$)-m($\tilde{\chi}^0_1$)<5 GeV	*To appear*
	$\tilde{q}\tilde{q}$, $\tilde{q}\to q(\ell\ell/\ell\nu/\nu\nu)\tilde{\chi}^0_1$	2 e,μ (off-Z)	2 jets	Yes	20.3	$\tilde{q}$ 🟩 820 GeV	m($\tilde{\chi}^0_1$)=0 GeV	1503.03290
	$\tilde{g}\tilde{g}$, $\tilde{g}\to q\bar{q}\tilde{\chi}^0_1$	0	2-6 jets	Yes	3.2	$\tilde{g}$ 🟦 1.52 TeV	m($\tilde{\chi}^0_1$)=0 GeV	ATLAS-CONF-2015-062
	$\tilde{g}\tilde{g}$, $\tilde{g}\to qq\tilde{\chi}^\pm_1\to qqW^\pm\tilde{\chi}^0_1$	1 e,μ	2-6 jets	Yes	3.3	$\tilde{g}$ 🟦 1.6 TeV	m($\tilde{\chi}^0_1$)<350 GeV, m($\tilde{\chi}^\pm$)=0.5(m($\tilde{\chi}^0_1$)+m($\tilde{g}$))	ATLAS-CONF-2015-076
	$\tilde{g}\tilde{g}$, $\tilde{g}\to qq(\ell\ell/\ell\nu/\nu\nu)\tilde{\chi}^0_1$	2 e,μ	0-3 jets	-	20	$\tilde{g}$ 🟩 1.38 TeV	m($\tilde{\chi}^0_1$)=0 GeV	1501.03555
	$\tilde{g}\tilde{g}$, $\tilde{g}\to qqWZ\tilde{\chi}^0_1$	0	7-10 jets	Yes	3.2	$\tilde{g}$ 🟦 1.4 TeV	m($\tilde{\chi}^0_1$) =100 GeV	1602.06194
	GMSB ($\tilde{\ell}$ NLSP)	1-2 τ + 0-1 ℓ	0-2 jets	Yes	20.3	$\tilde{g}$ 🟩 1.63 TeV	tanβ >20	1407.0603
	GGM (bino NLSP)	2 γ	-	Yes	20.3	$\tilde{g}$ 🟩 1.34 TeV	$c\tau$(NLSP)<0.1 mm	1507.05493
	GGM (higgsino-bino NLSP)	γ	1 b	Yes	20.3	$\tilde{g}$ 🟩 1.37 TeV	m($\tilde{\chi}^0_1$)<950 GeV, $c\tau$(NLSP)<0.1 mm, μ<0	1507.05493
	GGM (higgsino-bino NLSP)	γ	2 jets	Yes	20.3	$\tilde{g}$ 🟩 1.3 TeV	m($\tilde{\chi}^0_1$)<850 GeV, $c\tau$(NLSP)<0.1 mm, μ>0	1507.05493
	GGM (higgsino NLSP)	2 e,μ (Z)	2 jets	Yes	20.3	$\tilde{g}$ 🟩 900 GeV	m(NLSP)>430 GeV	1503.03290
	Gravitino LSP	0	mono-jet	Yes	20.3	$F^{1/2}$ scale 🟩 865 GeV	m($\tilde{G}$)>1.8×10^{-4} eV, m($\tilde{g}$)=m($\tilde{q}$)=1.5 TeV	1502.01518
3^{rd} gen. $\tilde{g}$ med.	$\tilde{g}\tilde{g}$, $\tilde{g}\to b\bar{b}\tilde{\chi}^0_1$	0	3 b	Yes	3.3	$\tilde{g}$ 🟦 1.78 TeV	m($\tilde{\chi}^0_1$)<800 GeV	ATLAS-CONF-2015-067
	$\tilde{g}\tilde{g}$, $\tilde{g}\to t\bar{t}\tilde{\chi}^0_1$	0-1 e,μ	3 b	Yes	3.3	$\tilde{g}$ 🟦 1.76 TeV	m($\tilde{\chi}^0_1$)=0 GeV	*To appear*
	$\tilde{g}\tilde{g}$, $\tilde{g}\to b\bar{t}\tilde{\chi}^+_1$	0-1 e,μ	3 b	Yes	20.1	$\tilde{g}$ 🟩 1.37 TeV	m($\tilde{\chi}^0_1$)<300 GeV	1407.0600
3^{rd} gen. squarks direct production	$\tilde{b}_1\tilde{b}_1$, $\tilde{b}_1\to b\tilde{\chi}^0_1$	0	2 b	Yes	3.2	$\tilde{b}_1$ 🟦 840 GeV	m($\tilde{\chi}^0_1$)<100 GeV	ATLAS-CONF-2015-066
	$\tilde{b}_1\tilde{b}_1$, $\tilde{b}_1\to t\tilde{\chi}^\pm_1$	2 e,μ (SS)	0-3 b	Yes	3.2	$\tilde{b}_1$ 🟦 325-540 GeV	m($\tilde{\chi}^0_1$)=50 GeV, m($\tilde{\chi}^\pm_1$)= m($\tilde{\chi}^0_1$)+100 GeV	1602.09058
	$\tilde{t}_1\tilde{t}_1$, $\tilde{t}_1\to b\tilde{\chi}^\pm_1$	1-2 e,μ	1-2 b	Yes	4.7/20.3	$\tilde{t}_1$ 🟩 117-170 GeV 🟩 200-500 GeV	m($\tilde{\chi}^\pm_1$) = 2m($\tilde{\chi}^0_1$), m($\tilde{\chi}^0_1$)=55 GeV	1209.2102, 1407.0583
	$\tilde{t}_1\tilde{t}_1$, $\tilde{t}_1\to Wb\tilde{\chi}^0_1$ or $t\tilde{\chi}^0_1$	0-2 e,μ	0-2 jets/1-2 b	Yes	20.3	$\tilde{t}_1$ 🟩 90-198 GeV 🟩 205-715 GeV 🟦 745-785 GeV	m($\tilde{\chi}^0_1$)=1 GeV	1506.08616, ATLAS-CONF-2016-007
	$\tilde{t}_1\tilde{t}_1$, $\tilde{t}_1\to c\tilde{\chi}^0_1$	0	mono-jet/c-tag	Yes	20.3	$\tilde{t}_1$ 🟩 90-245 GeV	m($\tilde{t}_1$)-m($\tilde{\chi}^0_1$)<85 GeV	1407.0608
	$\tilde{t}_1\tilde{t}_1$ (natural GMSB)	2 e,μ (Z)	1 b	Yes	20.3	$\tilde{t}_1$ 🟩 150-600 GeV	m($\tilde{\chi}^0_1$)>150 GeV	1403.5222
	$\tilde{t}_2\tilde{t}_2$, $\tilde{t}_2\to\tilde{t}_1+Z$	3 e,μ (Z)	1 b	Yes	20.3	$\tilde{t}_2$ 🟩 290-610 GeV	m($\tilde{\chi}^0_1$)<200 GeV	1403.5222
	$\tilde{t}_2\tilde{t}_2$, $\tilde{t}_2\to\tilde{t}_1+h$	1 e,μ	6 jets + 2 b	Yes	20.3	$\tilde{t}_2$ 🟩 320-620 GeV	m($\tilde{\chi}^0_1$)=0 GeV	1506.08616
EW direct	$\tilde{\ell}_{L,R}\tilde{\ell}_{L,R}$, $\tilde{\ell}\to\ell\tilde{\chi}^0_1$	2 e,μ	0	Yes	20.3	$\tilde{\ell}$ 🟩 90-335 GeV	m($\tilde{\chi}^0_1$)=0 GeV	1403.5294
	$\tilde{\chi}^+_1\tilde{\chi}^-_1$, $\tilde{\chi}^+_1\to\tilde{\ell}\nu(\ell\tilde{\nu})$	2 e,μ	0	Yes	20.3	$\tilde{\chi}^\pm_1$ 🟩 140-475 GeV	m($\tilde{\chi}^0_1$)=0 GeV, m($\tilde{\ell},\tilde{\nu}$)=0.5(m($\tilde{\chi}^\pm_1$)+m($\tilde{\chi}^0_1$))	1403.5294
	$\tilde{\chi}^+_1\tilde{\chi}^-_1$, $\tilde{\chi}^+_1\to\tilde{\tau}\nu(\tau\tilde{\nu})$	2 τ	-	Yes	20.3	$\tilde{\chi}^\pm_1$ 🟩 355 GeV	m($\tilde{\chi}^0_1$)=0 GeV, m($\tilde{\tau},\tilde{\nu}$)=0.5(m($\tilde{\chi}^\pm_1$)+m($\tilde{\chi}^0_1$))	1407.0350
	$\tilde{\chi}^\pm_1\tilde{\chi}^0_2\to\tilde{\ell}_L\nu\tilde{\ell}_L\ell(\tilde{\nu}\nu)$, $\ell\tilde{\nu}\tilde{\ell}_L\ell(\tilde{\nu}\nu)$	3 e,μ	0	Yes	20.3	$\tilde{\chi}^\pm_1,\tilde{\chi}^0_2$ 🟩 715 GeV	m($\tilde{\chi}^\pm_1$)=m($\tilde{\chi}^0_2$), m($\tilde{\chi}^0_1$)=0, m($\tilde{\ell},\tilde{\nu}$)=0.5(m($\tilde{\chi}^\pm_1$)+m($\tilde{\chi}^0_1$))	1402.7029
	$\tilde{\chi}^\pm_1\tilde{\chi}^0_2\to W\tilde{\chi}^0_1Z\tilde{\chi}^0_1$	2-3 e,μ	0-2 jets	Yes	20.3	$\tilde{\chi}^\pm_1,\tilde{\chi}^0_2$ 🟩 425 GeV	m($\tilde{\chi}^\pm_1$)=m($\tilde{\chi}^0_2$), m($\tilde{\chi}^0_1$)=0, sleptons decoupled	1403.5294, 1402.7029
	$\tilde{\chi}^\pm_1\tilde{\chi}^0_2\to W\tilde{\chi}^0_1h\tilde{\chi}^0_1$, $h\to b\bar{b}/WW/\tau\tau/\gamma\gamma$	e,μ,γ	0-2 b	Yes	20.3	$\tilde{\chi}^\pm_1,\tilde{\chi}^0_2$ 🟩 270 GeV	m($\tilde{\chi}^\pm_1$)=m($\tilde{\chi}^0_2$), m($\tilde{\chi}^0_1$)=0, sleptons decoupled	1501.07110
	$\tilde{\chi}^0_2\tilde{\chi}^0_3$, $\tilde{\chi}^0_{2,3}\to\tilde{\ell}_R\ell$	4 e,μ	0	Yes	20.3	$\tilde{\chi}^0_{2,3}$ 🟩 635 GeV	m($\tilde{\chi}^0_2$)=m($\tilde{\chi}^0_3$), m($\tilde{\chi}^0_1$)=0, m($\tilde{\ell},\tilde{\nu}$)=0.5(m($\tilde{\chi}^0_2$)+m($\tilde{\chi}^0_1$))	1405.5086
	GGM (wino NLSP) weak prod.	1 e,μ + γ	-	Yes	20.3	$\tilde{W}$ 🟩 115-370 GeV	$c\tau$<1 mm	1507.05493
Long-lived particles	Direct $\tilde{\chi}^+_1\tilde{\chi}^-_1$ prod., long-lived $\tilde{\chi}^\pm_1$	Disapp. trk	1 jet	Yes	20.3	$\tilde{\chi}^\pm_1$ 🟩 270 GeV	m($\tilde{\chi}^\pm_1$)-m($\tilde{\chi}^0_1$)~160 MeV, τ($\tilde{\chi}^\pm_1$)=0.2 ns	1310.3675
	Direct $\tilde{\chi}^+_1\tilde{\chi}^-_1$ prod., long-lived $\tilde{\chi}^\pm_1$	dE/dx trk	-	Yes	18.4	$\tilde{\chi}^\pm_1$ 🟩 495 GeV	m($\tilde{\chi}^\pm_1$)-m($\tilde{\chi}^0_1$)~160 MeV, τ($\tilde{\chi}^\pm_1$)<15 ns	1506.05332
	Stable, stopped $\tilde{g}$ R-hadron	0	1-5 jets	Yes	27.9	$\tilde{g}$ 🟩 850 GeV	m($\tilde{\chi}^0_1$)=100 GeV, 10 μs<τ($\tilde{g}$)<1000 s	1310.6584
	Metastable $\tilde{g}$ R-hadron	dE/dx trk	-	-	3.2	$\tilde{g}$ 🟦 1.54 TeV	m($\tilde{\chi}^0_1$)=100 GeV, τ>10 ns	*To appear*
	GMSB, stable $\tilde{\tau}$, $\tilde{\chi}^0_1\to\tilde{\tau}(\tilde{e},\tilde{\mu})+\tau(e,\mu)$	1-2 μ	-	-	19.1	$\tilde{\chi}^0_1$ 🟩 537 GeV	10<tanβ<50	1411.6795
	GMSB, $\tilde{\chi}^0_1\to\gamma\tilde{G}$, long-lived $\tilde{\chi}^0_1$	2 γ	-	Yes	20.3	$\tilde{\chi}^0_1$ 🟩 440 GeV	1<τ($\tilde{\chi}^0_1$)<3 ns, SPS8 model	1409.5542
	$\tilde{g}\tilde{g}$, $\tilde{\chi}^0_1\to ee\nu/e\mu\nu/\mu\mu\nu$	displ. $ee/e\mu/\mu\mu$	-	-	20.3	$\tilde{\chi}^0_1$ 🟩 1.0 TeV	7 <$c\tau$($\tilde{\chi}^0_1$)< 740 mm, m($\tilde{g}$)=1.3 TeV	1504.05162
	GGM $\tilde{g}\tilde{g}$, $\tilde{\chi}^0_1\to Z\tilde{G}$	displ. vtx + jets	-	-	20.3	$\tilde{\chi}^0_1$ 🟩 1.0 TeV	6 <$c\tau$($\tilde{\chi}^0_1$)< 480 mm, m($\tilde{g}$)=1.1 TeV	1504.05162
RPV	LFV $pp\to\tilde{\nu}_\tau+X$, $\tilde{\nu}_\tau\to e\mu/e\tau/\mu\tau$	$e\mu,e\tau,\mu\tau$	-	-	20.3	$\tilde{\nu}_\tau$ 🟩 1.7 TeV	λ'_{311}=0.11, $\lambda_{132/133/233}$=0.07	1503.04430
	Bilinear RPV CMSSM	2 e,μ (SS)	0-3 b	Yes	20.3	$\tilde{q},\tilde{g}$ 🟩 1.45 TeV	m($\tilde{q}$)=m($\tilde{g}$), $c\tau_{LSP}$<1 mm	1404.2500
	$\tilde{\chi}^+_1\tilde{\chi}^-_1$, $\tilde{\chi}^+_1\to W\tilde{\chi}^0_1$, $\tilde{\chi}^0_1\to ee\tilde{\nu}_\mu, e\mu\tilde{\nu}_e$	4 e,μ	-	Yes	20.3	$\tilde{\chi}^\pm_1$ 🟩 760 GeV	m($\tilde{\chi}^0_1$)>0.2×m($\tilde{\chi}^\pm_1$), $\lambda_{121}\neq0$	1405.5086
	$\tilde{\chi}^+_1\tilde{\chi}^-_1$, $\tilde{\chi}^+_1\to W\tilde{\chi}^0_1$, $\tilde{\chi}^0_1\to\tau\tau\tilde{\nu}_e, e\tau\tilde{\nu}_\tau$	3 e,μ + τ	-	Yes	20.3	$\tilde{\chi}^\pm_1$ 🟩 450 GeV	m($\tilde{\chi}^0_1$)>0.2×m($\tilde{\chi}^\pm_1$), $\lambda_{133}\neq0$	1405.5086
	$\tilde{g}\tilde{g}$, $\tilde{g}\to qqq$	0	6-7 jets	-	20.3	$\tilde{g}$ 🟩 917 GeV	BR(t)=BR(b)=BR(c)=0%	1502.05686
	$\tilde{g}\tilde{g}$, $\tilde{g}\to qq\tilde{\chi}^0_1$, $\tilde{\chi}^0_1\to qqq$	0	6-7 jets	-	20.3	$\tilde{g}$ 🟩 980 GeV	m($\tilde{\chi}^0_1$)=600 GeV	1502.05686
	$\tilde{g}\tilde{g}$, $\tilde{g}\to\tilde{t}_1t$, $\tilde{t}_1\to bs$	2 e,μ (SS)	0-3 b	Yes	20.3	$\tilde{g}$ 🟩 880 GeV		1404.2500
	$\tilde{t}_1\tilde{t}_1$, $\tilde{t}_1\to bs$	0	2 jets + 2 b	-	20.3	$\tilde{t}_1$ 🟩 320 GeV		1601.07453
	$\tilde{t}_1\tilde{t}_1$, $\tilde{t}_1\to b\ell$	2 e,μ	2 b	-	20.3	$\tilde{t}_1$ 🟩 0.4-1.0 TeV	BR($\tilde{t}_1\to be/\mu$)>20%	ATLAS-CONF-2015-015
Other	Scalar charm, $\tilde{c}\to c\tilde{\chi}^0_1$	0	2 c	Yes	20.3	$\tilde{c}$ 🟩 510 GeV	m($\tilde{\chi}^0_1$)<200 GeV	1501.01325

*Only a selection of the available mass limits on new states or phenomena is shown.

You don't have to study this table by hearth of course ☺

SAPIENZA
UNIVERSITÀ DI ROMA

End of chapter 11